I. A NUMERICAL METHOD FOR SMOOTHING THERMODYNAMIC DATA

II. DIFFUSION COEFFICIENTS IN BINARY HYDROCARBON LIQUIDS

III. CORRELATION OF DIFFUSION COEFFICIENTS OF LIQUID HYDROCARBONS

Thesis by

Dennis Jerome Graue

In Partial Fulfillment of the Requirements

For the Degree of

Doctor of Philosophy

California Institute of Technology

Pasadena, California

1965

(Submitted April 16, 1965)

ACKNOWLEDGMENT

I wish to express my appreciation to my advisor, Professor B. H. Sage, for his guidance and counsel throughout my graduate research program.

The many contributions which were made in discussions by my fellow students, especially Mr. J. W. Woodward, were invaluable.

I acknowledge with gratitude the financial support of the National Science Foundation during the four years in which I was a graduate student.

To my wife, Mary Beth, I am indebted for her years of unselfish encouragement.

ABSTRACT

I. A numerical method was developed for smoothing thermodynamic data with a digital computer. As a feasibility study, data on specific volume and enthalpy from the skeleton tables of the Sixth International Conference on the Properties of Steam and from the tables of Keenan and Keyes were smoothed and interpolated. Orthogonal polynomials of temperature and pressure were used as the smoothing functions. In order to maintain thermodynamic consistency between the smoothed values of the two thermodynamic properties, Lagrange multipliers were used in conjunction with least squares techniques to accomplish the curve fitting. Excellent agreement was obtained between tabulated and smoothed values of the above properties and their derivatives except near the critical region where data were sparse. The method is recommended for the smoothing of the above and other thermodynamic properties which may be subject to consistency restrictions.

II. Data on the Chapman-Cowling diffusion coefficients of liquid hydrocarbons were expressed analytically in terms of the physical properties of the liquid phase and the nature of the components. The weight fraction of the light component, temperature, and the molecular weight of the heavy component served satisfactorily as independent variables to describe the recent data of Sage for binary hydrocarbon systems. The results permit the calculation of the Chapman-Cowling diffusion coefficients in the liquid phase for saturated hydrocarbons from methane through n-decane.

III. The above data were used in the testing and formulation of correlations of diffusion coefficients of binary liquid mixtures. The correlation methods which were tested were the following: empirical, rate process theory, hole theory, and kinetic theory. The hole theory was inadequate for describing the available data on mutual diffusion; accurate empirical and rate-process expressions were developed for calculating Chapman-Cowling diffusion coefficients for binary mixtures of methane and ethane with heavier hydrocarbons through n-decane and a heavier "white oil;" although the expressions which were tested from kinetic theory did not predict correctly the dependence of the data on temperature and composition, they presented good approximations and appeared to be a promising area for future development.

TABLE OF CONTENTS

I. A NUMERICAL METHOD FOR SMOOTHING THERMODYNAMIC DATA

INTRODUCTION

The use of programmed numerical methods to smooth and interpolate tables of thermodynamic data is becoming increasingly justified in terms of time, energy, and money required to do the work. This work describes a feasibility study for such numerical smoothing and interpolation of the recently published skeleton table of the Sixth International Conference on the Properties of Steam (4).

In general, the easiest method to smooth data is to express the data in a characteristic form which varies slowly within finite limits (2). Keenan and Keyes (5) used such a procedure and approximated the thermodynamic behavior of steam with equations. Then they smoothed the residual values of the data graphically. Their technique would be satisfactory for present purposes if the residual values could be smoothed numerically. To accomplish this smoothing when the behavior of the residual values is arbitrary and the independent variables number more than one, a very convenient method uses orthogonal polynomials in the manner of Pings and Sage (6). In fact, Bright and Dawkins (1) found that the use of orthogonal polynomials often produces curves which fit the data much better than would the curves of conventional polynomials. However, to overcome the necessity for data points at equally spaced intervals which accompanied the particular orthogonal polynomials used by Pings and Sage, the generalized orthogonal polynomials of Forsythe (3) are preferred.

Thus, it should be possible to fit any reasonable function by a least squares analysis and interpolate and smooth it with sums of orthogonal polynomials.

THEORY

Forsythe (3) suggested the following as a recursion formula to generate a set of orthogonal polynomials for a set of I data points, arbitrarily spaced.

$$P_1(x) = 1 \tag{1}$$

$$P_2(x) = (x - \alpha_2)P_1(x) \tag{2}$$

$$P_3(x) = (x - \alpha_3)P_2(x) - \beta_2 P_1(x) \tag{3}$$

$$P_n(x) = (x - \alpha_n)P_{n-1}(x) - \beta_{n-1}P_{n-2}(x) \tag{4}$$

The α's and β's are found as follows. Multiply each side of Equation 4 by $P_{n-1}(x)$ and sum over the I data points, as

$$\sum_{i=1}^{I} P_{n-1}(x_i)P_n(x_i) = \sum_{i=1}^{I} x_i P_{n-1}^2(x_i) - \alpha_n \sum_{i=1}^{I} P_{n-1}^2(x_i)$$

$$- \beta_{n-1} \sum_{i=1}^{I} P_{n-1}(x_i)P_{n-2}(x_i) . \tag{5}$$

An orthogonal polynomial is defined by the equation for discrete variables

$$\sum_{i=1}^{I} P_j(x_i)P_k(x_i) = \delta_{jk} \times \text{constant.} \tag{6}$$

Therefore, Equation 5 reduces to give

$$\alpha_n = \left(\sum_{i=1}^{I} x_i P_{n-1}^2(x_i) \right) \Bigg/ \left(\sum_{i=1}^{I} P_{n-1}^2(x_i) \right) \tag{7}$$

Similarly, β_{n-1} is found to be

$$\beta_{n-1} = \left(\sum_{i=1}^{I} x_i P_{n-2}(x_i)P_{n-1}(x_i) \right) \Bigg/ \left(\sum_{i=1}^{I} P_{n-2}^2(x_i) \right) . \tag{8}$$

However, from Equations 4 and 6, it is seen that

$$\sum_{i=1}^{I} P_n^2(x_i) = \sum_{i=1}^{I} x_i P_n(x_i) P_{n-1}(x_i) \quad . \tag{9}$$

Combining Equations 8 and 9 gives the expression for the calculation of β_{n-1}:

$$\beta_{n-1} = \left(\sum_{i=1}^{I} P_{n-1}^2(x_i) \right) \Bigg/ \left(\sum_{i=1}^{I} P_{n-2}^2(x_i) \right) \quad . \tag{10}$$

In least squares fitting with orthogonal polynomials, it is very convenient to know the relative contributions of the individual polynomials in the series. If it is known that the polynomials all range in value from about 0.01 to 1.0, the relative size of the coefficient of each polynomial gives directly the relative importance of the polynomial's contribution to the function. Therefore, it is very convenient to define an orthonormal polynomial by the equation

$$\sum_{i=1}^{I} P_j^o(x_i) P_k^o(x_i) = \delta_{jk} \quad . \tag{11}$$

From Equations 6 and 11, it is found that

$$\frac{1}{F_j} = \text{constant} = \sum_{i=1}^{I} P_j^2(x_i) \tag{12}$$

and

$$P_j^o(x_i) = P_j(x_i) F_j \quad . \tag{13}$$

Now $P_j^o(x_i)$ will always be ≤ 1.0 and may be used to advantage as described above in place of a polynomial which is only orthogonal.

A least squares fit of data by such polynomials would be of the following form. Dependent variable y is a function of x. Therefore, express y as

$$y = \sum_{k=1}^{K} A_k P_k^o(x) \quad . \tag{14}$$

Given I data points of x and y , the K coefficients A_k can be determined by minimizing the sum S with respect to the A_k's .

$$S = \sum_{i=1}^{I} [y_i - \sum_{k=1}^{K} A_k P_k^o(x_i)]^2 \tag{15}$$

$$\frac{1}{2}\frac{\partial S}{\partial A_j} = -\sum_{i=1}^{I} y_i P_j^o(x_i) + \sum_{i=1}^{I}\sum_{k=1}^{K} A_k P_k^o(x_i) P_j^o(x_i) = 0 \tag{16}$$

Combining Equations 16 and 11 gives the expression for the calculation of A_k .

$$A_k = \sum_{i=1}^{I} y_i P_k^o(x_i) \tag{17}$$

The complication of having more than one independent variable can be handled by obtaining sets of orthonormal polynomials for each independent variable and forming all of the cross-products of them, as illustrated here for two such variables. The polynomials will be $P^o(x)$ and $T^o(z)$, where $y = f(x, z)$. y is expressed as

$$y = \sum_{k=1}^{K}\sum_{\ell=1}^{L} A_{k\ell} P_k^o(x) T_\ell^o(x) \ . \tag{18}$$

Again, a least squares manipulation gives the expression for the coefficients

$$\sum_{i=1}^{I}\sum_{k,\ell}^{K,L} A_{k\ell} P_k^o(x_i) T_\ell^o(z_i) P_m^o(x_i) T_n^o(z_i) = \sum_{i=1}^{I} y_i P_m^o(x_i) T_n^o(z_i) \tag{19}$$

or

$$\sum_{k,\ell}^{K,L} A_{k\ell} \sum_{i=1}^{I} P_k^o(x_i) P_m^o(x_i) T_\ell^o(z_i) T_m^o(z_i) = \sum_{i=1}^{I} y_i P_m^o(x_i) T_n^o(z_i) \ . \tag{20}$$

Unlike Equation 17, this expression involves all of the coefficients $A_{k\ell}$ since $P_m^o(x_i)$ and $T_n^o(z_i)$ are not necessarily orthogonal to each other. Thus, unless additional conditions are met by the data,

K+L simultaneous equations like Equation 20 would have to be solved as in the normal multiple linear regression procedure. However, if the data consist of a rectangular set -- that is, there are data points at the same set of x's for each value of z -- the sum over i in the left portion of Equation 20 can be replaced with a double sum over x values and z values. The inner sum then covers the entire range of its variable and results in the orthogonality relationship 11, giving

$$A_{mn} = \left(\sum_{i=1}^{I} y_i P^o_m(x_i) T^o_n(z_i) \right) \Big/ \left(\sum_{i=1}^{I} P^{2o}_m(x_i) T^{2o}_n(z_i) \right) . \qquad (21)$$

It can be shown that, for orthonormal polynomials of a rectanglular set of data,

$$\sum_{i=1}^{I} P_k^{2o}(x_i) T_\ell^{2o}(z_i) = \frac{1}{I} , \qquad (22)$$

for any k or ℓ. Therefore, Equation 21 becomes

$$A_{mn} = I \sum_{i=1}^{I} y_i P^o_m(x_i) T^o_n(z_i) . \qquad (23)$$

When data for two different but related functions such as volume and enthalpy are being smoothed simultaneously, the least squares fit may be forced to conform to the interrelation between the functions. In the case of volume and enthalpy, the smoothed points would have to satisfy the thermodynamic relation

$$\left(\frac{\partial H}{\partial P} \right)_T = V - T \left(\frac{\partial V}{\partial T} \right)_P . \qquad (24)$$

Up to this point, the fitting of data by least squares has not involved inverting a matrix except when the data were not a rectangular set. Thus, unless the data were taken very close to a two-phase boundary, they could be a rectangular set; if a rectangular set

were used, a diagonal matrix would result and give the trivial inversion solution of Equation 23. However, when restrictions such as Equation 24 are placed on a fit of data, the least squares matrix is always non-diagonal. It may be simplified to give a matrix of the order of the number of restrictions only if the data are a rectangular set. This matrix, of relatively low order, then should not be difficult to invert. The least squares coefficients could then be calculated from the Lagrange multipliers which were obtained from the inverted restriction matrix. As an example, the development will be given for a least squares fit of PV/T and H/(T+a) in the gas phase, assuming a rectangular set of data points.

Define

$$\alpha = \frac{H}{T+a} - b \tag{25}$$

and

$$\gamma = \frac{PV}{T} - R \ . \tag{26}$$

In terms of α and γ, Equation 24 becomes

$$(T + a)\left(\frac{\partial \alpha}{\partial P}\right)_T = - \frac{T^2}{P} \left(\frac{\partial \gamma}{\partial T}\right)_P \ . \tag{27}$$

γ will be expressed in terms of the K temperature polynomials $T_k^o(T)$, the L pressure polynomials $P_\ell^o(P)$, and the coefficients $A_{k\ell}$. α will be expressed in terms of the N temperature polynomials $U_n^o(T)$, the M pressure polynomials $Q_m^o(P)$, and the coefficients B_{mn}. Thus,

$$\gamma = \sum_{k=1}^{K} \sum_{\ell=1}^{L} A_{k\ell} T_k^o(T) P_\ell^o(P) \tag{28}$$

and

$$\alpha = \sum_{m=1}^{M} \sum_{n=1}^{N} B_{mn} U_n^o(T) Q_m^o(P) \quad . \tag{29}$$

Restriction 27 can be expressed at temperature T_r and pressure P_r as

$$R_1 = (T+a) \sum_{m,n}^{M,N} B_{mn} Q_m^{o'}(P_r) U_n^o(T_r) + \frac{T_r^2}{P_r} \sum_{k,\ell}^{K,L} A_{k\ell} T_k^{o'}(T) P_\ell(P_r) = 0 \tag{30}$$

with the associated Lagrange multiplier λ_1. An additional restriction on the fit may be that $\gamma \to 0$ as $P \to 0$ at T_r, or

$$R_2 = \sum_{k,\ell}^{K,L} A_{k\ell} T_k^o(T_r) P_\ell^o(0) = 0 \tag{31}$$

with the associated Lagrange multiplier λ_2. Now, for convenience, additional functions will be defined as

$$f_{k\ell} = \sum_{i=1}^{I} \gamma_i P_\ell^o(P_i) T_k^o(T_i) \tag{32}$$

$$q_{k\ell} = T_k^o(T_r) P_\ell^o(0) \tag{33}$$

$$p_{k\ell} = T_k^{o'}(T_r) P_\ell^o(P_r) \tag{34}$$

$$g_{mn} = \sum_{j=1}^{J} \alpha_j Q_m^o(P_j) U_n^o(T_j) \tag{35}$$

$$h_{mn} = Q_m^{o'}(P_r) U_n^o(T_r) \tag{36}$$

The least squares sum for the simultaneous fits of γ and α, with the two restrictions 30 and 31 included by using the Lagrange multipliers, is

$$S = \sum_{i=1}^{I} \left[\gamma_i - \sum_{k,\ell}^{K,L} A_{k\ell} T_k^o(T_i) P_\ell^o(P_i)\right]^2 + \sum_{j=1}^{J} \left[\alpha_j - \sum_{m,n}^{M,N} B_{mn} U_n^o(T_j) Q_m^o(P_j)\right]^2$$

$$+ \lambda_1 \left[(T_r+a) \sum_{m,n}^{M,N} B_{mn} Q_m^{o'}(P_r) U_n^o(T_r) + \frac{T_r^2}{P_r} \sum_{k,\ell}^{K,L} A_{k\ell} T_k^{o'}(T_r) P_\ell^o(P_r)\right] +$$

$$+ \lambda_2 \sum_{k,\ell}^{K,L} A_{k\ell} T_k^o(T_r) P_\ell^o(0) \quad . \tag{37}$$

The A's and B's are found by minimizing the sum S with respect to the λ's , A's , and B's . Then α and γ (or H and V) and their derivatives may be determined at the point T_r, P_r . The minimization of S gives

$$A_{k\ell} = I\left(f_{k\ell} - \lambda_1 q_{k\ell} - \lambda_2 p_{k\ell} \frac{T_r^2}{P_r}\right) \tag{38}$$

$$B_{mn} = J(g_{mn} - \lambda_2 h_{mn}[T_r+a]) \tag{39}$$

where the λ's are found from the solution of the matrix equation

$$\begin{bmatrix} \sum_{k,\ell}^{K,L} q_{k\ell}^2 & \frac{T_r^2}{P_r} \sum_{k,\ell}^{K,L} p_{k\ell} q_{k\ell} \\ I\frac{T_r^2}{P_r} \sum_{k,\ell}^{K,L} q_{k\ell} p_{k\ell} & I\frac{T_r^4}{P_r^2} \sum_{k,\ell}^{K,L} p_{k\ell}^2 + J(T_r+a)^2 \sum_{m,n}^{M,N} h_{mn}^2 \end{bmatrix} \begin{bmatrix} \lambda_1 \\ \lambda_2 \end{bmatrix} =$$

$$\begin{bmatrix} \sum_{k,\ell}^{K,L} f_{k\ell} q_{k\ell} \\ I\frac{T_r^2}{P_r} \sum_{k,\ell}^{K,L} f_{k\ell} p_{k\ell} + J(T_r+a) \sum_{m,n}^{M,N} g_{mn} h_{mn} \end{bmatrix} \tag{40}$$

The derivatives of the polynomials are necessary to the above analysis. Differentiation of Equation 4 gives

$$P_n'(x) = P_{n-1}(x) + (x-\alpha_n)P_{n-1}'(x) - \beta_{n-1}P_{n-2}'(x) \tag{41}$$

$$P_n'(x) = P_{n-1}(x) + (x-\alpha_n)P_{n-2}(x) + [(x-\alpha_n)(x-\alpha_{n-1}) - \beta_{n-1}]P_{n-2}'(x)$$
$$- \beta_{n-2}(x-\alpha_n)P_{n-3}'(x) \quad . \tag{42}$$

It is seen that the following recursion formula applies:

$$P'_J(x) = \sum_{j=1}^{J-1} (E_{j,1} - E_{j,2}) P_j(x) \tag{43}$$

where

$$E_{j,1} = E_{j+1,1}(x-\alpha_{j+1})$$

$$E_{j,2} = E_{j+2,1}\beta_{j+1}$$

$$E_{J,1} = 1$$

$$E_{J,2} = 0$$

$$E_{J+1,1} = 0$$

Also,

$$P^{o'}_J(x) = P'_J(x)F_J \ . \tag{44}$$

PROCEDURE

The step-by-step method for obtaining smoothed or interpolated values of specific volumes and enthalpies from a set of data points is as follows.

1. Select a grid of data points of desired size in the range of interest (either manually or by machine).
2. Generate the appropriate orthonormal polynomials in each independent variable from the data.
3. Calculate the polynomials and their appropriate derivatives at the point of interest (the latter if thermodynamic restrictions are to be imposed).
4. Set up the thermodynamic restriction matrix and solve for the Lagrange multipliers.
5. Calculate the least squares constants.
6. Evaluate the least squares fit (optional).
7. Calculate the smoothed or interpolated properties at the point of interest.

All of these steps except the first have been programmed by the author in Fortran IV language for calculation on an IBM 7094 computer. The first step is easily programmed as well.

RESULTS

The data which were used in this feasibility study are given in Tables 1 through 5. The data in the first four tables were converted from data published by the Sixth International Conference on the Properties of Steam (4); those in Table 5 were taken directly from the smoothed tables of Keenan and Keyes (5).

When the smooth gas phase properties of Keenan and Keyes given in Table 5 were fitted, the results were as shown in Table 6. Fitting PV/T with no restrictions on the behavior of the function gave an average absolute deviation from the input values for specific volume of 0.005 per cent. The same was true when that property was described by a function with one restriction on it: that $PV/T \rightarrow R$ as $P \rightarrow 0$ at the temperature to be smoothed. The third case given in Table 6 shows that the simultaneous fit of $PV/T - R$ and $H/(T+340) - 1.200$, with the above restriction and the additional restriction that Equation 24 be satisfied, has greater deviation from the input data points than the other two cases. The average absolute deviations from the input volume and enthalpy data were about 0.02 and 0.002 per cent, respectively. Good agreement was obtained in each case with the smoothed values of Keenan and Keyes for values of volume, enthalpy, and heat capacity, which was calculated by analytical differentiation of the equation for enthalpy.

Table 7 was produced using gas phase data from the skeleton table of the Sixth International Conference on the Properties of Steam. Since the data covered a much wider range than did those used in Table 6, the fit was considerably poorer than in the latter.

Further, since the data points in the gas phase were few, a rectangular set was not used and matrix had to be inverted as described in the THEORY section. However, the predicted values agreed to within less than one per cent with the values given by Keenan and Keyes, though the data used for the equation, Table 1, may not have been completely compatible with those of Keenan and Keyes. The cases with zero and one restrictions were analogous to those in Table 6. A simultaneous fit of volumetric and enthalpy data was not made because of the above mentioned necessity for inverting a matrix. In the latter case, a non-diagonal matrix of the order of 18 or 20 would have to be inverted to give little or no accuracy in results. It is therefore concluded that, in the absence of enough data to comprise a rectangular set, the volume and enthalpy data should be interpolated separately at first. Then rectangular sets of more closely spaced points could be smoothed simultaneously (without matrix inversion) to give a thermodynamically consistent table.

The interpolated points in Table 8 were located in the compressed liquid and superheat regions of the skeleton table. The fits with one restriction were simultaneous fits of specific volumes and enthalpies restricted by Equation 24. Since the properties varied rather slowly in the regions, the standard deviations from the input data were small. Keenan and Keyes' tables did not extend far enough for comparison of these interpolated values.

The two interpolated points in Table 9 were also obtained using skeleton table values as input data. The restriction was the same as in Table 8. As would be expected, the fits were poorer in

the critical region than in any other. The agreement with Keenan and Keyes' values was quite poor, also. To obtain accurate interpolations very near the critical point, it may be necessary to add additional data from other sources or smooth functions other than those used in this study.

In all probability, the functions which were used in the smoothing (PV/T and H/(T+a)-b) were not the optimum ones. However, the best fits of the skeleton table data were probably satisfactory in each region except near the critical point. In fact, good values for derivative properties in addition to the heat capacity were obtained but not reported in most cases. There is room for improvement in the form of the functions which are smoothed, in the details of how many temperature and pressure polynomials are used, and when to apply restrictions in each region of the table.

CONCLUSIONS AND RECOMMENDATIONS

1. Smoothing of thermodynamic data when the smoothed and interpolated values must obey certain restrictions can be accomplished accurately and efficiently by using least squares fits of orthogonal polynomials. Specifically, enthalpy and volumetric data from the skeleton table of the Sixth International Conference on the Properties of Steam may be smoothed in this way.

2. The function to be smoothed and the numbers of temperature and pressure polynomials to be used must be optimized in any specific case of smoothing or curve fitting.

NOMENCLATURE

A	A constant determined by a least squares fit of data
a	An arbitrary constant
B	A constant determined by a least squares fit of data
b	An arbitrary constant
E	A matrix defined by Equation 43
F	A normalizing vector defined by Equation 12
f	A matrix defined by Equation 32
g	A matrix defined by Equation 35
H	Enthalpy, Btu/lb
h	A matrix defined by Equation 36
I	The limit of a sum on i
J	The limit of a sum on j
K	The limit of a sum on k
L	The limit of a sum on ℓ
M	The limit of a sum on m
N	The limit of a sum on n
P	Pressure, psi
$P_i(x)$	The i^{th} orthogonal polynomial P evaluated at x
p	A matrix defined by Equation 34
Q	A set of polynomials
q	A matrix defined by Equation 33
R	The gas constant: R_1, restricting Equation 30; R_2, restricting Equation 31
S	The sum to be minimized by a least squares fit of data
T	Temperature, degrees R; a set of polynomials

U	A set of polynomials
V	Volume, ft^3/lb
x	An arbitrary independent variable or data point
y	An arbitrary dependent variable or data point
z	An arbitrary independent variable or data point
α	Recursion vector defined by Equations 4 and 6; residual variable defined by Equation 25
β	Recursion vector defined by Equations 4 and 6
γ	Residual variable defined by Equation 28
δ_{ij}	The Kronecker delta
λ	Lagrange multiplier

Superscripts

o	Indicates an orthonormal polynomial
'	Indicates a derivative with respect to the independent variable

Subscripts

i, j k, ℓ m, n	Indicate elements of a series
r	Indicates a particular value of an independent variable at which interpolation is desired

REFERENCES

1. Bright, J. W. and Dawkins, G. S., Ind. Eng. Chem. Fund. 4, 93 (1965).

2. Deming, W. E. and Shupe, L. E., Phys. Rev. 37, 638 (1931).

3. Forsythe, G. E., J. Soc. Indust. Appl. Math. 5, 74 (1957).

4. Haywood, R. W., Proceedings of the Sixth International Conference on the Properties of Steam, The Secretariat of the International Conference on the Properties of Steam, New York (October 1963).

5. Keenan, J. H. and Keyes, F. G., Thermodynamic Properties of Steam, John Wiley and Sons, New York (1936).

6. Pings, C. J., Jr. and Sage, B. H., Ind. Eng. Chem. 49, 1315 (1957).

LIST OF TABLES

TABLE 1. Thermodynamic Properties of Steam from the Sixth International Conference on the Properties of Steam, Gas Phase

Temperature deg. F	Pressure psi	Volume ft^3/lb
482	14.5038	38.5404
482	72.5190	7.59916
482	145.038	3.72750
482	362.595	1.39361
572	14.5038	42.2727
572	72.5190	8.36965
572	145.038	4.13116
572	362.595	1.58423
572	725.190	0.726277
572	1087.785	0.427853
662	14.5038	45.9890
662	72.519	9.13213
662	145.038	4.52361
662	362.595	1.75723
662	725.190	0.831839
662	1087.785	0.519639
662	1450.38	0.359454
662	1812.975	0.258538
662	2175.57	0.184052

TABLE 2. Thermodynamic Properties of Steam from the Sixth International Conference on the Properties of Steam, Liquid Phase

Temperature deg. F	Pressure psi	Volume ft^3/lb	Enthalpy Btu/lb
32	8702.28	0.0148539	25.2794
32	9427.47	0.0155427	27.3001
32	10152.7	0.0155091	29.2777
32	10877.8	0.0154770	31.2554
32	11603.0	0.0154450	33.2330
122	8702.28	0.0158150	111.952
122	9427.47	0.0157846	113.758
122	10152.7	0.0157558	115.563
122	10877.8	0.0157269	117.369
122	11603.0	0.0156981	119.132
212	8702.28	0.0162700	199.742
212	9427.47	0.0162379	201.376
212	10152.7	0.0162043	202.966
212	10877.8	0.0161722	204.643
212	11603.0	0.0161402	206.277
302	8702.28	0.0169091	288.048
302	9428.47	0.0168674	289.768
302	10152.7	0.0168274	291.187
302	10877.8	0.0167873	292.648
302	11603.0	0.0167489	294.069
392	8702.28	0.0177404	378.805
392	9427.47	0.0176844	379.966
392	10152.7	0.0176299	381.169
392	10877.8	0.0175771	382.330
392	11603.0	0.0175258	383.577

TABLE 3. Thermodynamic Properties of Steam from the Sixth International Conference on the Properties of Steam, Critical Region

Temperature deg. F	Pressure psi	Volume ft^3/lb	Enthalpy Btu/lb
707	2900.76	0.123022	1119.95
707	3263.35	0.0398860	851.247
707	3625.95	0.0317166	795.357
707	3988.54	0.0298744	779.880
707	4351.14	0.0287852	769.991
752	2900.76	0.159384	1211.95
752	3263.35	0.125905	1167.24
752	3625.95	0.0961108	1109.20
752	3988.54	0.0671174	1024.51
752	4351.14	0.0451721	927.343
797	2900.76	0.183732	1270.42
797	3263.35	0.152336	1240.33
797	3625.95	0.126386	1206.79
797	3988.54	0.104120	1168.53
797	4351.14	0.0848658	1123.82
842	2900.76	0.203595	1316.42
842	3263.35	0.172359	1293.64
842	3625.95	0.146889	1269.13
842	3988.54	0.125745	1242.48
842	4351.14	0.107900	1213.24

TABLE 4. Thermodynamic Properties of Steam from the Sixth International Conference on the Properties of Steam, Superheat Region

Temperature deg. F	Pressure psi	Volume ft^3/lb	Enthalpy Btu/lb
932	5076.33	0.110976	1288.91
932	5801.52	0.0900238	1429.36
932	6526.71	0.0741334	1209.37
932	7251.90	0.0622157	1170.68
932	7977.09	0.0535337	1135.43
1022	5076.33	0.133594	1382.63
1022	5801.52	0.111809	1355.55
1022	6526.71	0.0950536	1327.60
1022	7251.90	0.0819184	1299.66
1022	7977.09	0.0715064	1272.57
1112	5076.33	0.152432	1460.02
1112	5801.52	0.129525	1438.95
1112	6526.71	0.111841	1417.88
1112	7251.90	0.0978408	1396.82
1112	7977.09	0.0865638	1375.75
1202	5076.33	0.169155	1529.23
1202	5801.52	0.144983	1512.47
1202	6526.71	0.125825	1495.27
1202	7251.90	0.111489	1478.50
1202	7977.09	0.0994586	1461.74
1292	5076.33	0.184533	1594.15
1292	5801.52	0.159063	1580.40
1292	6526.71	0.139361	1566.21
1292	7251.90	0.123663	1552.45
1292	7977.09	0.111008	1538.69

TABLE 5. Thermodynamic Properties of Steam from the Tables of Keenan and Keyes, Gas Phase

Temperature deg. F	Pressure psi	Volume ft^3/lb	Enthalpy Btu/lb
260	8	53.28	1175.7
260	9	47.32	1175.4
260	10	42.56	1175.1
260	11	38.66	1174.9
260	12	35.41	1174.6
260	13	32.66	1174.3
280	8	54.80	1185.0
280	9	48.67	1184.8
280	10	43.76	1184.5
280	11	39.77	1184.3
280	12	36.43	1184.0
280	13	33.61	1183.8
300	8	56.31	1194.3
300	9	50.03	1194.1
300	10	45.00	1193.9
300	11	40.88	1193.6
300	12	37.45	1193.4
300	13	34.55	1193.2
320	8	57.82	1203.6
320	9	51.37	1203.4
320	10	46.21	1203.2
320	11	41.99	1203.0
320	12	38.47	1202.8
320	13	35.49	1202.6
340	8	59.33	1212.9
340	9	52.71	1212.7
340	10	47.42	1212.5
340	11	43.09	1212.4
340	12	39.48	1212.2
340	13	46.43	1212.0
360	8	60.84	1222.2
360	9	54.06	1222.0
360	10	48.63	1221.9
360	11	44.19	1221.7
360	12	40.49	1221.6
360	13	37.36	1221.4

TABLE 6. Fit of Keenan and Keyes' Smooth Values in the Gas Phase

Smoothed point at 320°F and 11 psi

Keenan and Keyes: $V = 41.99\ ft^3/lb$
$H = 1203.0\ Btu/lb$
$C_p = 0.47\ Btu/lb\ deg.\ F$

Number of Restrictions	Smoothed Values			Standard Deviation of Fit	
	V	H	C_p	V	H
0	41.99	-		0.00459	-
1	41.99	-		0.00483	-
2	41.99	1203.	0.467	0.0141	0.0427

Interpolated point at 310°F and 10.5 psi

Number of Restrictions	Smoothed Values			Standard Deviation of Fit	
	V	H	C_p	V	H
0	43.42	-		0.00459	-
1	43.42	-		0.00484	-
2	43.42	1198.	0.467	0.0157	0.0385

These predictions were made using the data in Table 5. Four temperature polynomials and four pressure polynomials were used for the volume fits; three temperature polynomials and three pressure polynomials were used for the enthalpy fits.

TABLE 7. Fit of Data of the Sixth International Conference on the Properties of Steam in the Gas Phase

Interpolated point at 600°F and 150 psi

(Keenan and Keyes: $V = 4.113\ ft^3/lb$)

Number of Restrictions	Smoothed Values V	Standard Deviation of Fit V
0	4.101	0.0267
1	4.100	0.0141

Interpolated point at 600°F and 1000 psi

(Keenan and Keyes: $V = 0.5140\ ft^3/lb$)

Number of Restrictions	Smoothed Values V	Standard Deviation of Fit V
0	0.5104	0.0267
1	0.5103	0.0141

These predictions were made using the data in Table 1. Two temperature polynomials and four pressure polynomials were used.

TABLE 8. Fit of Data of the Sixth International Conference on the Properties of Steam in the Liquid Phase and Superheat Region

Interpolated point at 200°F and 10,000 psi

(Keenan and Keyes extrapolated C_p = 0.97 Btu/lb deg. F)

Number of Restrictions	Smoothed Values V	H	C_p	Standard Deviation of Fit V	H
0	0.01612	-		4.26×10^{-5}	-
1	0.01599	190.8	0.974	7.68×10^{-4}	0.164

These predictions were made using the data in Table 2. Four temperature polynomials and four pressure polynomials were used for both the volume and enthalpy fits.

Interpolated point at 1100°F and 6500 psi

Number of Restrictions	Smoothed Values V	H	C_p	Standard Deviation of Fit V	H
0	0.1104	-		1.38×10^{-4}	-
1	0.1111	1409.	0.952	4.20×10^{-3}	1.40

These predictions were made using the data in Table 4. Four temperature polynomials and four pressure polynomials were used for both the volume and enthalpy fits.

TABLE 9. Fit of Data of the Sixth International Conference on the Properties of Steam near the Critical Point

Interpolated point at 750°F and 3400 psi

Keenan and Keyes: $V = 0.1129\ ft^3/lb$
$H = 1143.6$ Btu/lb
$C_p = 3.5$ Btu/lb deg. F

Number of Restrictions	Smoothed Values			Standard Deviation of Fit	
	V	H	C_p	V	H
0	0.1044	-		6.41×10^{-3}	-
1	0.0893	1103.6	4.98	3.3×10^{-2}	28.1

Interpolated point at 825°F and 3400 psi

Estimated from Keenan and Keyes: $V = 0.1550\ ft^3/lb$
$H = 1266.6$ Btu/lb

Number of Restrictions	Smoothed Values			Standard Deviation of Fit	
	V	H	C_p	V	H
0	0.1599	-		6.41×10^{-3}	-
1	0.1604	1285.4	-0.14	6.89×10^{-3}	28.1

These predictions were made using data in Table 3. Four temperature polynomials and three pressure polynomials were used for both the volume and enthalpy fits.

II. DIFFUSION COEFFICIENTS IN BINARY HYDROCARBON LIQUIDS*

* This section is to be presented as a paper by D. J. Graue and B. H. Sage at the meeting of the American Petroleum Institute in Montreal, Canada, May 10, 1965.

A number of measurements of molecular transport in the liquid phase were made by Lacey and co-workers some thirty years ago (3, 4, 9). More recently, additional measurements involving binary hydrocarbon liquids have been carried out and the results are available in a recent monograph (12). These later investigations indicated a substantial influence of temperature and composition upon the molecular, material transport characteristics in a binary hydrocarbon liquid phase. All of the measurements referred to above have been carried out in heterogeneous systems where the surface of the liquid phase is at bubble point. The effect of pressure upon the self-diffusion characteristics of light paraffin hydrocarbons was found by McCall, Douglass, and Anderson(7, 8) to be a change of about five per cent per thousand pounds per square inch change in pressure. The influence of the composition of the phase upon the material transport characteristics is evident, as is the large effect of the nature of the hydrocarbon components involved. Any analytical representation of these characteristics should take into account the effects of temperature, concentration, and the nature of the components and, therefore, is necessarily somewhat complicated.

It is the purpose of this discussion to present the advantages and limitations of several methods of describing the available experimental data on diffusion for binary paraffin hydrocarbon systems at temperatures between 40° and 400° F. and throughout a rather wide range of concentration of the components. The results are presented in analytical form with statistical measures of the agreement of the

predictions with experimental values.

Diffusion Coefficients

Fick (2) was perhaps the first to relate the molecular transport of a component to a potential gradient and a coefficient. The so-called Fick coefficient is related to the component flux in the following way:

$$\mathring{m}_k = \sigma_k u - D_{Fk} \frac{\partial \sigma_k}{\partial x} \quad . \tag{1}$$

The Chapman-Cowling coefficient (1) is numerically equal for the two components and is related to the material flux as follows:

$$\mathring{m}_k = \sigma_k u - D_{Ckj}\, \sigma \frac{\partial n_k}{\partial x} \quad . \tag{2}$$

It may be shown (6) that the Fick diffusion coefficient for each of the components may be evaluated from the Chapman-Cowling coefficient by:

$$D_{Fk} = D_{Ckj} (V / \overline{V}_j) \quad . \tag{3}$$

Recently the several relationships among the molecular transport coefficients and fluxes have been reviewed (6). For this reason no extended discussion of the application of the diffusion coefficients will be given. All of the results are presented here in terms of the Chapman-Cowling coefficient since it is symmetrical with respect to both components and does not involve a singularity at states where the partial volume of the component passes through zero, as is the case for the Fick coefficient. Such behavior for the latter component is apparent from consideration of Equation 3.

Sources of Data

Measurements of the molecular transport at bubble point have

been made for a variety of binary systems (12). The range of concentrations, weight fractions, and temperatures for which experimental information has been obtained is indicated in Table 1. These data have been smoothed with respect to the state of the system by graphical means (12) and the standard error of estimate of the experimental data, together with the number of experimental points obtained, have been included in Table 1. The standard error of estimate affords a semiquantitative clue to the reproducibility of the measurements. In some instances the reproducibility is rather poor and contributes a significant basic uncertainty to the analytical descriptions of the results.

Analytical Descriptions

Two classes of analytical expressions were investigated: empirical and quasi-theoretical. Of the many empirical forms which were studied, the following gave the best agreement with the experimental data for the nine binary systems described in Table 1:

$$D_{Ckj} = A + B(T-D) + Cn_k(T-D) \quad . \qquad (4)$$

The expression is linear in temperature and fortunately, in addition, the constant D was found by least squares analysis to be remarkably close to 460 for nearly all of the systems investigated. For simplicity in calculation and ease of visualizing the contributions of the individual terms, the following form of Equation 4 was chosen:

$$D_{Ckj} = A + (B + Cn_k)(T - 459.69) \quad . \qquad (5)$$

It is apparent that the temperature expressed in° F may be substituted for the last term, as is indicated in Equation 6:

$$D_{Ckj} = A + (B + Cn_k)t \quad . \tag{6}$$

The most useful quasi-theoretical expression which was studied is as follows:

$$D_{Ckj} = \exp\left[A + \frac{B + Cn_k}{T}\right] \quad . \tag{7}$$

Equation 7 is based upon a quasi-theoretical expression developed by Eyring (10). His basic relationship was of the form:

$$D = \alpha \exp\left[-\frac{\epsilon}{RT}\right] \quad . \tag{8}$$

From Equation 8 it is apparent that the coefficients and exponents are related to the constants of Equation 7 in the following way:

$$\alpha = \exp[A] \quad , \tag{9}$$

$$-\frac{\epsilon}{R} = B + Cn_k \quad . \tag{10}$$

The Eyring expression has been used to describe the Chapman-Cowling diffusion coefficient by a number of investigators to extend or to interpolate available experimental measurements. It is the only one of the foregoing expressions that has any theoretical background. For example, Equations 4, 5, and 6 are entirely empirical in nature. There are a number of other quasi-theoretical expressions which purport to describe the effect of temperature and composition upon the Chapman-Cowling diffusion coefficient. However, these are for the most part more complicated than Equation 7 and require a larger number of coefficients than the three associated with the latter equation.

In Table 2 are shown the results obtained for six hydrocarbon systems containing methane and three such systems involving ethane. Each binary system was considered individually in the representation

of Table 2 for each of two types of expressions. The first is Equation 6, which is linear in temperature and composition; the second is Equation 7, and involves an exponential term. The standard and the average deviations for each of the two expressions have been indicated for each binary system along with the values of the coefficients. It should be noted that the significance of the two measures of uncertainty loses some statistical meaning in several instances because of the paucity of experimental data. In some instances, such as for the ethane-n-pentane system, there were insufficient data to make the evaluation of the three coefficients significant. It should be noted further that there is a limiting absolute uncertainty in the experimental measurements amounting to approximately 0.2×10^{-8} square foot per second, which accounts for the much larger fractional deviation in the case of measurements where the absolute value of the diffusion coefficient is small. There is shown in Figure 1 the agreement of the ethane-n-decane system with Equations 6 and 7. The agreements shown in Table 2 and illustrated for the ethane-n-decane system in Figure 1 are based upon the application of least squares techniques to the data available.

In Figure 2 is depicted the effect of the molecular weight of the less volatile component upon the Chapman-Cowling diffusion coefficient for several different weight fractions of methane and of ethane at a temperature of 160° F. It is apparent that the molecular weight of the less volatile component exerts a pronounced influence on the Chapman-Cowling diffusion coefficient which, in some cases, overshadows the effect of temperature and composition.

Equation 6 was modified to apply to all of the systems containing methane or ethane in the following forms:

$$D_{Ckj} = A + (B + Cn_k)t + \frac{(D + En_k t)}{M_j} \tag{11}$$

$$D_{Ckj} = A + \left[B + \frac{(C + Dn_k)}{M_j}\right]t \tag{12}$$

$$D_{Ckj} = A + \left[B + \frac{(C + Dn_k)}{M_j^2}\right]t \tag{13}$$

In each case, the molecular weight of the less volatile component was used as the additional variable. In a similar fashion, Equation 7 was modified in the two following forms:

$$D_{Ckj} = \exp\left[A + \frac{(B + CM_j^{0.25} + Dn_k)}{T}\right] \tag{14}$$

$$D_{Ckj} = \exp\left[A + \frac{(B + C/M_j + Dn_k)}{T}\right] \tag{15}$$

The agreement of the predictions of Equations 12 and 15 with the data for the ethane-n-decane system is shown in Figure 3. The application of Equations 11, 12, 14, and 15 to the six binary systems containing methane and of Equations 12, 13, 14, and 15 to the three systems containing ethane is shown in Table 3. In the application of these expressions, the uncertainty at the 95 per cent conficence level (5) exceeds the value of the coefficients in some cases. It is apparent that for both the methane and ethane systems a somewhat smaller deviation was obtained with the Eyring (10) type of expression shown in Equations 14 and 15 than with linear expressions such as Equation 12.

It should be recognized that in using the molecular weight of

the less volatile component as an independent variable, discreet values of this molecular weight corresponding to the values for the pure components were employed in all cases except the "white oil." If attempts are made to employ the average molecular weight of several components to describe the molecular transport behavior of a multicomponent system, an unknown uncertainty will be introduced.

It is probable that, when the range of molecular weights in the heavier components is not large, a reasonable approximation may be obtained by treating the system as binary. Such an approximation was done with the white oil (11, 13). The variation in the characteristics of the components of the white oil were not large when compared with the molecular weight of methane and ethane. However, the symmetry of application of the Chapman-Cowling diffusion coefficients is lost except as a gross approximation for the heavier components when a multicomponent system is treated as a restricted binary (14).

As a matter of convenience, there are tabulated in Table 4 values of the Chapman-Cowling diffusion coefficient (12) for the binary systems listed in Table 1. The values of the coefficients have been recorded as a function of temperature and weight fraction of the more volatile component and were tabulated to at least one more significant figure than is justified by the accuracy of the results. This action has been taken to ensure ease of utilization of the values in graphical or numerical operations.

ACKNOWLEDGMENT

The assistance of Virginia Berry in connection with the assembly of the information reported here is acknowledged. B. Lawson Miller contributed to the preparation of the manuscript. The experimental work referred to was carried out as a part of the activities of Project 37 of the American Petroleum Institute. However, the work reported here was not obtained as a part of the activities of that project.

NOMENCLATURE

A, B, C, D, E	Coefficients used in equations
D_{Ckj}	Chapman-Cowling diffusion coefficient for components k and j , sq. ft. per sec.
D_{Fk}	Fick diffusion coefficient for component k , sq. ft. per sec.
D	Diffusion coefficient in Equation 8, sq. ft. per sec.
M	Molecular weight, lb. per lb-mole
$\mathring{m}_k$	Material flux of component k , lb. per (sec)(sq. ft.)
N_C	Number of equation constants
N_P	Number of experimental data points
n_k	Weight fraction of component k
R	Universal gas constant, Btu per (lb-mole)($^\circ$ R)
s	Average deviation, defined in Table 1
s'	Average deviation, defined in Table 2
T	Thermodynamic temperature, $^\circ$R
t	Temperature, $^\circ$F
u	Local or momentum velocity, ft. per sec.
V	Specific volume, cu. ft. per lb.
$\overline{V}$	Partial specific volume, cu. ft. per lb.
x	Coordinate, ft.
α	Coefficient defined by Equation 8, sq. ft. per sec.
ϵ	Eyring activation energy defined by Equation 8, Btu per lb-mole
σ	Specific weight, lb. per cu. ft. ; standard error of estimate, defined in Table 1
σ_k	Concentration of component k , lb. per cu. ft.

σ'	Standard deviation, defined in Table 2
exp	Exponential
∂	Partial differential operator
Σ	Summation operator

Subscripts

j	Component j , the less volatile or stagnant component
k	Component k , the more volatile or diffusing component
av	Average
sm	Smoothed
cal	Calculated
ex	Experimental

REFERENCES

1. Chapman, Sidney, and Cowling, T. G., The Mathematical Theory of Non-Uniform Gases, 2nd. ed., University Press, Cambridge, England (1952).

2. Fick, Adolph, "On Diffusion," Ann. Phys. Chem. 94, 59 (1855).

3. Hill, E. S., and Lacey, W. N., "Rate of Solution of Methane in Quiescent Liquid Hydrocarbons, II," Ind. Eng. Chem. 26, 1324 (1934).

4. Hill, E. S., and Lacey, W. N., "Rate of Solution of Propane in Quiescent Liquid Hydrocarbons," Ind. Eng. Chem. 26, 1327 (1934).

5. Kempthorne, Oscar, The Design and Analysis of Experiments, John Wiley and Sons, New York (1952).

6. Longwell, P. A., and Sage, B. H., "Some Molecular Transport Characteristics in Binary Homogeneous Systems," A.I. Ch. E. J. 11, 46 (1965).

7. McCall, D. W., Douglass, D. C., and Anderson, E. W., "Diffusion in Liquids," J. Chem. Phys. 31, 1555 (1959).

8. McCall, D. W., Douglass, D. C., and Anderson, E. W., "Self-Diffusion in Liquids: Paraffin Hydrocarbons," Phys. Fluids 2, 87 (1959).

9. Pomeroy, R. D., Lacey, W. N., Scudder, N. F., and Stapp, F. P., "Rate of Solution of Methane in Quiescent Liquid Hydrocarbons," Ind. Eng. Chem. 25, 1014 (1933).

10. Powell, R. E., Roseveare, W. E., and Eyring, Henry, "Diffusion, Thermal Conductivity and Viscous Flow of Liquids," Ind. Eng. Chem. 33, 430 (1941).

11. Reamer, H. H., Duffy, C. H., and Sage, B. H., "Diffusion Coefficients in Hydrocarbon Systems: Methane-White Oil-Methane in Liquid Phase," Ind. Eng. Chem. 48, 285 (1956).

12. Sage, Bruce H., Some Material Transport Properties of the Lighter Hydrocarbons in the Liquid Phase, American Petroleum Institute, New York (1964).

13. Sage, B. H., Backus, H. S., and Lacey, W. N., "Phase Equilibria in Hydrocarbon Systems: Methane-Crystal Oil System," Ind. Eng. Chem. 27, 686 (1935).

14. Sage, B. H., and Lacey, W. N., Volumetric and Phase Behavior of Hydrocarbons, Gulf Publishing Company, Houston, Texas (1949).

LIST OF FIGURES

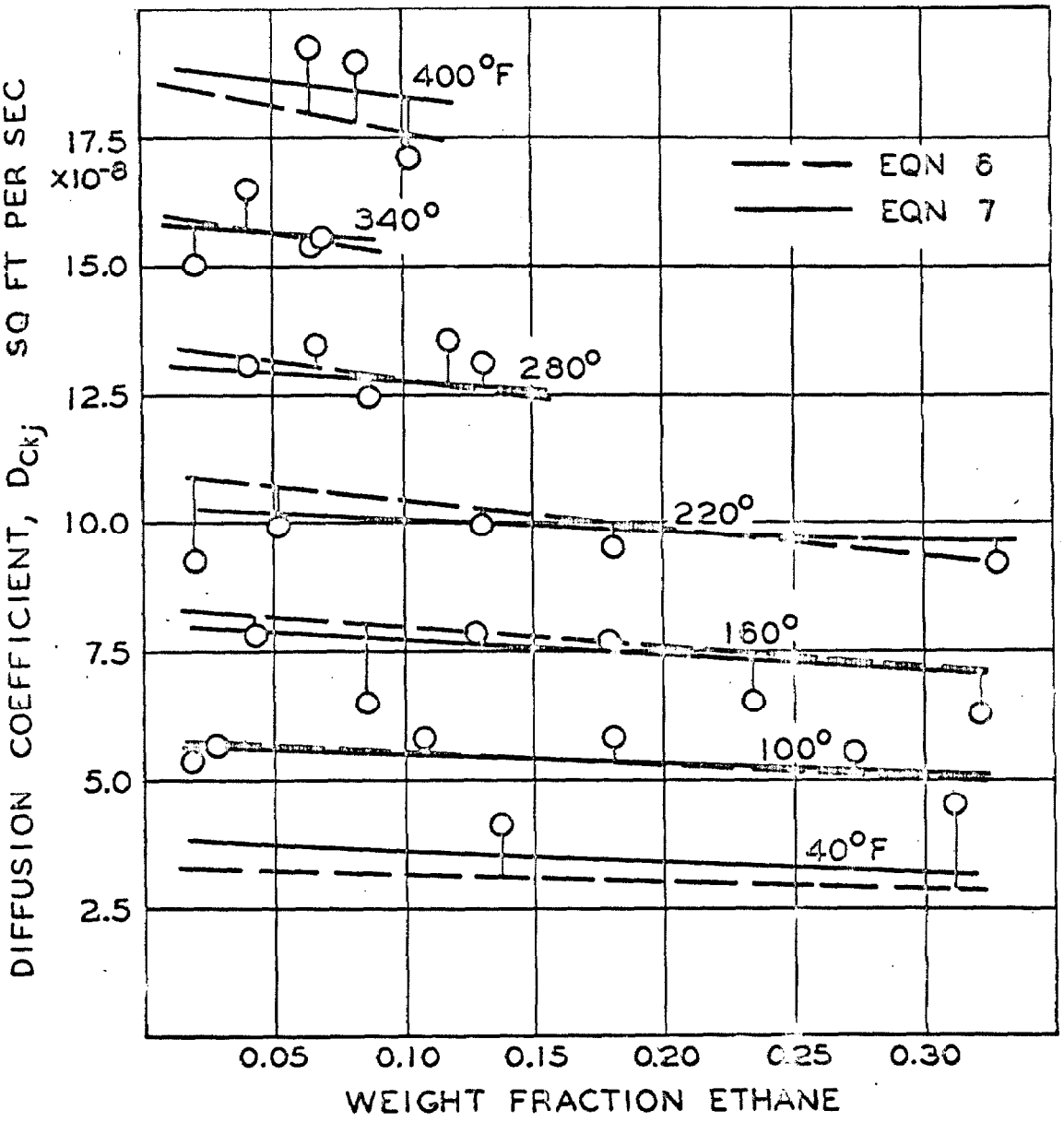

Fig. 1. Comparison of Calculated and Experimental Diffusion Coefficients in the Ethane-n-Decane System

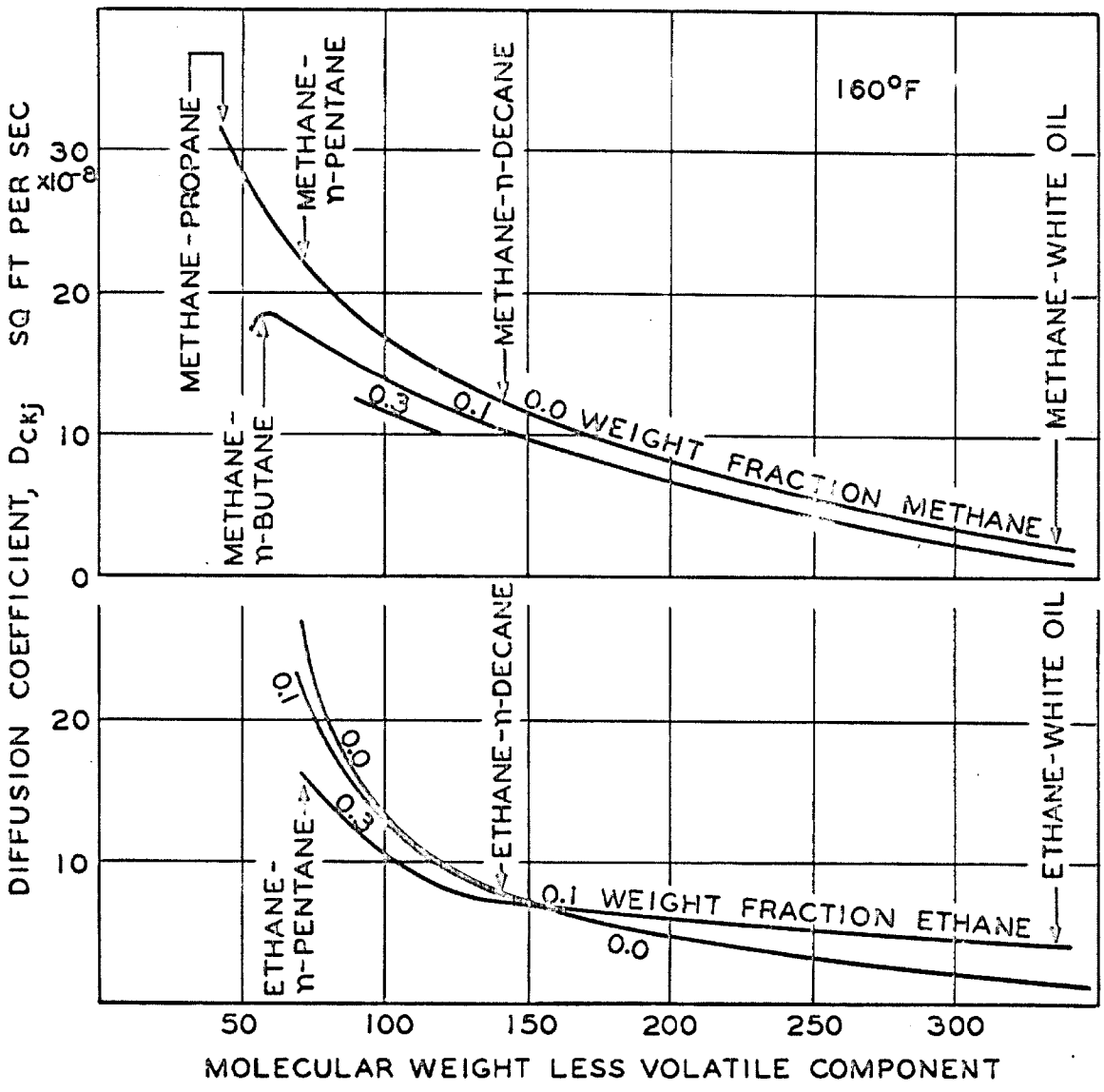

Fig. 2. Influence of Molecular Weight of the Less Volatile Component upon Diffusion Coefficients at 160° F.

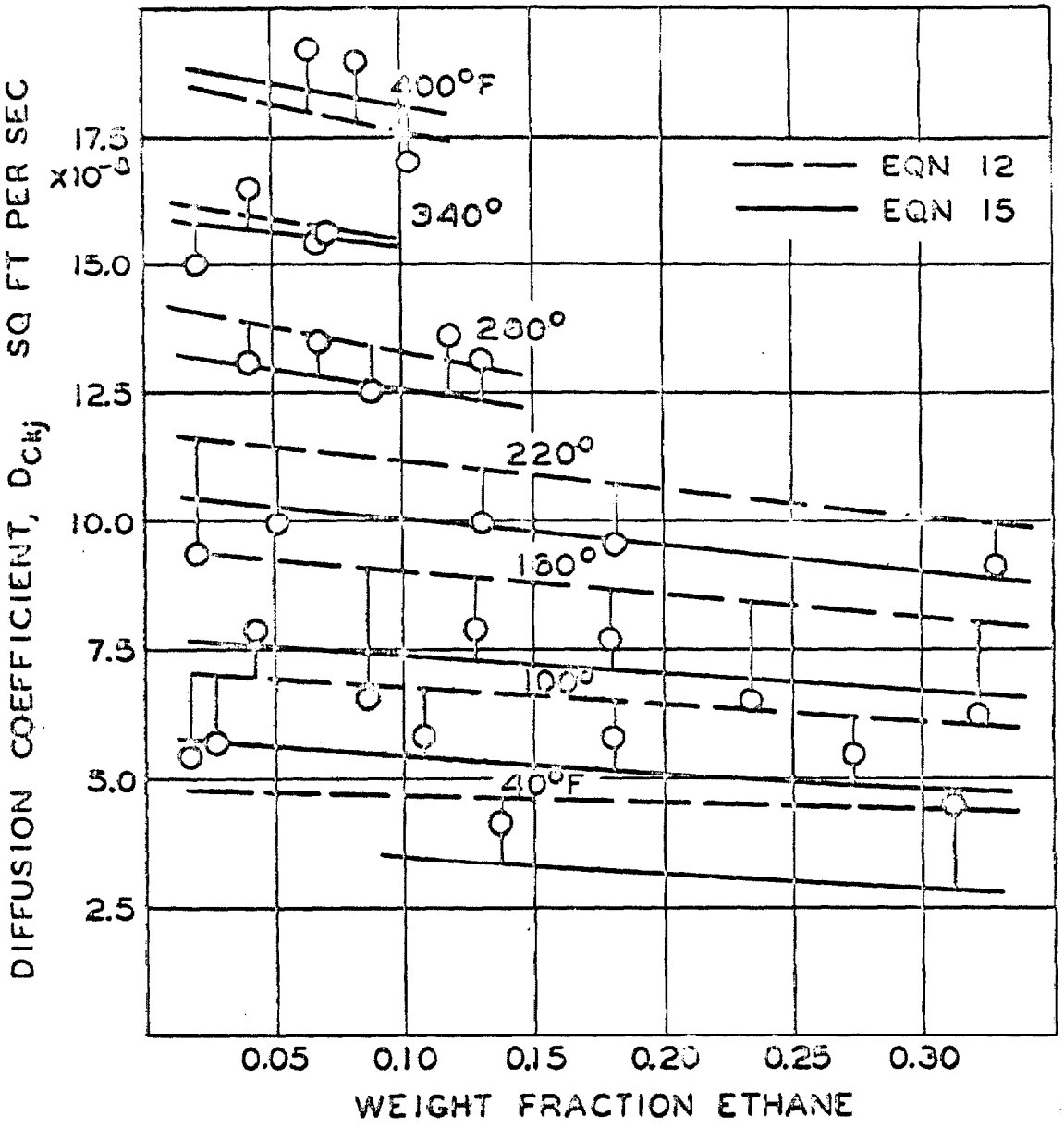

Fig. 3. Comparison of Calculated and Experimental Diffusion Coefficients in the Ethane-n-Decane System

LIST OF TABLES

TABLE 1. Range of Experimental Conditions.

System	Number of Points	Range of Data: Temp. °F	Range of Data: Weight Fraction Component k	Range of Data: Concentration Component k	Graphical*: Standard Error of Estimate**	Graphical*: Average Deviation Fraction†
Methane-Propane	14	40-130	0.03-0.14	0.8-3.7	0.8×10^{-8}	0.050
Methane-n-Butane	18	10-220	0.03-0.18	0.9-5.4	0.6×10^{-8}	0.036
Methane-n-Pentane	14	40-280	0.02-0.18	0.8-5.3	1.3×10^{-8}	0.071
Methane-n-Heptane	13	40-220	0.03-0.14	0.8-5.2	1.5×10^{-8}	0.098
Methane-n-Decane	17	40-280	0.01-0.18	0.4-6.5	0.6×10^{-8}	0.054
Methane-White Oil	16	40-340	0.01-0.06	0.4-2.9	0.3×10^{-8}	0.091
Ethane-n-Pentane	8	40-280	0.03-0.36	1.2-11.6	2.1×10^{-8}	0.114
Ethane-n-Decane	30	40-400	0.02-0.33	0.7-11.1	0.6×10^{-8}	0.060
Ethane-White Oil	11	100-400	0.02-0.18	0.8-8.5	0.2×10^{-8}	0.065

* Graphically smoothed experimental data (12).

** Standard error of estimate expressed in sq. ft./sec. and defined by:

$$\sigma = \left[\frac{\sum_{1}^{N_p} \left[(D_{Ckj})_{ex} - (D_{Ckj})_{sm} \right]^2}{N_p} \right]^{\frac{1}{2}} .$$

† Average deviation defined by: $s = \sigma / [(D_{Ckj})_{ex\ av}]$.

TABLE 2. Coefficients for Diffusion Correlations for Individual Binary Systems

System	Coefficient A $\times 10^8$	Coefficient B $\times 10^8$	Coefficient C $\times 10^8$	Deviation Standard* $\times 10^8$	Deviation Average†
Equation 6					
Methane-Propane	20.7	0.0531	-1.14	0.995	0.0422
Methane-n-Butane	12.1	0.0890	-0.411	1.03	0.0490
Methane-n-Pentane	7.45	0.0854	-0.291	1.76	0.0652
Methane-n-Heptane	5.99	0.0697	-0.157	1.70	0.0954
Methane-n-Decane	1.07	0.0688	-0.115	0.878	0.0740
Methane-White Oil	-1.22	0.0306	-0.219	0.674	0.267
Ethane-n-Pentane	7.90	0.0873	-0.131	2.36	0.118
Ethane-n-Decane	1.45	0.0429	-0.025	0.806	0.0747
Ethane-White Oil	-3.24	0.0225	0.321	1.56	0.268
Equation 7**	A	B	C		
Methane-Propane	-16.4	664	-2800	2.18	0.110
Methane-n-Butane	-13.7	-916	-1500	1.57	0.0717
Methane-n-Pentane	-13.1	-1450	-1130	2.15	0.0908
Methane-n-Heptane	-13.1	-1500	-1010	1.55	0.0912
Methane-n-Decane	-12.5	-2150	-1120	0.944	0.0689
Methane-White Oil	-12.0	-3270	-6390	0.512	0.130
Ethane-n-Pentane	-13.2	-1330	-523	2.31	0.117
Ethane-n-Decane	-13.3	-1910	-190	0.675	0.0624
Ethane-White Oil	-11.9	-3610	5300	2.04	0.295

* Standard deviation expressed in sq. ft./sec. and defined by:

$$\sigma = \left[\frac{\sum_{1}^{N_p} \left[(D_{Ckj})_{ex} - (D_{Ckj})_{cal} \right]^2}{N_p - N_C} \right]^{\frac{1}{2}}.$$

† Average deviation without regard to sign was expressed as a fraction and defined by:

$$s' = \frac{\sum_{1}^{N_p} \left| \frac{(D_{Ckj})_{ex} - (D_{Ckj})_{cal}}{(D_{Ckj})_{ex}} \right|}{N_p}$$

** Coefficients for Equation 7 are not $\times 10^8$.

TABLE 3. Coefficients for Diffusion Correlations for Binary Systems Containing Methane or Ethane

Equation No.	Number of Points	Coefficient A	B	C	D	E	Deviation Standard*	Deviation Average†
Methane-Hydrocarbon Systems**								
11	92	-6.83×10^{-8}	0.0500×10^{-8}	0.245×10^{-8}	1130×10^{-8}	26.4×10^{-8}	3.56×10^{-8}	0.392
12	92	6.71×10^{-8}	-0.0228×10^{-8}	8.35×10^{-8}	-22.2×10^{-8}		3.50×10^{-8}	0.707
14	92	-13.4	561	-600	-1320		2.20×10^{-8}	0.253
15	92	-13.6	-1580	30000	-1130		3.01×10^{-8}	0.385
Ethane-Hydrocarbon Systems**								
13	49	2.83×10^{-8}	0.00883×10^{-8}	581×10^{-8}	-685×10^{-8}		2.03×10^{-8}	0.231
12	49	3.13×10^{-8}	-0.0162×10^{-8}	7.85×10^{-8}	-3.90×10^{-8}		2.16×10^{-8}	0.217
14	49	-13.5	1180	-8.17	-337		1.85×10^{-8}	0.156
15	49	-13.3	-2490	85100	-369		1.45×10^{-8}	0.160

* Standard deviation expressed in sq. ft. /sec. and defined by:

$$\sigma' = \left[\frac{\sum_{1}^{N_p} \left[(D_{Ckj})_{ex} - (D_{Ckj})_{cal} \right]^2}{N_p - N_C} \right]^{\frac{1}{2}}$$

** Hydrocarbon systems as given in Table 1.

† Average deviation without regard to sign was expressed as a fraction and defined by:

$$s' = \frac{\sum_{1}^{N_p} \left| \frac{(D_{Ckj})_{ex} - (D_{Ckj})_{cal}}{(D_{Ckj})_{ex}} \right|}{N_p}$$

TABLE 4. Diffusion Coefficients at 160° F for Several Binary Hydrocarbon Systems

Weight Fraction Component k*	Diffusion Coefficient, (sq. ft. /sec.) × 10^8 (Chapman-Cowling)					
	Graphical	Equation 12	Equation 15	Graphical	Equation 12	Equation 15
	Methane-n-Butane			Ethane-n-Pentane		
0.020	23.6	24.83	21.49	23.5	17.77	19.97
0.040	22.6	23.60	20.72	22.8	17.60	19.73
0.060	21.4	22.38	19.98	22.2	17.43	19.50
0.080	20.4	21.16	19.26	21.6	17.25	19.26
0.100	19.4	19.94	18.57	21.0	17.08	19.04
0.125	18.4	18.41	17.74	20.4	16.87	18.76
0.150	17.4	16.88	16.95	19.6	16.65	18.48
	Methane-n-Pentane			Ethane-n-Decane		
0.020	18.7	20.59	18.27	7.67	9.278	7.813
0.040	17.9	19.61	17.62	7.58	9.190	7.721
0.060	17.2	18.63	16.99	7.51	9.103	7.629
0.080	16.5	17.64	16.38	7.46	9.015	7.539
0.100	15.8	16.66	15.79	7.40	8.927	7.450
0.125	15.1	15.43	15.09	7.33	8.817	7.340
0.150	14.5	14.19	14.42	7.27	8.708	7.231
	Methane-n-Heptane			Ethane-White Oil		
0.020	15.8	15.69	15.15	1.75	4.228	4.473
0.040	15.2	14.98	14.60	2.32	4.191	4.420
0.060	14.8	14.27	14.08	2.93	4.154	4.368
0.080	14.3	13.56	13.58	3.66	4.117	4.316
0.100	13.9	12.85	13.09	4.41	4.080	4.265
0.125	13.4	11.96	12.51	5.36	4.034	4.202
0.150	13.0	11.08	11.95	6.32	3.987	4.140

* Weight fraction of diffusion of more volatile component, Methane or Ethane.

III. CORRELATION OF DIFFUSION COEFFICIENTS OF LIQUID HYDROCARBONS

INTRODUCTION

Attempts to correlate or predict liquid phase transport behavior date from the last century. Since that time the theoretical and commercial importance of this undertaking has been evidenced by the many diverse methods which have been used to describe transport properties. The purpose of this work was to investigate the use of some of these methods of prediction and correlation with recent data on binary hydrocarbon systems to give an accurate method of calculating diffusion coefficients for engineering use.

The next section will survey a spectrum of prediction and correlation techniques ranging from the simple, semi-empirical relation of Einstein to the very sophisticated and complicated work of Kirkwood. Since the efforts to describe transport properties of liquids often are closely tied to those aimed at describing equilibrium properties of liquids, the success of the latter is sometimes a necessary condition for the success of the former. It is notable that, although progress is being made at the present time in the theory of transport in liquids, the improvements to date in the description of diffusion properties of liquids have been indecisive. That is, although there are several expressions which have had some success in correlating diffusion coefficients for liquids, none has yet had such outstanding success as to be clearly indicated as having the correct approach. Of the many relations reported, a number of the more promising were tested in this study. The availability of time and auxiliary data limited the extent of the testing. The scope of this

work was confined also to binary mixtures of light, normal, paraffin hydrocarbons for two reasons: other authors have correlated data for widely differing systems; and the extensive data of Sage permitted the more detailed study of a particular homologous series of compounds.

Part II of this work presents results which were part of the following investigation; therefore, there is some duplication in the two parts. However, the results reported in the two sections are not duplicated.

In the Appendix are presented two examples of uses of a correlation of diffusion coefficients in solving problems involving diffusion.

METHODS OF PREDICTION AND CORRELATION OF LIQUID PHASE DIFFUSION COEFFICIENTS

General

The earliest relation which was used to correlate liquid diffusion coefficients was the Stokes-Einstein equation (23). The liquid model for which this equation was derived was that of a sphere of solute moving through a continuum of solvent. The drag on a molecule of solute was calculated from Equation 1.

$$D_k = kT/\xi \tag{1}$$

Einstein's substitution of the Stokes' Law drag for ξ in Equation 1 resulted in the Stokes-Einstein relation:

$$D_k = \frac{kT}{6\pi r_k \eta_j} . \tag{2}$$

Thus, the diffusion coefficient for the solute k was considered to be dependent on the viscosity of the pure solvent j .

Quite closely related to the Stokes-Einstein equation and the Exner rule (2), which is

$$D\eta M^{\frac{1}{2}} = C , \tag{3}$$

was an empirical relation developed by Wilke and Chang (71):

$$D_{vk} = \frac{C'(xM_j)^{\frac{1}{2}}T}{\eta V^{0.6}} . \tag{4}$$

Their relation gave the most accurate results of any equation developed for dilute binary liquid systems in general. In Equation 4, the variable x is the association factor which has a value of unity for nonassociated solvents. In this equation, the viscosity is that

of the solution, the molecular weight is that of the solvent, and the diffusion coefficient is the volumetric coefficient for the solute as defined by Longwell (36).

$$\dot{m}_k = \sigma_k u - D_{vk} \nabla \sigma_k \tag{5}$$

Thakar and Othmer (67) have reported a relation which is somewhat like that of Wilke and Chang. The relation used water as a reference substance and was more complicated and less accurate than that of Wilke and Chang. Sitaraman (64) also modified the Wilke-Chang equation so that latent heats of vaporization instead of the factor x accounted for association.

Sutherland (66) suggested another modification of the Stokes-Einstein relation which included a correction for "slip" at the particle - solvent interface:

$$D_k = \frac{kT}{6\pi\gamma_k\eta_j}\left[\frac{3\eta_j + \gamma_k\beta_{kj}}{2\eta_j + \gamma_k\beta_{kj}}\right]. \tag{6}$$

Li and Chang (34) used this new equation to predict self-diffusion coefficients for a number of substances. It is obvious that his modification is not a large one, because as β_{kj} varies from a value of zero to infinity, the bracketed factor only varies from 3/2 to one.

Hill (26) attempted with fair success to predict liquid diffusion coefficients from a model based on relaxation of a polar molecule in a non-polar solvent. Her equation resembled Equation 2

$$D_{Fk} = \frac{kT}{6}\left[\frac{\sigma_j \bar{V}_j}{n_k\eta_k\gamma_k + n_j\eta\gamma_{kj}} + \frac{\sigma_k \bar{V}_k}{n_k\eta\gamma_{kj} + n_j\eta_j\gamma_j}\right] \tag{7}$$

and involved only molecular and volumetric parameters besides the

viscosity and diffusion coefficient. Of the relations mentioned thus far, hers was the only one to take composition into account.

Arnold in an early work (2) combined the kinetic theory of gases, the Stokes-Einstein equation, and the Exner rule to give the relation

$$D_k = \frac{B\left(\frac{1}{M_k} + \frac{1}{M_j}\right)^{1/2}}{A_k A_j \eta_j^{1/2} \left(v_k^{1/3} + v_j^{1/3}\right)^2} \quad . \tag{8}$$

However, his equation lacks generality because of his inclusion of the abnormality factors A_k and A_j, which are not easily predictable.

An interestingly different approach to the problem of correlating diffusion coefficients was taken by Olson and Walton (43) who related diffusion coefficients of binary liquid systems to the lowering of their surface tensions upon mixing. They related the quantity $D\eta/T$ to $\Delta\gamma/\sigma$ to give quite good results in the limited systems for which they had data. Their model involved the balancing of surface tension with a concentration gradient at the liquid surface.

Corresponding States

Bird (8) has suggested a corresponding states approach for correlation of self-diffusion coefficients. Naghizadeh and Rice (41) and Gaven and co-workers (22) have tested the theory for a few simple substances. Their work indicated that only very nearly spherical molecules behave according to a corresponding states law.

Irreversible Thermodynamics

Bearman (3) and several others (4, 14, 24, 31) have derived

from non-equilibrium thermodynamics expressions relating self-diffusion coefficients to a mutual diffusion coefficient. One widely obtained expression is

$$D = D_k \left(\frac{\partial \ell n\, a_k}{\partial \ell n\, n_{\cdot k}} \right) \left[n_{\cdot k} \frac{\bar{V}_k}{\bar{V}_j} + n_{\cdot j} \right] \tag{9}$$

where now the variation of the diffusion coefficient with composition is approximated. Equation 9 states that the diffusion coefficient divided by the term containing the activity of species k should be a simple function of the mole fraction of component k and the viscosity. Some authors (27) have had good results using these expressions to describe the effect of composition on the diffusion behavior in liquids. Others such as Kozicki (30) and Dullien and Shemilt (19) found that the activity correction did not improve significantly the description of that transport property. By contrast, Longwell and Sage (36) have shown that simply the use of the Chapman-Cowling diffusion coefficient instead of the Fick coefficient improves the linearity of the variation of that transport property with composition, at least for light hydrocarbon systems.

A very simple method of correlation was suggested by Van Geet and Adamson (70). They proposed that for liquid paraffins having five or more carbon atoms the following relation would hold:

$$D_{FC_{\bar{N}}} \bar{V}_{C_{\bar{N}}} = \sum_{i=1}^{n} n_{\cdot i} D_{Fi} \bar{V}_i \tag{10}$$

where the average chain length $\bar{N}$ was related to the chain length of the components in the mixture by

$$\overline{N} = \sum_{i=1}^{n} n_i N_i \quad . \tag{11}$$

Roughly speaking, their theory states that systems (regular solutions) of the same average molecular weight have the same sum of Equation 10. Because their work was very recent, their ideas have not been confirmed by the data from investigations other than their own.

Non-equilibrium Statistical Mechanics

The prediction of factor ξ of Equation 1 has been the subject of extensive work by Kirkwood (57) and others from a statistical mechanical approach. They have attempted to approximate non-equilibrium radial distribution functions in highly complicated expressions to predict diffusion coefficients. The work is in a state of development which is not easily used by engineers.

Kamal and Canjar (28) used an equation of Davis and Rice (15) to obtain diffusion coefficients for a large number of systems, but at infinite dilution of the solutes. Their equations were quite complicated, involving thermodynamic properties of the solute and solvent and the quantity v_f/v which represents the ratio of the occupied volume to the total volume per molecule. Rice and Davis used a dense rigid sphere approximation for the derivation of their equations.

Hole Theory

Some transport properties have been described well (1, 10) over a large range of temperatures and pressures as functions of the volume of the fluid only. It has, therefore, been supposed that what

would hold for viscosity and thermal conductivity would also hold for diffusion coefficients.

The rate process approach of Eyring (23, 56) has been impressively successful for correlating diffusion data. That is not to say that his theory is able to predict diffusion behavior from molecular properties, however; the model which he used has been criticized for this lack. But, the success of the final equations cannot be discounted (18, 39, 40).

Eyring proposed that diffusion occurred in liquids by a mechanism of molecules jumping into vacancies, or holes, at adjacent locations in a semi-crystalline structure. In the process of this movement the diffusing molecules attain activated energy states before reaching the hole position. The rate of motion of the molecules to and from the activated states was described by kinetic-type rate expressions which yielded temperature dependencies of the Arrhenius form. Examples of his resultant equations follow:

$$D = \frac{\lambda^2 kT}{h} e^{-\Delta F^{\ddagger}/RT}, \tag{12}$$

$$D = \frac{\lambda^2}{v_f^{1/3}} \left(\frac{kT}{2\pi m}\right)^{1/2} e^{-\Delta E/RT}, \tag{13}$$

and

$$D = A\, e^{-E/RT}. \tag{14}$$

Equations 12 and 13 are different expressions of the same idea, according to the derivation of Eyring. To obtain Equation 14 from Equation 13, one assumes, as Eyring suggested, that the variation of $(\lambda^2/v_f^{1/3})T^{1/2}$ and ΔE with temperature compensate to give a result

which has temperature appearing only once. In addition, when Equation 12 is combined with a corresponding expression for viscosity, Equation 15 is obtained which resembles very closely the Stokes-Einstein equation. His factor ξ is

$$\frac{D\eta}{kT} = \frac{k'}{\xi\lambda k''} \quad , \tag{15}$$

numerically about 5.6, and his jumping frequencies for viscosity and diffusion, k' and k'', respectively, are not necessarily equal (42). However, they are usually assumed to be so.

Naghizadeh (41) has successfully predicted the same temperature dependence for diffusion as Eyring did without resorting to an activation energy concept. One other factor associated with the Eyring theory is the fact that the activation energy is sometimes (21) a strong function of temperature itself. Chu (13) has suggested raising the temperature to a power greater than unity to compensate.

Kinetic Theory

Enskog (12) derived several expressions which were based solely upon molecular and thermodynamic parameters for a dense fluid of hard spheres. However, the theory has had difficulty (8), reportedly because it only considered binary collisions.

More recently, Longuet-Higgins and Pople (35) have derived a similar and relatively simple expression for describing self-diffusion in liquids. They started from the equation for Brownian motion

$$D = \langle r^2 \rangle / 6\theta \tag{16}$$

and estimated $\langle r^2 \rangle$ by assuming that the velocity autocorrelation function for a molecule decayed exponentially with time. Their result was

$$D = \frac{a}{2}\left(\frac{\pi RT}{M}\right)^{1/2}\left(\frac{PV}{RT} - 1\right)^{-1} . \qquad (17)$$

Equation 16 is similar in some respects to the results of Enskog, who suggested using the "thermal pressure" instead of P in the relation to compensate for using a hard sphere model fluid. McCall and coworkers (39, 40) have had quite good results using Equation 16. It is probable that this technique may be able to be improved in the near future.

Activity in the subject area was reported in the recent results of Rahman (45) who simulated liquid argon at 94.4° K by calculating an 864 body problem on a digital computer. He used a Lennard-Jones potential for the molecules, and calculated the self-diffusion coefficient, velocity autocorrelation function, and other characteristic properties. Two interesting results were the remarkable agreement with the diffusion coefficients measured by Naghizadeh and Rice (41) and the fact that the velocity autocorrelation function did not decay exponentially. Rather, it decreased less slowly, but went negative before approaching zero asymptotically with time. Douglass, McCall, and Anderson (17) recently included this "damped-oscillatory" effect in a derivation similar to that of Equation 17 to give the two-parameter equation

$$D = \frac{\pi^{1/2} kT}{2ma_2^{1/2}}\left(1 + \frac{\delta^2}{2}\right)^{1/2} e^{-\delta^2/4} \qquad (18)$$

where the value of the temperature-dependent parameter δ indicates the importance of the oscillation. When Equation 17 is combined with a similar expression for viscosity derived by Longuet-Higgins and Pople, the familiar-looking expression results:

$$\frac{D\eta V}{RT} = \frac{2}{5} a^2 \quad . \tag{19}$$

DATA

Most of the data on diffusion in binary liquid-paraffin hydrocarbon systems have been obtained by Sage and co-workers (46-55). Nearly all of these data are also published in smoothed form (59). Undoubtedly, the reason why more data are not available is the difficulty of determining quantitatively the changes in composition which a liquid undergoes under conditions of elevated pressure. The pertinent data which have been obtained to date by Sage are listed in Table 1 in the form of Chapman-Cowling diffusion coefficients. All of the data in Table 1 were obtained for liquids very close to the bubble point. Therefore, only two of the variables -- temperature, pressure, and composition -- were independent.

Fishman (20) obtained self-diffusion coefficients for n-pentane and n-heptane over a wide range of temperatures. McCall and co-workers (18, 39, 40) measured self-diffusion coefficients for those and several other normal paraffin liquids. However, even though they varied conditions of temperature and pressure, the latter authors only reported explicitly their data at one condition. Van Geet and Adamson (70) measured diffusion coefficients of a somewhat heavy binary system, n-octane-n-dodecane. Trevoy and Drickamer (68) also measured diffusion coefficients for a series of relatively heavy binary systems, but only at a single composition of each system. They covered mixtures of n-heptane with four longer hydrocarbons. Bidlack and Anderson (6, 7) obtained data for three heavy binary systems. The self-diffusion coefficients of liquid methane (22, 38, 41, 58) and liquid ethane (21) have been measured but not considered here because

their liquid states exist at temperatures far from the region of interest. The only other data found on binary mixtures of very light hydrocarbons were obtained at low temperatures also. They were the measurements by Manzhelii and Verkin (37) for the methane-propylene system at 90.2° K in an apparatus using the same principle as that of Sage.

Auxiliary data consisted largely of viscosity data and volumetric data. The viscosities of the methane-white oil and ethane-white oil systems were those of Sage (60, 61); viscosities for the methane-propane and methane-n-butane systems were estimated from the correlation of Lee (33) and the data of Bicher and Katz (5). Volumetric data were those of Sage (62, 63).

The values used for molecular weights in this study were as follows:

methane	16.04
ethane	30.07
propane	44.09
n-butane	58.12
n-pentane	72.15
n-heptane	100.20
n-decane	142.28
"white oil"	337.

Although the "white oil" was not a single straight-chain hydrocarbon, it approximated one and was assigned its average estimated molecular weight.

EVALUATION OF DIFFUSION COEFFICIENTS

Derivation of Equations

The calculation of diffusion coefficients from the laboratory data of Sage (59) requires a knowledge of the rate of addition of material to a transient diffusion cell and of the volumetric properties of the binary system in the cell. Although the transient diffusion process which is used has been described analytically earlier (48, 59), a somewhat more complete analysis will be developed here.

Figure 1 shows a diagram of the unsteady state diffusion cell used for liquid phase studies in the Chemical Engineering Laboratory (50). It is an isochoric, isothermal pressure vessel which, before a diffusion measurement, contains a binary liquid system of light hydrocarbons in physical equilibrium with its vapor phase in the region R . To begin a measurement, the pressure is raised a predetermined amount by the addition of a quantity of the lighter of the two components through the small diameter tubing S . Then, the amount of the lighter component which is required to maintain the system under isobaric conditions at the higher pressure is determined as a function of time.

It is assumed that diffusion in the gas phase is sufficiently more rapid than that in the liquid phase to justify the assumption of equilibrium in the gas phase. It is further assumed, after the analysis of Drickamer (69), that there is no resistance to transport at the interface and that the liquid at that point is in equilibrium with the gas phase.

In addition, it is assumed that the temperature of the fluid at the interface is the same as that of the rest of the fluid in the cell. This assumption is justified by two factors. First, the rate of diffusion is slow, and, therefore, the rate of generation of heat due to condensation at the interface is slow. Secondly, in practice, a number of small-diameter copper tubes stand vertically inside the cell and pass through the two-phase interface and provide excellent means for conducting away the heat of condensation. The presence of the many vertical tubes within the cell also justifies the assumptions of a negligible velocity gradient across the diameter of the cell and of negligible convection in the liquid phase.

The concentration changes imposed within the cell are assumed to be sufficiently small to allow the partial specific volumes of the components in the liquid phase to be approximated over the entire run by their values at the equilibrium conditions at the interface. The Chapman-Cowling diffusion coefficient is also assumed constant over the small concentration range used during an experiment and thus independent of position within the liquid phase. As a further aid to the theoretical analysis of the diffusion process, the liquid phase is treated as being infinitely deep; this approximation is applicable during the initial part of a run.

The total rate of introduction of the lighter component, k , to the cell may be related to the rate at which it enters the liquid and gas phases by:

$$\mathring{m}_{kc} = \mathring{m}_{k\ell} + \mathring{m}_{kg} \quad . \tag{1}$$

A similar relationship applies for component j :

$$\dot{m}_{jc} = 0 = \dot{m}_{j\ell} + \dot{m}_{jg} \quad . \tag{2}$$

Since the vessel is isochoric, it follows that

$$\underline{\dot{V}} = 0 = \underline{\dot{V}}_g + \underline{\dot{V}}_\ell \quad . \tag{3}$$

The gas phase composition is constant, so that

$$\dot{m}_{jg} = -\sigma_{jd}\underline{\dot{V}}_\ell = -(\sigma_{jd}\overline{V}_{k\ell}\dot{m}_{k\ell} + \sigma_{jd}\overline{V}_{j\ell}\dot{m}_{j\ell}) \tag{4}$$

and

$$\dot{m}_{kg} = -\sigma_{kd}\underline{\dot{V}}_\ell = -(\sigma_{kg}\overline{V}_{k\ell}\dot{m}_{k\ell} + \sigma_{kg}\overline{V}_{j\ell}\dot{m}_{j\ell}) \tag{5}$$

where the partial specific volumes are assumed constant throughout the change of state associated with the measurement. Combining Equations 1 and 5 and rearranging results in

$$\dot{m}_{k\ell} = \dot{m}_{kc}\left[1 + \frac{\sigma_{kg}\overline{V}_{k\ell}}{1 - \sigma_{kg}\overline{V}_{k\ell} - \sigma_{jg}\overline{V}_{j\ell}}\right] \quad . \tag{6}$$

This is the flux of component k into the liquid phase; therefore, it is the flux across the interface, referred to a coordinate system there. A similar manipulation yields the expression for component j at the interface:

$$\dot{m}_{j\ell} = \dot{m}_{kc}\left[\frac{\overline{V}_{k\ell}\sigma_{jg}}{1 - \sigma_{kg}\overline{V}_{k\ell} - \sigma_{jg}\overline{V}_{j\ell}}\right] \quad . \tag{7}$$

The velocity of the interface related to the cell is

$$u_i = -\dot{m}_{k\ell i}\overline{V}_{k\ell} - \dot{m}_{j\ell i}\overline{V}_{j\ell} \tag{8}$$

where the subscripts "i" denote reference to the interface. Combining Equations 6, 7, and 8 results in

$$u_i = - \dot{m}_{kc} \frac{\overline{V}_{k\ell}}{1 - \sigma_{kg}\overline{V}_{k\ell} - \sigma_{jg}\overline{V}_{j\ell}} \quad . \tag{9}$$

The flux at the interface with respect to a fixed frame of reference is related to that with respect to the interface by

$$\dot{m}_{k\ell} = \dot{m}_{kc} + u_i \sigma_k \quad . \tag{10}$$

A combination of Equations 9 and 10 with some rearrangement results in

$$\dot{m}_{k\ell} = \dot{m}_{kc} \left[1 - \frac{\overline{V}_{k\ell}(\sigma_{kb} - \sigma_{kd})}{1 - \sigma_{kd}\overline{V}_{k\ell} - \sigma_{jd}\overline{V}_{j\ell}} \right] \quad . \tag{11}$$

Similarly, for component j ,

$$\dot{m}_{j\ell} = - \frac{\overline{V}_{k\ell}}{\overline{V}_{j\ell}} \dot{m}_{k\ell} \tag{12}$$

at the interface. Since the partial volumes are assumed to be constant, Equation 12 holds true throughout the liquid phase.

The flux of components k and j relative to the diffusion cell may be expressed in terms of the Chapman-Cowling diffusion coefficient by the relationships (36):

$$\dot{m}_{k\ell} = \sigma_k u - \sigma D_{Ckj} \frac{\partial n_k}{\partial x} \tag{13}$$

and

$$\dot{m}_{j\ell} = \sigma_j u - \sigma D_{Ckj} \frac{\partial n_j}{\partial x} = \sigma_j u + \sigma D_{Ckj} \frac{\partial n_k}{\partial x} \quad . \tag{14}$$

Combining Equations 12, 13, and 14 gives

$$\dot{m}_{k\ell} = - \sigma^2 \overline{V}_{j\ell} D_{Ckj} \frac{\partial n_k}{\partial x} \quad . \tag{15}$$

From the definition of n_k ,

$$n_k = \sigma_k/\sigma \tag{16}$$

and the relation

$$V = 1/\sigma = n_k \overline{V}_{k\ell} + n_j \overline{V}_{j\ell} \ , \tag{17}$$

the simplifying relation results:

$$\frac{\partial \sigma_k}{\partial n_k} = \sigma^2 \overline{V}_{j\ell} \ . \tag{18}$$

When Equations 15 and 18 are combined, a very simple relation describing the material flux in the liquid phase is produced:

$$\mathring{m}_{k\ell} = - D_{Ckj} \frac{\partial \sigma_k}{\partial x} \ . \tag{19}$$

The equation of continuity is

$$\frac{\partial \sigma_k}{\partial \theta} = - \frac{\partial \mathring{m}_k}{\partial x} \ . \tag{20}$$

If it is assumed that D_{Ckj} is independent of position, the equation that results is

$$\frac{\partial \sigma_k}{\partial \theta} = D_{Ckj} \frac{\partial^2 \sigma_k}{\partial x^2} \ . \tag{21}$$

The initial and boundary conditions which apply in fixed coordinates are

$$\begin{aligned} \sigma_k(x, 0) &= \sigma_{ko} \\ \sigma_k(\infty, \theta) &= \sigma_{ko} \\ \sigma_k(x_i, \theta) &= \sigma_{kb} \end{aligned} \tag{22}$$

where

$$x_i = x_o + \int_0^\theta u_i d\theta \ . \tag{23}$$

The coordinates will be transformed by setting

$$x' = x - x_o - \int_0^\theta u_i d\theta \quad . \tag{24}$$

After substitution for u_i, Equation 21 in the new coordinate system becomes

$$\frac{\partial \sigma_k}{\partial \theta} = - \mathring{m}_{kc} \frac{\overline{V}_{k\ell}}{1-\sigma_{kd}\overline{V}_{k\ell}-\sigma_{jd}\overline{V}_{j\ell}} \frac{\partial \sigma_k}{\partial x'} + D_{Ckj} \frac{\partial^2 \sigma_k}{\partial x'^2} \quad . \tag{25}$$

The variables are now normalized in terms of dimensionless variables

$$S = \frac{\sigma_k - \sigma_{ko}}{\sigma_{kb} - \sigma_{ko}}$$

$$X = \frac{x'}{\sqrt{4D_{Ckj}\theta}} \tag{26}$$

$$M = - \mathring{m}_{kc} \frac{\overline{V}_{k\ell}}{1-\sigma_{kd}\overline{V}_{k\ell}-\sigma_{jd}\overline{V}_{j\ell}} \sqrt{\frac{\theta}{D_{Ckj}}}$$

If M is assumed independent of X, Equation 25 is given as

$$\frac{d^2S}{dX^2} + 2(X + M)\frac{dS}{dX} = 0 \quad . \tag{27}$$

The straightforward solution of Equation 27 with Equations 22 as boundary conditions is

$$S = \text{erfc}\,(X + M)/\text{erfc}\,M \quad . \tag{28}$$

From Equations 17, 19, and 28, the relation for evaluating the quantity M is found to be

$$\sqrt{\pi}\, M\, e^{M^2}\, \text{erfc}\, M = - \frac{\overline{V}_{k\ell}}{\overline{V}_{j\ell}} \left[\frac{\sigma_{kb} - \sigma_{ko}}{\sigma_{jb} - \sigma_{jd}} \right] \quad . \tag{29}$$

The value of M satisfying Equation 29 can be found quite easily by an

iterative method or by plotting it as a function of the volumetric term in the equation. Now that the value of M is known, rearrangement of Equation 26 yields the Chapman-Cowling diffusion coefficient:

$$D_{Ckj} = \left(\frac{\dot{m}_{kc}\sqrt{\theta}}{M}\right)^2 \left[\frac{\bar{V}_{k\ell}}{1-\sigma_{kd}\bar{V}_{k\ell}-\sigma_{jd}\bar{V}_{j\ell}}\right]^2 . \qquad (30)$$

It is seen from Equations 29 and 30 that the information which is necessary to evaluate the Chapman-Cowling diffusion coefficient from an experiment is: the concentrations of the two components in each phase at the interface conditions, their partial volumes in the liquid phase, the initial concentration of the lighter component in the liquid phase, and the product $\dot{m}_{kc}\sqrt{\theta}$. The volumetric properties are taken from previous measurements (62, 63), and the value of $\dot{m}_{kc}\sqrt{\theta}$ is determined by fitting the following equation to laboratory data for weight added to the cell, m_{kc}, versus time after initiation of the measurement, θ:

$$m_{kc} = m_o + b\sqrt{\theta} . \qquad (31)$$

The desired product is then, simply, $\frac{1}{2}b$. With this last substitution, Equation 30 is

$$D_{Ckj} = \frac{b^2}{4M^2}\left[\frac{\bar{V}_{k\ell}}{1-\sigma_{kd}\bar{V}_{k\ell}-\sigma_{jd}\bar{V}_{j\ell}}\right]^2 . \qquad (32)$$

The Approximate Description of the Diffusion Process

The equation which was used recently (48, 59) to calculate the Chapman-Cowling diffusion coefficients from the above experiments is:

$$D_{Ckj} = \pi \left(\frac{\dot{m}_{kc}\sqrt{\theta}}{\sigma_{kb}-\sigma_{ko}} \right)^2 \left[1 - \frac{\overline{V}_{k\ell}(\sigma_{kb}-\sigma_{kd})}{1-\sigma_{kd}\overline{V}_{k\ell}-\sigma_{jd}\overline{V}_{j\ell}} \right]^2 . \qquad (33)$$

In the derivation of Equation 33, a small effect due to the movement of the two-phase interface was neglected. However, the error which was thus introduced is small, as will be shown now by consideration of Equations 29 and 30.

The following relation is obtained when Equation 29 is solved for $1/M$ and the exponential and error functions are given by infinite series:

$$\frac{1}{M} = \sqrt{\pi}\left(1+M^2+\frac{1}{2}M^4+\ldots\right)\left(1-M+\frac{1}{3}M^3-\ldots\right)\frac{\overline{V}_{j\ell}}{\overline{V}_{k\ell}}\left(\frac{\sigma_{jb}-\sigma_{jd}}{\sigma_{kb}-\sigma_{ko}}\right) . \qquad (34)$$

Thus, $1/M^2$ becomes

$$\frac{1}{M^2} = \pi\left(1-2M+3M^2+\ldots\right)\left[\frac{\overline{V}_{j\ell}}{\overline{V}_{k\ell}}\left(\frac{\sigma_{jb}-\sigma_{jd}}{\sigma_{kb}-\sigma_{ko}}\right)\right]^2 . \qquad (35)$$

It is obvious that a combination of Equations 17, 30, and 35 results in Equation 33 if the infinite series in Equation 35 is truncated at the first term. The systematic error which is introduced by this truncation is of the order of $-200\times M$ per cent, since M is usually much less than unity.

Table 3 compares data for the methane-n-pentane and the methane-n-decane systems which were calculated from Equations 30 and 33. Table 3 also gives the value of M for each experiment. The values of the diffusion coefficients in Table 3 which were calculated from the truncated formula differ very slightly from those in Table 1 because the two tables were calculated at different times with two different people reading graphs of volumetric properties, rounding

off numbers, etc. The truncation after the first term of the infinite series in Equation 35 introduced an error of about five per cent for a typical value of 0.025 for M in the table; this error is probably within the uncertainty of the measurement.

Analysis of Calculation Uncertainties

The general formula for estimating the uncertainty in a calculated function

$$y = y(x_1, x_2, \ldots, x_n) \tag{36}$$

is given (16) as

$$\sigma_y^2 = \sum_{i=1}^{n} \left(\frac{\partial y}{\partial x_i}\right)^2 \sigma_{x_i}^2 \tag{37}$$

where the quantities σ_{x_i} are the estimated uncertainties in each of the variables x_i. Such an analysis of Equations 17, 29, and 32 shows that the variance of the calculated diffusion coefficient may be estimated if the uncertainties in the variables $\sigma_{kb}, \sigma_{ko}, \sigma_{jb}, \overline{V}_{j\ell}$, and b are known or can be approximated. The variable $\overline{V}_{k\ell}$ is not included above because it is not independent of the other variables, as seen in Equations 16 and 17. The quantities σ_{jd} and σ_{kd} are neglected in the error analysis because they are very small and contribute little to the overall propagation of uncertainty.

When the manipulation in Equation 37 is carried out on Equation 32, the following equation results:

$$\frac{1}{4}\left(\frac{\sigma_{D_{ckj}}}{D_{Ckj}}\right)^2 = \left(\frac{\sigma_b}{b}\right)^2 + \left(\frac{\sigma_M}{M}\right)^2 + \frac{1}{(1-\sigma_{jd}\overline{V}_{j\ell}-\sigma_{kd}\overline{V}_{k\ell})^2}\left[\left(\frac{\sigma_{jb}-\sigma_{jd}}{1-\overline{V}_{j\ell}\sigma_{jb}}\right)^2 \sigma_{\overline{V}_{j\ell}}^2 +\right.$$

$$+\left(\frac{1-\overline{V}_{j\ell}\sigma_{jd}}{1-\overline{V}_{j\ell}\sigma_{jb}}\right)^2 \overline{V}_{j\ell}{}^2\sigma_{\sigma_{jb}}{}^2 + \left(\frac{1-\overline{V}_{j\ell}\sigma_{jd}}{\sigma_{kb}}\right)^2 \sigma_{\sigma_{kb}}{}^2\Bigg] \quad . \tag{38}$$

The contribution due to the uncertainty in M is found from a similar treatment of Equation 29.

$$\left(\frac{\sigma_M}{M}\right)^2 = 1\Bigg/\left[2M^2\left(1+\frac{\overline{V}_{j\ell}}{\overline{V}_{k\ell}}\cdot\frac{\sigma_{jb}-\sigma_{jd}}{\sigma_{kb}-\sigma_{ko}}\right)+1\right]^2\left[\left(\frac{\sigma_{\overline{V}_{j\ell}}}{\overline{V}_{j\ell}(1-\overline{V}_{j\ell}\sigma_{jb})}\right)^2\right.$$

$$\left.+\left(\frac{\sigma_{ko}}{\sigma_{kb}}\right)^2\left(\frac{\sigma_{\sigma_{ko}}}{\sigma_{kb}-\sigma_{ko}}\right)^2+\left(\frac{\sigma_{\sigma_{ko}}}{\sigma_{kb}-\sigma_{ko}}\right)^2+\left(\frac{1-\overline{V}_{j\ell}\sigma_{jd}}{1-\overline{V}_{j\ell}\sigma_{jb}}\right)^2\left(\frac{\sigma_{\sigma_{jb}}}{\sigma_{kb}-\sigma_{ko}}\right)^2\right] \tag{39}$$

In Table 4 are given the values and estimated uncertainties of the Chapman-Cowling diffusion coefficients for the methane-n-pentane system and the methane-n-decane system and the estimated uncertainties of the quantities in Equations 38 and 39. Figure 2 shows the relative uncertainties which were calculated for the diffusion coefficients of the methane-n-decane system at 100°F along with the Chapman-Cowling coefficients calculated from the truncated and untruncated formulas. The uncertainties for the diffusion coefficients are probably high, because the estimates of the uncertainties in the contributing terms were estimated as quite large. However, within the set of calculations, the error estimates for individual points provide a method for comparing them even if the estimates are not exact on an absolute basis.

Equations 38 and 39 and Table 4 demonstrate that calculated properties, such as the diffusion coefficient, which are dependent on a knowledge of a number of other properties, all of which have finite uncertainties, may have uncertainties appreciably greater than those

in the laboratory measurements.

RESULTS

Comparison of Data

Since no other investigators have reported data for the same substances under the same conditions as Sage, the data cannot be compared directly. It would therefore be hoped that the mutual diffusion coefficients of Sage could be compared, probably by extrapolation, to the self-diffusion coefficients measured by Fishman (20) and Douglass and McCall (18). However, Figure 3 shows that the above extrapolated mutual diffusion coefficients for n-pentane and n-heptane differ both in magnitude and in dependence on temperature from the self-diffusion coefficients for those substances.

The same can be said for a comparison of the limiting values of the mutual diffusion coefficients of Bidlack and Anderson (6), which do not agree well with measured self-diffusion coefficients. Their value of 1.911×10^{-8} sq. ft. per sec. for pure n-heptane in the n-heptane-n-hexadecane system compares very poorly with McCall's value of 3.36×10^{-8} for self-diffusion on n-heptane and Sage's value of 10.0×10^{-8} for pure heptane in the methane-n-heptane system at 77° F. It is obvious from Figure 3 that the values of Sage for pure n-pentane for the methane-n-pentane and the ethane-n-pentane systems differ by about twenty per cent over the entire temperature range covered by the data. However, in this case the slopes of the data for these two systems in Figure 3 are very nearly the same.

Similarly, Bidlack and Anderson's limiting values given in Table 2 for n-hexane differ between the n-hexane-n-dodecane, the n-hexane-carbon tetrachloride, and the n-hexane-n-hexadecane

systems. Those values of 2.94×10^{-8}, 4.15×10^{-8}, and 2.36×10^{-8}, respectively, all differed significantly from McCall's value of 4.54×10^{-8} sq. ft./sec. for the self-diffusion of n-hexane.

What has been said of the data for the systems involving n-pentane can be said of a comparison of the mutual diffusion coefficients of the methane-n-decane, the ethane-n-decane, and the n-butane-n-decane systems shown in Figure 3 extrapolated to pure n-decane. Also, there is a large disagreement between the limit of 1.561×10^{-8} for pure n-dodecane in the n-hexane-n-dodecane system of Bidlack and Anderson and the value of about 1.26×10^{-8} for the same substance in the n-octane-n-dodecane system of Van Geet and Anderson. The data of Van Geet and Anderson showed explicitly that the limit of a mutual diffusion coefficient was always different from the self-diffusion coefficient of the pure component at that limit.

In short, there is no basis for comparing diffusion data unless it is known that the compared quantities truly represent the same phenomenon in each case. In particular, extrapolated mutual diffusion coefficients do not compare with measured self-diffusion coefficients. Therefore, the present correlative study was limited to the data of Sage, except for purposes of comparison.

One distinctive difference between the composition dependence evidenced by the data of Sage and those of Van Geet and Anderson and of Bidlack and Anderson is the fact that the latter data show an increase in diffusion coefficients with mole fraction of the light component, while the data of nine of the ten binary systems in the former data do the opposite. The ethane-white oil system, the exception,

behaves similar to the heavy hydrocarbon systems of the other authors above and shows an increase in the Chapman-Cowling diffusion coefficient with mole fraction of ethane. It should be remembered that the data of the other authors were presented at isothermal, isobaric conditions, and the data of Sage were presented at isothermal conditions only, since they were measured on the two-phase envelope. Thus, Sage's data show the combined effect of pressure and composition at constant temperature. A further factor contributing to the difference in behavior could be the considerable difference between the characteristics of the very light hydrocarbons used by Sage and the heavier ones used by the other investigators. His data for the ethane-white oil system support this idea.

Throughout the rest of this section are discussed tests and uses of the theories and correlations mentioned in the INTRODUCTION. Those theories and correlations were chosen for testing which appeared to have promise, which were of theoretical interest, or for which the needed auxiliary data were available. Such auxiliary data consisted, for example, of partial volumetric data, viscosity data for two component systems, etc. Any numerical fitting of equations to data was carried out using standard linear (29) or nonlinear (16, 72) least squares techniques on a digital computer.

Empirical

The development of an empirical equation for predicting diffusion coefficients in liquid binary hydrocarbon mixtures was governed by three considerations: ease of use, graphical trends of the data,

and theories.

As stated earlier, all of the diffusion data used in the correlations were obtained very near to the bubble point in the liquid phase. Therefore, only two of the variables temperature, pressure, or composition were needed to completely specify the state or a state function, such as a mutual diffusion coefficient. Although Sage (59) presented the data in smoothed form using temperature and pressure as the independent variables, the work of McCall (39, 40) indicated that pressure had an effect on the diffusion properties of liquids (about five per cent change per thousand pounds per square inch change in pressure) which was less than the variation indicated in the data in Table 1 (as much as thirty per cent change per 0.1 change in weight fraction for the methane-n-pentane system at 280° F, for example). Therefore, it was convenient both from a theoretical standpoint and for calculations to use composition as an independent variable in addition to temperature. Specifically, the weight fraction of the lighter component, its mole fraction, and its concentration were employed at different times. The first of those named above was used largely because, although the correlation would not pretend universality, those who might use the empirical relations might know the weight fractions of various components more accurately than their mole fractions.

Fortunately, the composition dependence of the Chapman-Cowling diffusion coefficient was easily described by an equation which was linear in weight fraction of the light component. A statistical analysis showed only a first-order dependence on composition to

be significant. As indicated by Kozicki (30), this was not true of either the Fick diffusion coefficient or the activity-corrected Fick coefficient in Equation 9 of METHODS, contrary to Bearman's relation. In fact, Bidlack and Anderson (7), among others, have found the activity-corrected Fick coefficient to be "over-corrected."

In Table 5 are given most of the empirical equations which were tested for the ten individual systems in Table 1. In the equations the variable χ stands for any of the three composition variables mentioned above, and the temperatures were expressed in Fahrenheit, as explained below.

It is worthy of note that Equation III of Table 5 resembles very closely the empirical Nernst equation (2)

$$D = D_o[1 + b(T - 459.69)] \qquad (1)$$

which has been used to correlate data over relatively small temperature ranges. Table 6 presents the values of the term which is subtracted from the absolute temperature T in Equation 1 as determined from the constants in Equation III for various binary systems. As pointed out in Part II of this work, the convenient and centrally located value of 459.69 was used for the subtractive term in further generalization of the correlation.

The temperature dependence was also tested in another way, by fitting the equation

$$D_{Ckj} = C_1 + (C_2+C_3 n_k)(T-T_s)^P \qquad (2)$$

for varying values of the subtractive terms T_s and the power P. Figure 4 shows the standard deviation of the methane-n-butane sys-

tem, which was typical, as a function of T_s and P. Again, the value of 459.69 was indicated for T_s, and the power P was taken as 1.0, 1.5, or 2.0 for the equations in Table 5; the standard deviations in Figure 4 which correspond to these powers are 10.2×10^{-8}, 6.9×10^{-8}, and 8.0×10^{-8}, respectively, for the methane-n-butane system.

Table 7 gives the standard deviations of the least squares fits of the equations in Table 5 for the ten systems. The system n-butane-n-decane was not tested for every equation, since it was not available until the last part of the study.

The first point to be noted from Table 7 is that the use of the mole fraction of the light component usually gave a lower standard deviation than the use of the weight fraction or the concentration. This difference was as much as five to ten per cent in the methane-propane and ethane-white oil systems. A second characteristic is that four-term equations did no better job of describing the behavior of the diffusion coefficient than the three-term Equations V and VI. Although the trends in standard deviations were not extremely sharply defined, Equations V and VI produced the lowest standard deviations in three systems and two systems, respectively, and were equally low in another; Equation VIII was best in two systems. A choice does not have to be made between these three equations at this time, because they all can be generalized to apply to sets of systems such as the methane-hydrocarbon systems. However, for example, Equation VI resulted in average per cent deviations from the experimental values of 3.2 per cent for the methane-n-butane system to 15.0 per cent for the

ethane-white oil system.

Obviously, such an expression as temperature in degrees Fahrenheit raised to a power can only be empirical, but it results because of the lack of proper theoretical form in the Equations of Table 5 in the first place. The fact that the above equations provided the best fits to the data shows that the temperature dependence of the Chapman-Cowling diffusion coefficients for the hydrocarbons tested here is stronger than linear in the region of the data. Also, the success of the three-term equations over the four-term equations indicates that the term depending on concentration only was not needed and only the cross-product term involving concentration of the light component and temperature was necessary to describe the variation of the Chapman-Cowling diffusion coefficient with state.

In Table 8 are listed the equations which were tested for generalizing the correlation of diffusion properties. Table 9 then gives the standard deviations of their fits to the sets of data for the methane-hydrocarbon systems, ethane-hydrocarbon systems, or combined methane- and ethane-hydrocarbon systems. It is interesting that although many of the equations seem to have equivalent fits to the data, those containing the very empirical term with temperature expressed in degrees Fahrenheit to the power 1.5 were again consistently somewhat better than others. Not only is this difficult to explain on theoretical grounds, but it also prevents using the equation for extrapolation to temperatures below zero degrees Fahrenheit.

Table 9 shows that for the methane-hydrocarbon systems the weight fraction of methane as the composition variable consistently

provided from five to fifteen per cent lower standard deviations from the data. For example, Equation IX, when fitted to concentration, weight fraction, and mole fraction of methane, resulted in standard deviations from the data of 1.80×10^{-8}, 1.71×10^{-8}, and 1.89×10^{-8} sq. ft. per sec., respectively. In the ethane-hydrocarbon systems, where the dependence of the diffusion coefficients on composition was less than in the methane-hydrocarbon systems, there was less difference between the standard deviations obtained using the various composition variables. The greatest difference between the standard deviations occurred for Equation III (2.39×10^{-8}, 1.89×10^{-8}, and 2.33×10^{-8}, respectively), although that equation was one of the poorer ones in the table. Thus, the weight fraction of ethane was favored somewhat. The behavior of the standard deviations for the generalized equations with respect to composition variables is in contrast to the behavior for the equations in Table 5 in that the latter favored the use of the mole fraction of the light component.

Empirically, Equation IX of Table 8 was indicated as giving the best description of the Chapman-Cowling diffusion coefficient for methane-hydrocarbon systems -- it resulted in a standard deviation from the data of all of the six methane systems of 1.71×10^{-8} sq.ft. / sec. when weight fraction of methane was used as the composition variable. Equations III and XIII were alternates to number IX, giving standard deviations of 1.89×10^{-8} and 1.96×10^{-8}, respectively. The power of $\frac{1}{2}$ for the molecular weight of the heavy component was prominent in these equations, reminiscent of the Exner rule.

For the ethane-hydrocarbon systems, the choice was again

more difficult, but Equations II, VI, and VII produced the lowest standard deviations from the data, 1.35×10^{-8}, 1.33×10^{-8}, and 1.33×10^{-8} sq. ft. per sec., respectively.

The single attempt to describe both the methane- and ethane-hydrocarbon systems by one equation, Equation XXI, resulted in poor agreement between the equation and the data (a standard deviation of 5.11×10^{-8} sq. ft./sec. for weight fraction of the light component).

The constants and their 95 per cent uncertainties for the six generalized equations which were named above are found in Table 10 with weight fraction of the light component as an independent variable. The 95 per cent uncertainties indicate qualitatively which terms in the equation are significant statistically. For example, Equation III revealed a strong dependence on all variables in the equation; the least strong dependence was on the last two, composition and composition combined with molecular weight of the heavy component. Thus, it is seen from the 95 per cent uncertainties in Table 10 that, as stated earlier from graphical observations, the ethane-hydrocarbon systems exhibited less dependence of diffusion coefficients on composition than did the methane-hydrocarbon systems.

The empirical equations which were presented in Part II of this work were chosen because of their accuracy, simplicity, and acceptability with reference to the temperature dependence.

Abas-Zade

Figure 5 shows the relation between the Chapman-Cowling diffusion coefficient and total concentration of material in the liquid phase

for a typical binary system. From the figure, it is apparent that there exists a definite relation between the above two quantities; however, the relation is seen to be a strong function of temperature as a second independent variable. This behavior is markedly different from the dependence of thermal conductivity and viscosity of pure components, although Starling and Ellington (65) found a slight additional dependence of residual viscosity on temperature. Probably self-diffusion coefficients would behave much like viscosity and thermal conductivity. Unfortunately, the only data noted for liquid hydrocarbons over wide ranges of temperature and pressure in the single phase region have been reported very incompletely by Douglass and McCall (18).

As a quantitative measure of how well defined the relation was between the mutual diffusion coefficient and the total concentration, the equation

$$D_{Ckj} = C_1 + C_2 t + (C_3 + C_4 t)\sigma \qquad (3)$$

was fitted to the data at hand. The resulting standard deviations of the fits and the equation constants are presented in Table 11. Obviously, the goodness of fit was less than was obtained for the empirical equations in Table 5 (as an example, for the methane-n-pentane system, Equation 3 produced a standard deviation of 2.40×10^{-8} as compared to 1.31×10^{-8} for Equation V in Table 5).

The interpretation of these results would be that a transport property of a two-component system on the two-phase envelope is not a function of just the specific volume of the phase. This is in agreement with the findings of Lee, Starling, et al. (33) for viscosity of

binary liquid system. Going a step further, one can infer from the preceding information that the availability of "holes," or space, in binary liquids, depending on their specific volumes, is not the sole determining factor for their transport behavior. In addition, the distribution of the available energy over the various modes of the two species becomes important.

Wilke and Stokes-Einstein

Since neither the expressions of Wilke nor of Stokes-Einstein are significantly different from that of Eyring, Equation 15 of METHODS, they were not considered individually to an extent worthy of reporting. Their major lack was in their ability to describe the variation of diffusion coefficients with composition. Additional comments on these expressions will be made in the section dealing with the theory of Eyring.

Eyring

In addition to those equations reported in Part II of this work, Table 12 gives more equations of the Eyring types, and Table 13 gives the standard deviations of their fits to the data. It is apparent from Table 13 that the various forms given by Eyring are roughly equivalent in that they all may fit the available data equally well (the spread in standard deviations between Equations I, IV, and V was only about five per cent or less in the table). This result is reasonable, since the small change caused by multiplying the exponential by the absolute temperature merely counteracts a small part of the exponential of the reciprocal absolute temperature, and the function remains basically

the same.

The standard deviations of the fits of these equations in general compare favorably with the best of the empirical equations. In particular, the four-constant equation, number III in Table 12, usually gave the best fit for the methane-n-butane and methane-n-decane systems; for example, it resulted in standard deviations of 0.87×10^{-8} and 0.98×10^{-8}, respectively, as compared with 0.65×10^{-8} and 1.03×10^{-8} for the empirical Equation VI of Table 5 for the same systems. This result indicates that concentration dependence has a significant component which is independent of temperature.

Equations I and II of Table 12 and Equation 7 of Table 2, Part II, compare the effect of using mole fraction, concentration, or weight fraction of the lighter component as an independent variable. Although the different forms were almost equivalent, the mole fraction form was favored slightly (its standard deviations were about four per cent lower than those for concentration and even closer to those for weight fraction).

It is more interesting to compare the individual terms of the equations, since in this case they have some theoretical significance. Table 14 lists the energies of activation as defined in Equation 14 in METHODS; they were calculated from the constants of the indicated equations of Table 13 at zero mole fraction of the light component. Also listed for comparison are the values of the energy of activation found by Douglass and McCall (18) for self-diffusion of the same heavy components. In every case the calculated values were greater than those reported for the case of self diffusion. That is, the tem-

perature dependence was more pronounced for mutual diffusion than for self diffusion. For example, the activation for n-decane was 7.6 kcal/gmole and 6.9 kcal/gmole for the methane-n-decane and ethane-n-decane systems, respectively, as compared with 3.6 kcal/gmole for its self diffusion. The trends of the activation energies with molecular weight were the same in each case, however, with the activation energies increasing substantially with molecular weight of the heavy component. The order of magnitude of the activation energies fell between the Lennard-Jones ϵ for the compounds (0.6 kcal/gmole) (9) and the carbon-carbon bond energies (80 kcal/gmole) (44), roughly at the geometric mean of these two energies.

In Table 15 is listed the pertinent information on two equations which were generalized to apply to the methane-hydrocarbon systems and the ethane-hydrocarbon systems of binary mixtures. In the table, Equations 1 and 2 are generalizations of Equations I and III in Table 12, respectively. When the two white-oil systems were left out of the correlations, the fits of the equations to the data sometimes were improved and sometimes were not. Also, the shorter Equation 1 was found to be better than the longer one in the case of the ethane series; this merely indicates that the empirical parts of the equations -- the composition and molecular weight dependencies -- were constructed to describe more closely one series or the other.

Equation 2 resulted in a standard deviation for the methane series of 2.03×10^{-8} as compared with the best empirical equation's 1.71×10^{-8} sq. ft./sec.; for the ethane systems, Equation 1 compared well with the empirical fits also, with a standard deviation of

1.49×10^{-8} compared to 1.33×10^{-8} sq. ft./sec. for the best empirical equation for ethane.

The limited data on the viscosities of liquid mixtures of paraffin hydrocarbons were used to calculate the molecular radii according to Equation 15 where the k's were assumed equal. These radii are presented in Table 16 and Figure 6 and show immediately that the trend with molecular weight is just the reverse of what it should be. Unlike the radii calculated by the formula of Longuet-Higgins and Pople in the next section, Eyring's radii increase with decreasing average molecular weight. He apparently ignored this effect which was obvious in the correlations which he presented (56) for toluene and n-heptane diffusing in a series of normal paraffins. The Stokes-Einstein equation also has this problem of the inverted dependence of radius on molecular weight.

The major point to be noted in this section dealing with Eyring's work is the fact that he predicted the form of the temperature dependence of the diffusion coefficient better than anyone had previously.

A logical technique to use in generalizing the Eyring equations for the several binary systems presented here would be to use reduced temperatures in his equation. However, others (18, 40) have not had great success with this technique for self-diffusion coefficients, and for a binary system the task of devising pseudo-critical temperatures would probably be more trouble than it was worth.

Longuet-Higgins and Pople

Even though the equation derived by Longuet-Higgins and Pople to predict dense phase diffusion coefficients was intended for self-diffusion, it was tested here as a matter of interest.

In order to carry out the required calculations, the thermal pressure, P_t, had to be estimated. Since data were not available directly for this quantity, it was estimated from the correlations of Seader and Chao (11) which used Hildebrand's (25) solubility parameter $\delta = (\Delta E_v / \dot{V})^{\frac{1}{2}}$. Their tables of δ and molar volume are reported in Table 17. According to Seader and Chao, the quantity $\bar{\delta}$ for a binary mixture can be estimated by the relation

$$\bar{\delta} = \sum_i n_i v_i \delta_i / \sum_i n_i v_i \quad . \tag{4}$$

Then this property is used to calculate the following thermodynamic property:

$$\bar{\delta}^2 = \frac{\Delta E_v}{\dot{V}} \sim \left(\frac{\partial E}{\partial \dot{V}}\right)_T \quad . \tag{5}$$

From thermodynamics,

$$T\left(\frac{\partial P}{\partial T}\right)_V = T\left(\frac{\partial S}{\partial V}\right)_T = \left(\frac{\partial E}{\partial V}\right)_T + P \quad . \tag{6}$$

Thus, the thermal pressure can be estimated directly from the equation

$$P_t = \delta^2 + P \quad . \tag{7}$$

Figure 7 shows a check of this estimate for the ethane-n-decane system which was made using volumetric data which were available from the Chemical Engineering Laboratory. The agreement is not perfect, but adequate for a test of an admittedly very approximate relation.

In Table 18 are reported the results of calculating a molecular radius by Equation 17 of METHODS for eight of the binary systems. One of the systems is shown in graphical form in Figure 8. The dashed line indicates the molal average value of the Lennard-Jones σ (9). The agreement between the calculated solid lines and the dashed lines is close, all around five Angstroms, but obviously not perfect. They could be adjusted by including a constant multiplying factor such as in Equation 18 of METHODS. In fact, if Longuet-Higgins and Pople had used the function $e^{-\beta s}\cos\delta\beta s$ as the velocity autocorrelation function, the multiplicative factor would have been $1+\delta^2$. Then, if δ decreased with temperature as Douglass (17) said it should as the importance of oscillations (characteristic of solids) decreased as the system moved away from the melting temperature, the curves in Figure 8 could presumably be made to coincide. Thus, the form of the results in these figures is qualitatively correct, with the molecular radius increasing with increasing average molecular weight of the system.

The available data on viscosities of the systems methane-propane and methane-n-butane in the form of the correlation by Lee (33) were used to compile part of Table 16 and Figure 9. These calculated molecular radii are different from those in Table 18, of course, because of the gross approximations in the theory. However, the trend of the radii with molecular weight is logical, less dependent on temperature, and in qualitative agreement with a molal average Lennard-Jones σ. The characteristic of Figure 9 which is markedly different from that in Figure 8 is the temperature dependence. In

Figures 15 and 16 the calculated molecular radius decreases very definitely with increasing temperature. This confirms a comment of Douglass, et al. (17) that the temperature dependences for diffusion and viscosity are poorly understood and that major temperature effects are being left out of the derivations.

CONCLUSIONS

1. Several analytical expressions have been developed with which one can interpolate the Chapman-Cowling diffusion coefficient for binary mixtures of light hydrocarbons in the liquid phase over a wide range of temperature and composition. The values of the diffusion coefficient thus calculated are within the scatter of the experimental data. These expressions should be valuable for interpolating the diffusion data and for analytical representation of diffusion coefficients for machine calculations.

2. The variation of the Chapman-Cowling diffusion coefficient with composition was found to be linear with weight fraction or mole fraction of the light component. This variation was more pronounced for methane-hydrocarbon systems than for ethane-hydrocarbon systems. The data were not of sufficient precision to reveal more complicated behavior which has been predicted from nonequilibrium thermodynamics.

3. The temperature dependence of the Chapman-Cowling diffusion coefficient of binary, liquid, light hydrocarbons is best described by the exponent of the reciprocal absolute temperature, as proposed by Eyring.

4. The Chapman-Cowling diffusion coefficient of the above systems cannot be determined solely from a knowledge of the specific volume of the system.

5. It is recommended that future calculations of the Chapman-Cowling diffusion coefficient from the experiment described above employ the untruncated formula which was derived in this work.

6. The theory of Longuet-Higgins and Pople is useful for approximating diffusion coefficients for binary liquid mixtures. However, it does not predict the correct composition or temperature dependence of the coefficients.

NOMENCLATURE

A	A constant; area, sq. ft.; abnormality factor
a	Molecular radius, Ångstroms; a constant; chemical activity
B	A constant
b	A constant
C	A constant; concentration variable, lb./cu. ft.; symbol for a hydrocarbon; C', a constant
D	Diffusion coefficient, sq. ft./sec.
E	Energy of activation, kcal/gmole
$F^{\ddagger}$	Free energy of activation, kcal/gmole
g	Acceleration of gravity, ft./sec.^{2}
h	Distance increment, ft.; Planck's constant, erg sec.
k	Boltzmann's constant, erg/$^{\circ}$K; k', k'', Eyring's jump frequencies for viscosity and diffusion, respectively
L	Length of phase, ft.
M	Dimensionless weight flux variable; mole weight, lb./lb.-mole
m	Weight of material, lb./sq. ft.; molecular weight, grams
$\dot{m}$	Moles of material, lb.-mole/sq. ft.
N	Number of carbon atoms per molecule
n	Weight Fraction
$\dot{n}$	Mole fraction
P	Pressure, lb./sq. in.; power
R	The gas constant, Btu/lb.$^{\circ}$R
r	Mean distance of travel in Brownian motion, Ångstroms
S	Dimensionless concentration variable; entropy, Btu/lb.$^{\circ}$R
s	Factor in theory of Longuet-Higgins and Pople
T	Thermodynamic temperature, $^{\circ}$R

t	Temperature, ^{o}F
u	Velocity, ft./sec.
V	Specific volume, cu. ft./lb.; $\overline{V}$, partial specific volume, cu. ft./lb.
$\dot{V}$	Specific molal volume, cu. ft./lb.-mole
$\underline{V}$	Total volume, cu. ft.
v	Molal volume, cu. ft./lb.-mole
X	Dimensionless coordinate
x	Coordinate, ft.; independent variable; association factor; x', coordinate, ft.
y	Dependent variable
β	Factor in theory of Longuet-Higgins and Pople; slip factor
γ	Molecular radius, Ångstroms; surface tension, dynes/cm.
δ	Vibration factor; solubility parameter, $lb.^{\frac{1}{2}}/in.$
η	Viscosity, lb. sec./sq. ft.
θ	Time, sec. or hr.
λ	Jump distance or molecular dimension of Eyring, Ångstroms
ξ	Drag on a molecule, lb. sec./ft.; Eyring's constant of 5.6
σ	Concentration, lb./cu. ft.; uncertainty in a variable
$\dot{\sigma}$	Molar concentration, lb.-mole/cu. ft.
χ	Composition variable, lb./cu. ft., mole fraction, or weight fraction

Subscripts

b	Bubble point
C	Chapman-Cowling; symbol for a hydrocarbon
c	Into cell
D	Diffusion coefficient

d	Dew point
F	Fick
f	Free
g	Gas phase
i	Referred to interface or of interface; component i
j	Component j , heavy component
k	Component k , light component
ℓ	Liquid phase
m	Time increment number
N	Carbon number
n	Distance increment number
o	Initial value
P	Constant pressure
s	Subtracted term
T	Constant temperature
t	Thermal
V	Constant volume; $\overline{V}$, partial volume
v	Volumetric property
y	Dependent variable
σ	Concentration

1, 2, 3... Component number; end of increment in from boundary; number of carbon atoms in molecule; the number of a constant

REFERENCES

1. Abas-Zade, A. K., Zhur. Ekspl. i Teoret. Fiz. 23, 60 (1952).

2. Arnold, J., J. Am. Chem. Soc. 52, 3937 (1930).

3. Bearman, R. J., J. Phys. Chem. 65, 1961 (1961).

4. Bennett, C. O., Chem. Eng. Sci. 9, 45 (1958).

5. Bicher, L. B., and Katz, D. L., Ind. Eng. Chem. 35, 754 (1943).

6. Bidlack, D. L., and Anderson, D. K., J. Phys. Chem. 68, 206 (1964).

7. Bidlack, D. L., and Anderson, D. K., J. Phys. Chem. 68, 3790 (1964).

8. Bird, R. B., Curtiss, D. F., and Hirschfelder, J. O., Chem. Eng. Prog. Sympos. Series, No. 16, 51, 69 (1955).

9. Bird, R. B., Steward, W. E., and Lightfoot, E. N., Transport Phenomena, John Wiley and Sons, New York (1960).

10. Carmichael, L. T., and Sage, B. H., J. Chem. Eng. Data 8, 612 (1963).

11. Chao, K. C., and Seader, J. D., A. I. Ch. E. J. 7, 598 (1961).

12. Chapman, S., and Cowling, T. G., The Mathematical Theory of Non-uniform Gases, 2nd Ed., University Press, Cambridge, England (1952).

13. Chu, Chieh-Hsi, Hua Kung Hsueh Pao 2, 172 (1959).

14. Darken, Trans. A. I. M. E. 175, 184 (1948).

15. Davis, H. T., Rice, S. A., and Sengers, J. V., J. Chem. Phys. 31, 575 (1959).

16. Deming, W. E., Statistical Adjustment of Data, John Wiley and Sons, New York (1943).

17. Douglass, D. C., McCall, D. W., and Anderson, E. W., J. Chem. Phys. 34, 152 (1961).

18. Douglass, D. C., and McCall, D. W., J. Phys. Chem. 62, 1102 (1958).

19. Dullien, F. A. L., and Shemilt, L. W., Nature 190, 526 (1961).

20. Fishman, E., J. Phys. Chem. 59, 469 (1955).

21. Gaven, J. V., Stockmayer, W. H., and Waugh, J. S., J. Chem. Phys. 37, 1188 (1962).

22. Gaven, J. V., Waugh, J. S., and Stockmayer, W. H., J. Chem. Phys. 38, 287 (1963).

23. Glasstone, S., Laidler, K. J., and Eyring, H., Theory of Rate Processes, McGraw-Hill, New York (1941).

24. Hartley, G. S., and Crank, K., Trans. Faraday Soc. 45, 801, (1949).

25. Hildebrand, J. O., and Scott, R. L., Regular Solutions, Prentice-Hall, Englewood Cliffs, New Jersey (1962).

26. Hill, N. E., Proc. Phys. Soc. 68B, 209 (1955).

27. Horrocks, J. K., and McLaughlin, E., Trans. Faraday Soc. 58, 1357 (1962).

28. Kamal, M. R., and Canjar, L. N., A. I. Ch. E. J. 8, 329 (1962).

29. Kempthorn, O., The Design and Analysis of Experiments, John Wiley and Sons, New York (1952).

30. Kozicki, W., Ph. D. Thesis, California Institute of Technology (1962).

31. Lamm, O., J. Phys. and Colloid Chem. 51, 1063 (1947).

32. Lapidus, L., Digital Computation for Chemical Engineers, McGraw-Hill, New York (1962).

33. Lee, A. L., Starling, K. E., Dolan, J. P., and Ellington, R. T., A. I. Ch. E. J. 10, 694 (1964).

34. Li, J. C. M., and Chang, P., J. Chem. Phys. 23, 518 (1955).

35. Longuet-Higgins, H. C., and Pople, J. A., J. Chem. Phys. 25, 884, (1956).

36. Longwell, P. A., and Sage, B. H., A. I. Ch. E. J. 11, 46 (1965).

37. Manzhelii, V. G., and Verkin, B. T., Zhur. Fiz. Khim. 33, 1758 (1959).

38. Matyash, I. V., Galkin, O. O., and Tarasenko, L. M., Ukr.

Fiz. Zh. 8, 39 (1963).

39. McCall, D. W., Douglass, D. C., and Anderson, E. W., J. Chem. Phys. 31, 1555 (1959).

40. McCall, D. W., Douglass, D. C., and Anderson, E. W., Phys. Fluids 2, 87 (1959).

41. Naghizadeh, J., and Rice, S. A., J. Chem. Phys. 36, 2710 (1962).

42. Olander, D. R., A. I. Ch. E. J. 9, 207 (1963).

43. Olson, R. L., and Walton, J. S., Ind. Eng. Chem. 43, 703 (1951).

44. Overmars, J. D., and Blinder, S. M., J. Phys. Chem. 68, 1801 (1964).

45. Rahman, A., Phys. Rev. 136, 405 (1964).

46. Reamer, H. H., Duffy, C. H., and Sage, B. H., Ind. Eng. Chem. 48, 282 (1956).

47. Reamer, H. H., Duffy, C. H., and Sage, B. H., Ind. Eng. Chem. 48, 285 (1956).

48. Reamer, H. H., Lower, J. H., and Sage, B. H., J. Chem. Eng. Data 9, 54 (1964).

49. Reamer, H. H., Lower, J. H., and Sage, B. H., J. Chem. Eng. Data 9, 602 (1964).

50. Reamer, H. H., Opfell, J. B., Sage, B. H., and Duffy, C. H., Ind. Eng. Chem. 48, 275 (1956).

51. Reamer, H. H., and Sage, B. H., A. I. Ch. E. J. 3, 449 (1957).

52. Reamer, H. H., and Sage, B. H., J. Chem. Eng. Data 1, 71 (1956).

53. Reamer, H. H., and Sage, B. H., J. Chem. Eng. Data 3, 54 (1958).

54. Reamer, H. H., and Sage, B. H., J. Chem. Eng. Data 6, 180 (1961).

55. Reamer, H. H., and Sage, B. H., J. Chem. Eng. Data 6, 481 (1961).

56. Ree, F. H., Ree, T., and Eyring, H., Ind. Eng. Chem. 50, 1036 (1958).

57. Rice, S.A., and Kirkwood, J. G., J. Chem. Phys. 31, 901 (1959).

58. Rugheimer, J. H., and Hubbard, P. S., J. Chem. Phys. 39, 552 (1963).

59. Sage, B. H., Some Material Transport Properties of the Lighter Hydrocarbons in the Liquid Phase, American Petroleum Institute, New York (1964).

60. Sage, B. H., Inman, B. N., and Lacey, W. N., Ind. Eng. Chem. 29, 888 (1937).

61. Sage, B. H., and Lacey, W. N., Ind. Eng. Chem. 32, 587 (1940).

62. Sage, B. H., and Lacey, W. N., Some Properties of the Lighter Hydrocarbons, American Petroleum Institute, New York (1955).

63. Sage, B. H., and Lacey, W. N., Thermodynamic Properties of the Lighter Paraffin Hydrocarbons and Nitrogen, American Petroleum Institute, New York (1950).

64. Sitaraman, R., Ibrahim, S. H., and Kuloor, N. R., J. Chem. Eng. Data 8, 198 (1963).

65. Starling, K. E., and Ellington, R. E., A. I. Ch. E. J. 10, 11 (1964).

66. Sutherland, Phil. Mag. 9, 871 (1905).

67. Thakar, N. S., and Othmer, D. F., Ind. Eng. Chem. 45, 589 (1953).

68. Trevoy, D. J., and Drickamer, H. G., J. Chem. Phys. 17, 1117 (1949).

69. Tung, L. H., and Drickamer, H. G., J. Chem. Phys. 20, 6 (1952).

70. Van Geet, A. L., and Adamson, A. W., J. Phys. Chem. 68, 238 (1964).

71. Wilke, C. R., and Chang, P., A. I. Ch. E. J. 1, 264 (1955).

72. Woodward, J. W., Ph. D. Thesis, California Institute of

Technology (1965).

LIST OF FIGURES

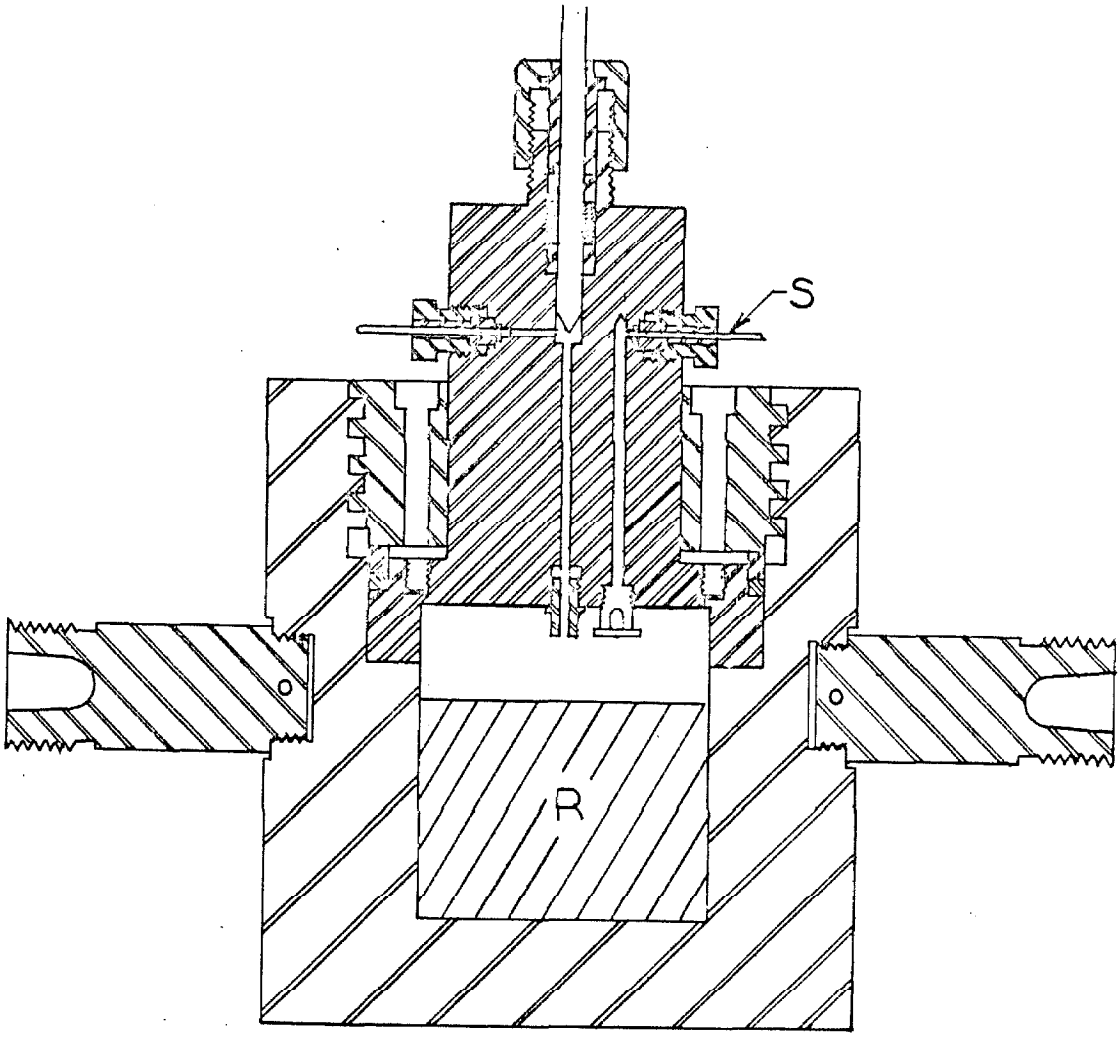

Fig. 1. Details of Diffusion Chamber

(Courtesy of Industrial and Engineering Chemistry)

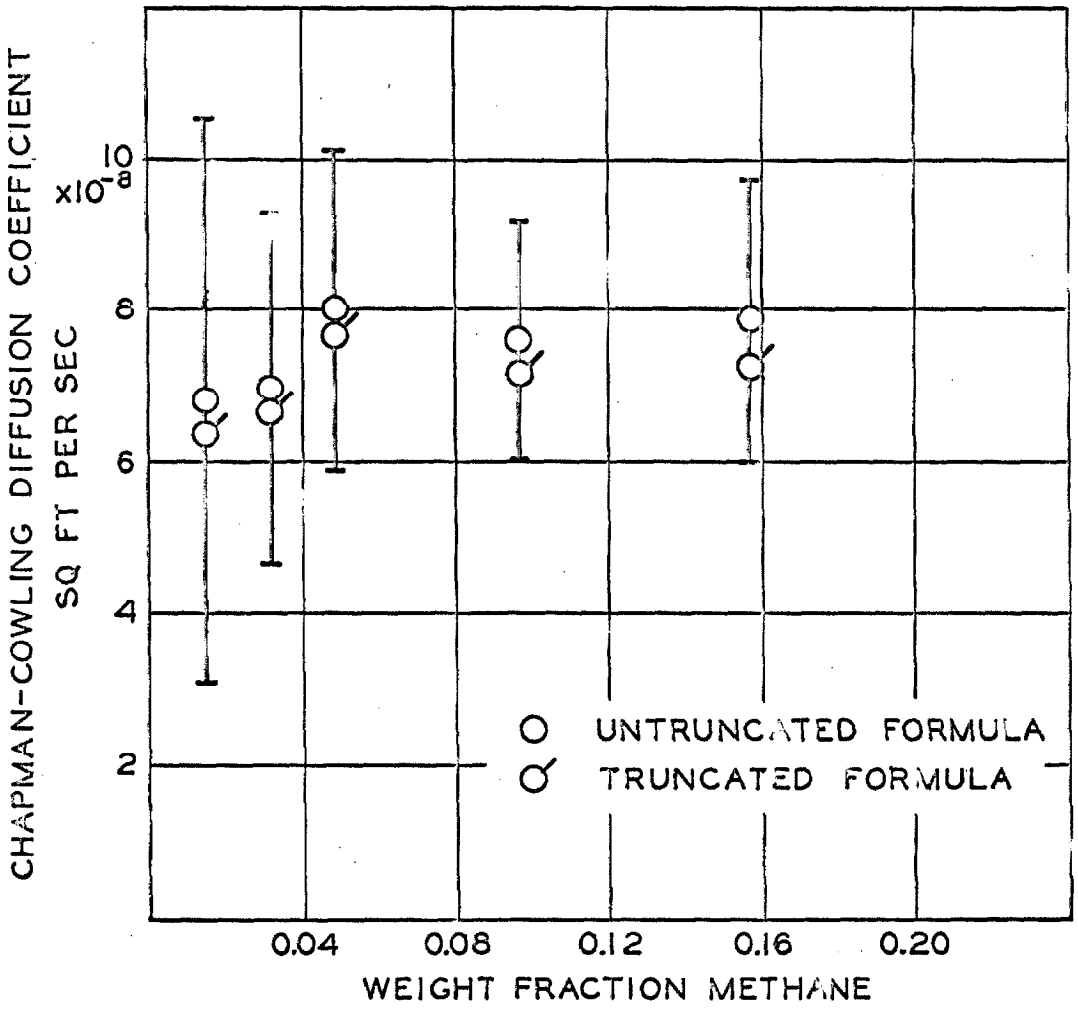

Fig. 2. Diffusion Coefficients and Their Estimated Relative Uncertainties for Methane-n-Decane at 100° F.

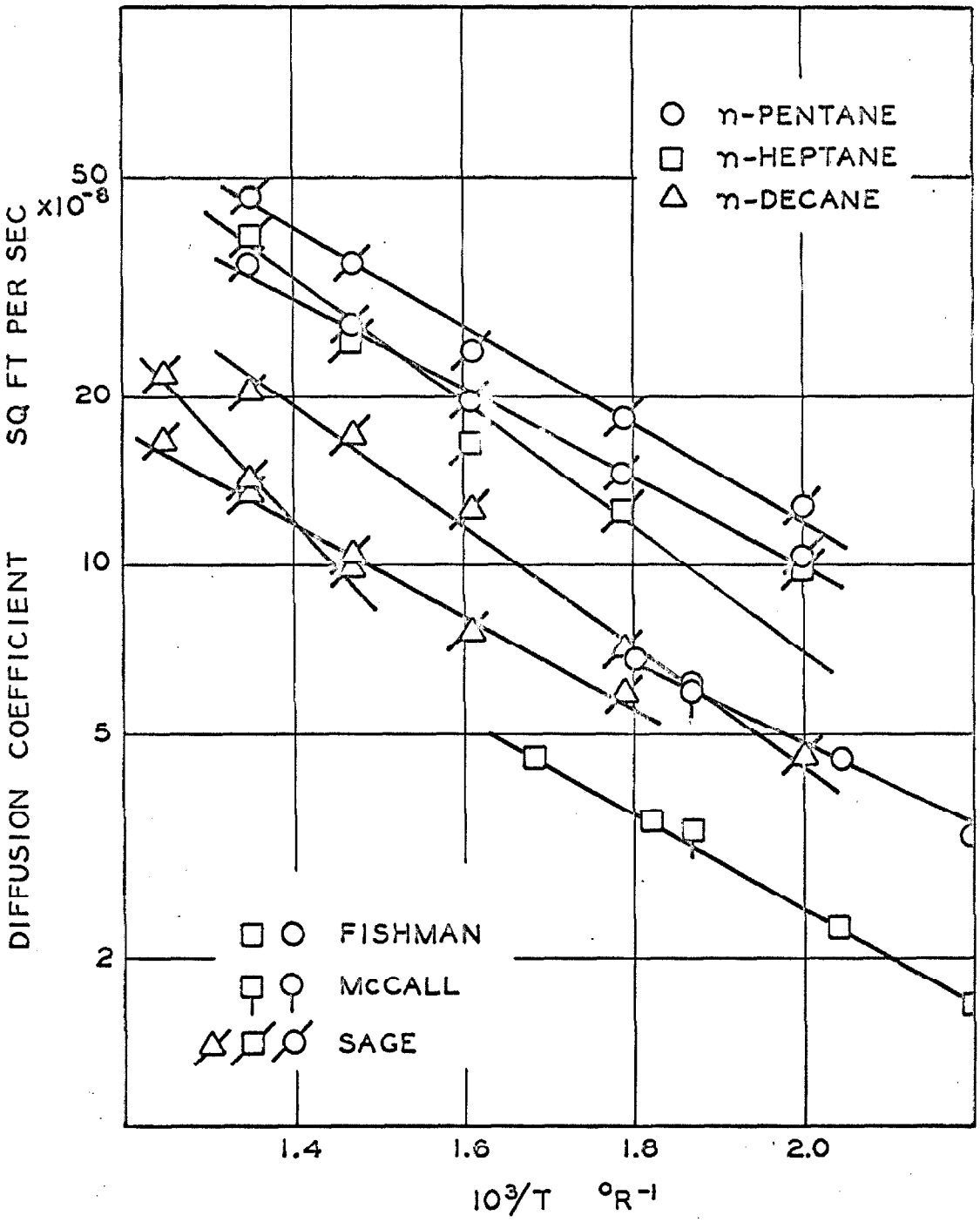

Fig. 3. Data of Several Authors for Self-Diffusion and Extrapolated Mutual Diffusion.

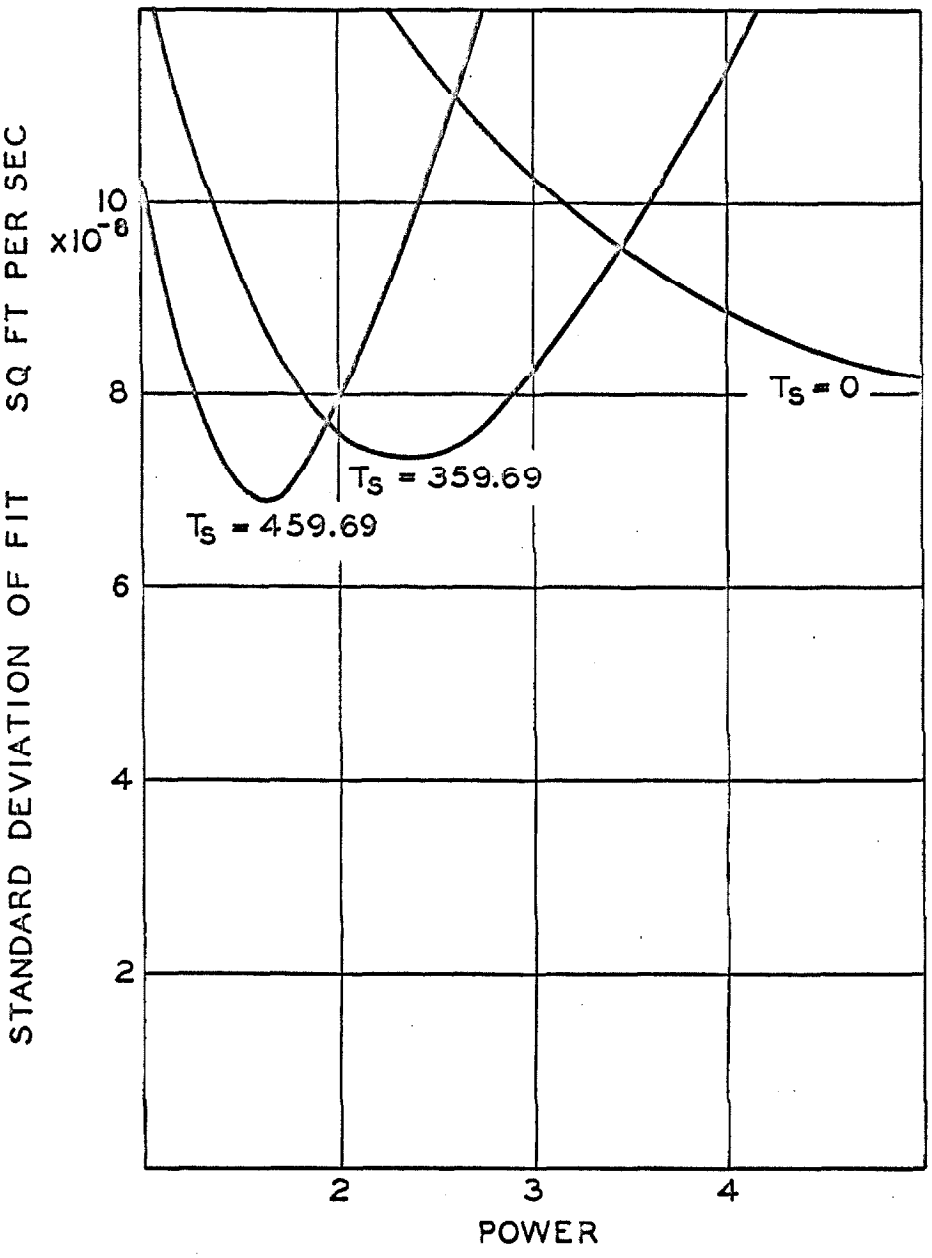

Fig. 4. Dependence of Standard Deviation on Empirical Equation Constants for the Methane-n-Butane System.

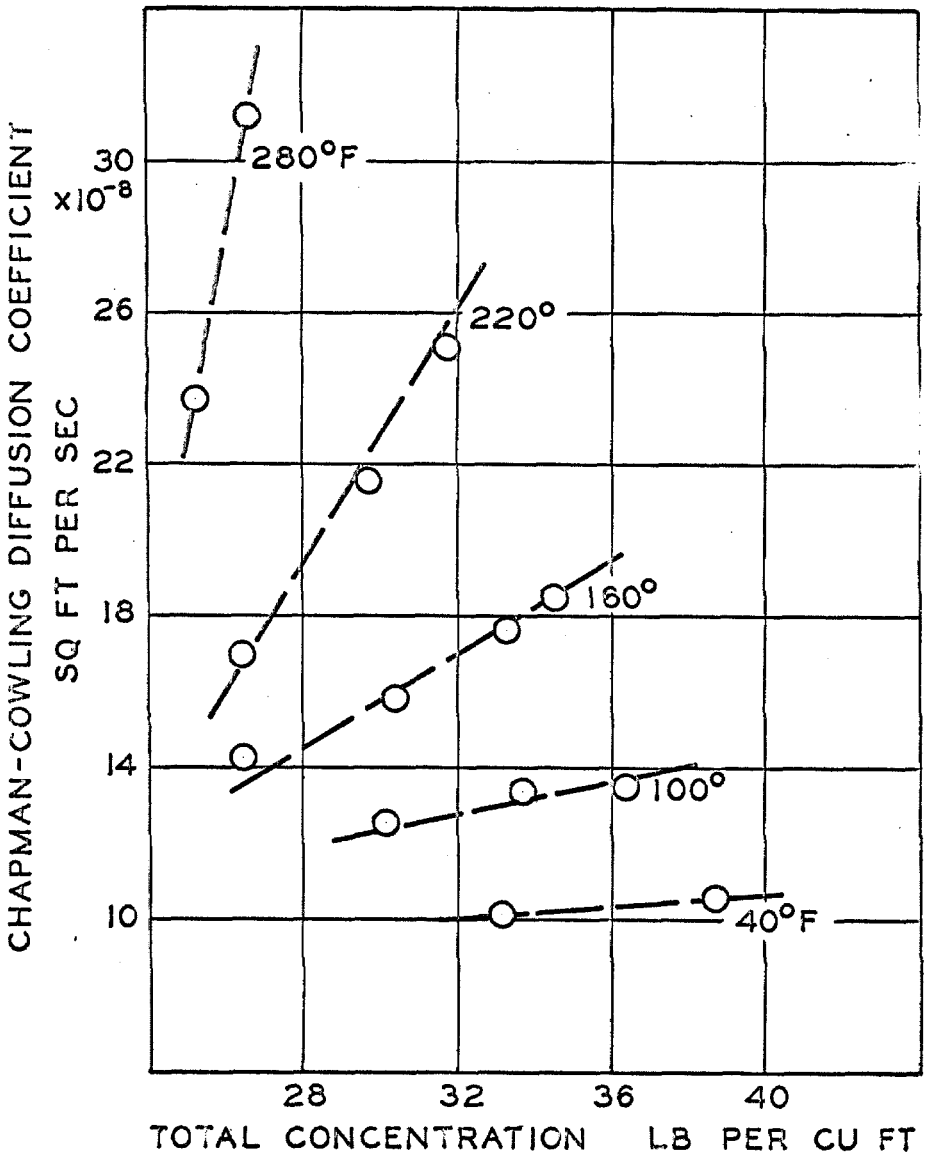

Fig. 5. Chapman-Cowling Diffusion Coefficient as a Function of Total Concentration in Liquid.

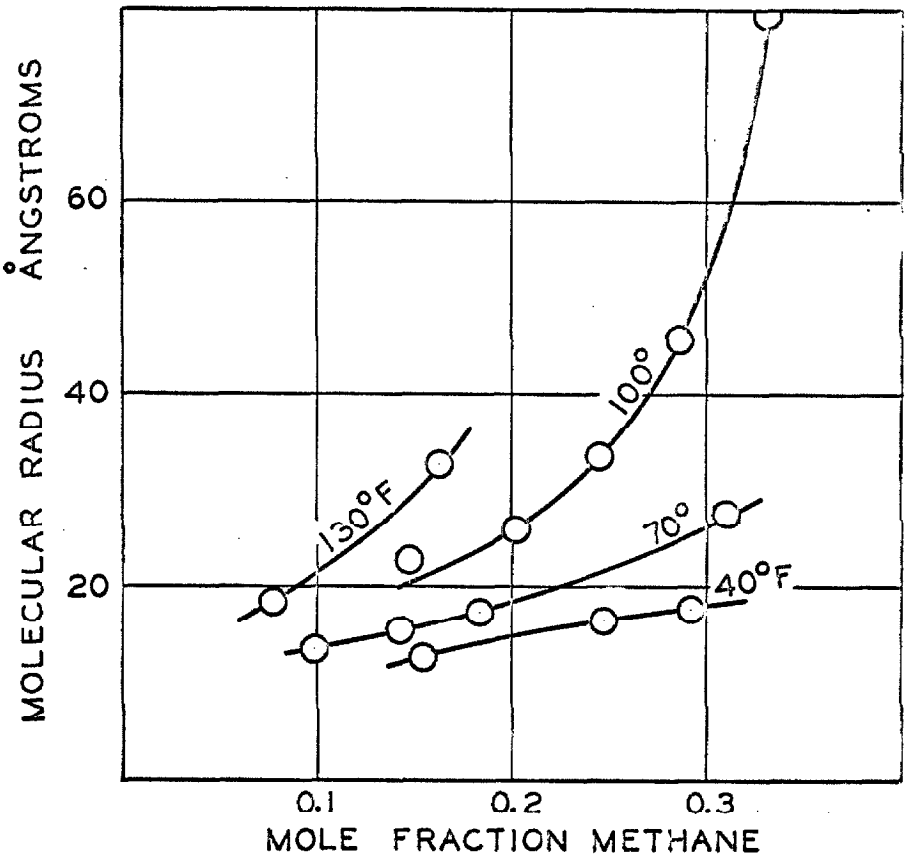

Fig. 6. Molecular Radius of Eyring Evaluated from Viscosity and Diffusion Coefficient for Methane-Propane.

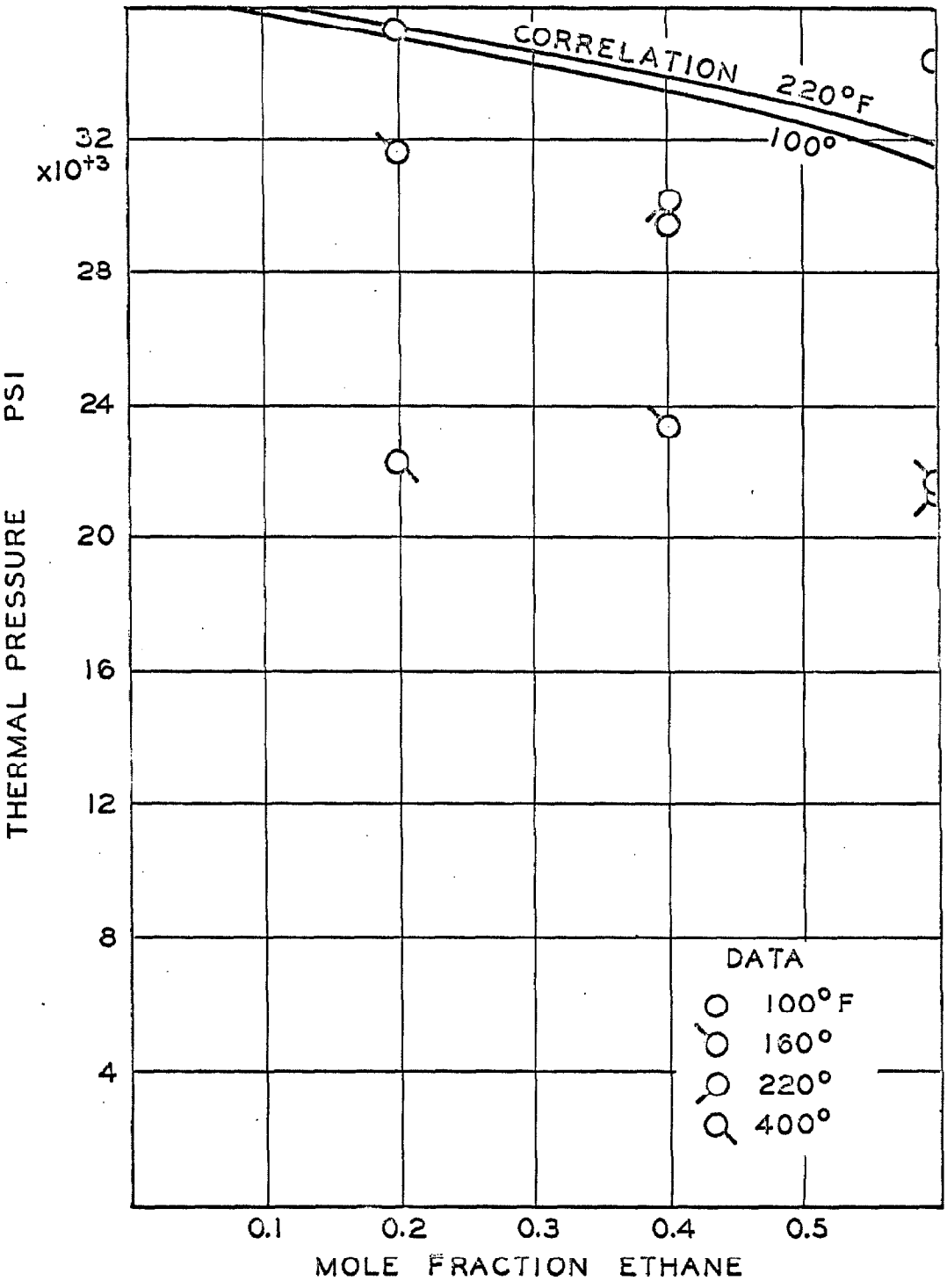

Fig. 7. Thermal Pressure of the Ethane-n-Decane System.

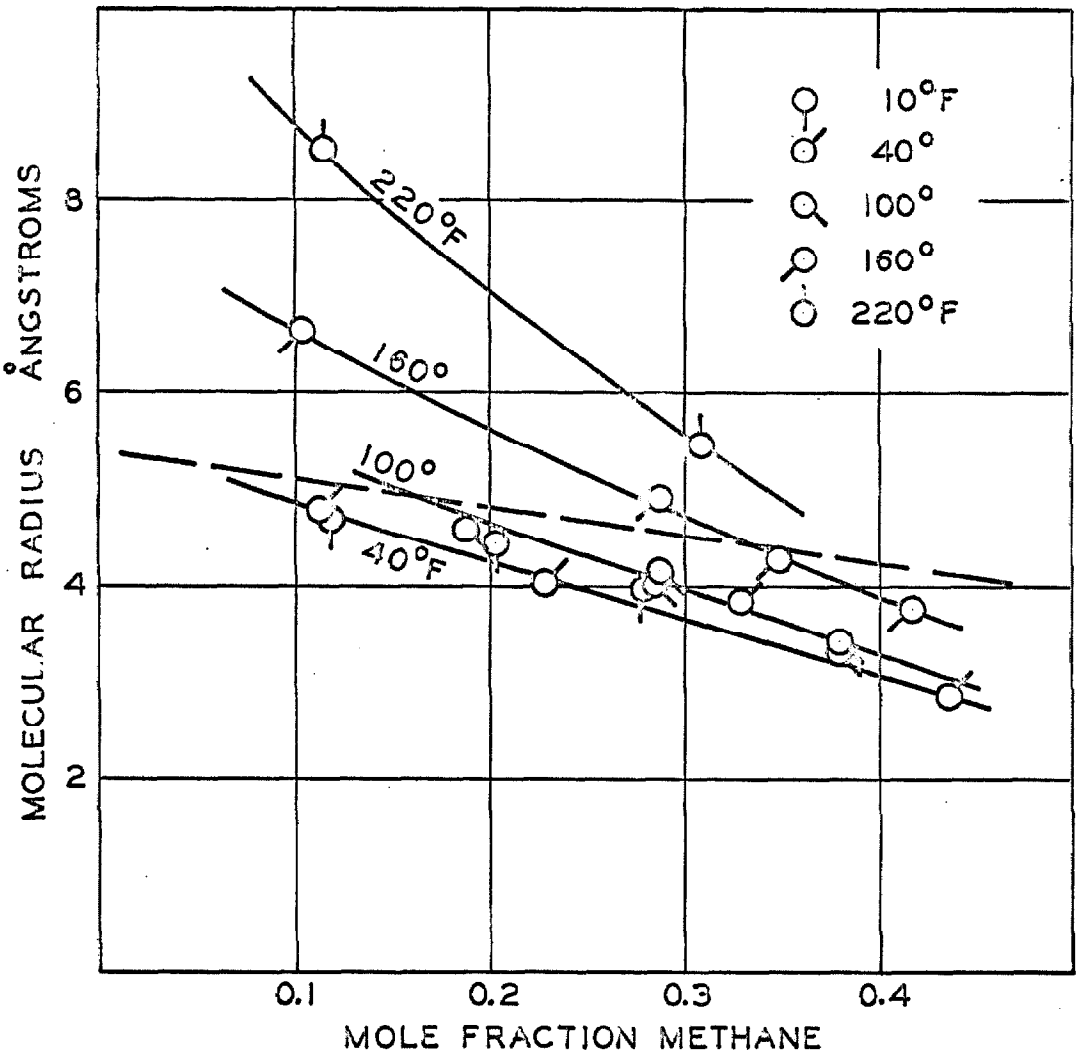

Fig. 8. Molecular Radius of Longuet-Higgins and Pople Calculated from Diffusion Coefficient and Estimated Thermal Pressure for Methane-n-Butane.

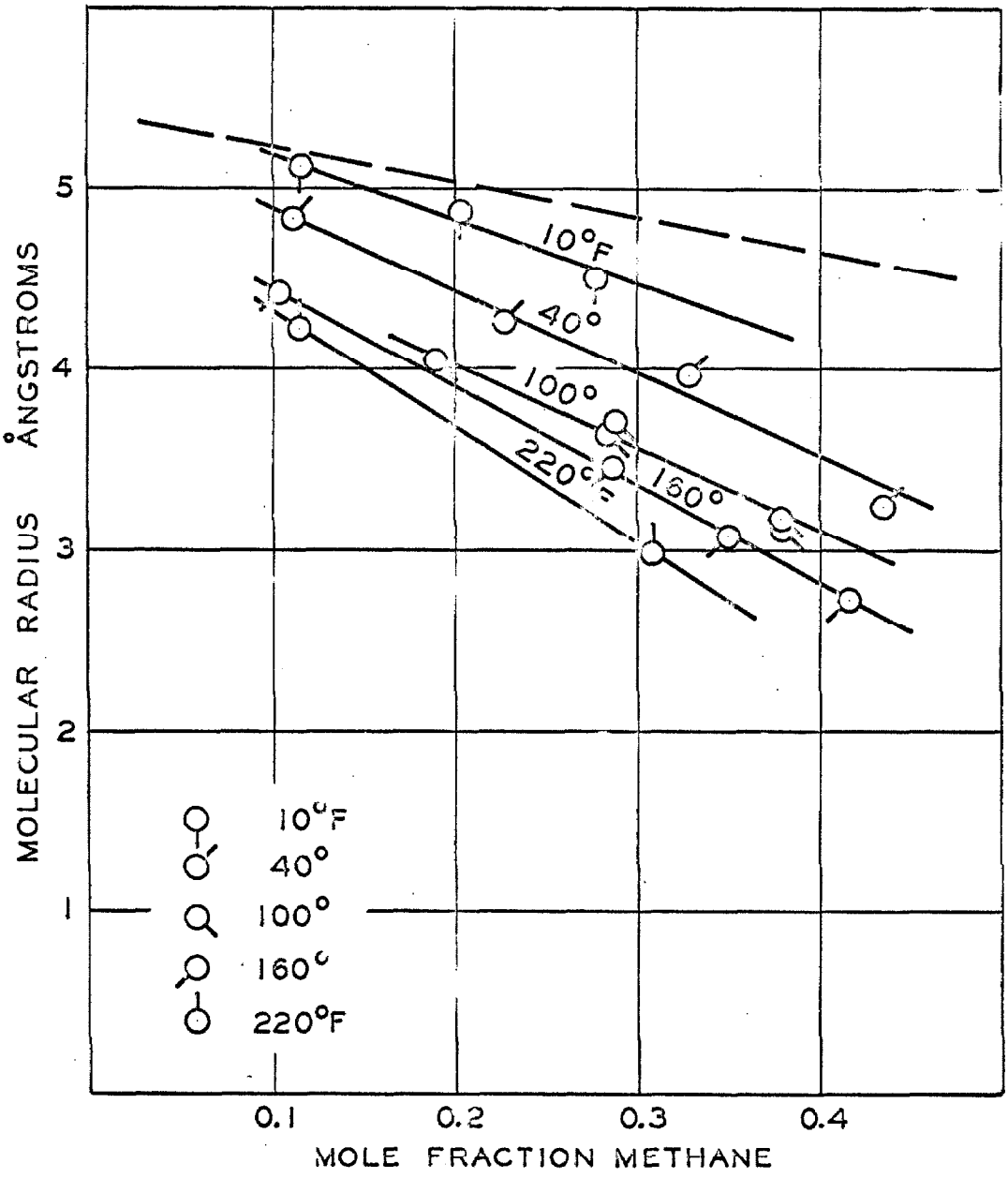

Fig. 9. Molecular Radius of Longuet-Higgins and Pople Evaluated from Viscosity and Diffusion Coefficient for Methane-n-Butane.

LIST OF TABLES

TABLE 1. Diffusion Data of Sage for Liquid Hydrocarbons

Chapman-Cowling Diffusion Coefficient sq ft/sec×10^8	Temp. deg. F	Concentration of Light Component lb/cu ft	Mole Fraction of Light Component	Pressure psi
		Methane-Propane		
19.48	40	1.909	0.1550	419.4
17.23	40	3.100	0.2474	621.1
17.15	40	3.690	0.2925	721.5
21.21	70	1.148	0.0994	360.8
19.67	70	1.657	0.1425	463.2
18.84	70	2.147	0.1838	563.1
14.64	70	3.656	0.3101	863.4
17.62	100	1.610	0.1482	565.0
17.01	100	2.213	0.2044	706.6
14.17	100	2.640	0.2446	807.1
11.19	100	3.076	0.2866	907.0
8.04	100	3.338	0.3325	1069.0
24.59	130	0.790	0.0793	484.4
16.42	130	1.599	0.1622	701.9
		Methane-n-Butane		
13.40	10	1.311	0.1174	284.5
13.91	10	2.360	0.2020	499.4
13.64	10	3.363	0.2765	700.1
14.51	40	1.221	0.1128	301.4
13.71	40	2.580	0.2262	603.0
14.64	40	3.912	0.3275	903.4
12.42	40	5.441	0.4349	1220.6
16.49	100	1.970	0.1888	598.5
15.95	100	3.070	0.2843	894.0
16.51	100	3.090	0.2858	899.7
14.37	100	4.208	0.3791	1195.4
14.84	100	4.206	0.3793	1193.7
23.58	160	0.949	0.1029	446.1
20.10	160	2.756	0.2864	1048.3
18.23	160	3.367	0.3491	1249.5
16.67	160	3.975	0.4158	1450.2
30.33	220	0.929	0.1149	615.6
21.23	220	2.460	0.3076	1218.8
		Methane-n-Pentane		
10.57	40	1.219	0.1274	342.2
10.14	40	5.408	0.4669	1484.8
13.71	100	3.218	0.3221	1053.5
13.48	100	1.187	0.1316	409.3
12.61	100	5.340	0.4920	1702.7

TABLE 1 (cont'd.)

Chapman-Cowling Diffusion Coefficient sq ft/sec $\times 10^8$	Temperature deg. F	Concentration of Light Component lb/cu ft	Mole Fraction of Light Component	Pressure psi
18.57	160	0.830	0.0999	377.2
17.63	160	2.074	0.2337	849.8
15.85	160	3.361	0.3584	1338.8
14.32	160	3.627	0.4170	1784.1
25.04	220	0.782	0.1019	452.7
21.54	220	1.636	0.2075	823.5
17.01	220	3.270	0.3888	1529.7
31.24	280	1.449	0.2059	918.1
23.64	280	1.881	0.2660	1123.2
		Methane-n-Heptane		
10.64	40	1.139	0.1453	410.6
8.74	40	2.147	0.2524	761.8
7.91	40	3.180	0.3454	1114.0
8.06	40	4.217	0.4256	1465.3
7.68	40	5.240	0.4943	1816.6
8.97	100	0.751	0.1049	335.7
13.26	100	2.459	0.2953	1062.4
12.53	100	3.347	0.3754	1426.3
11.68	100	4.222	0.4371	1777.6
15.24	160	1.489	0.2029	766.2
13.22	160	3.682	0.4186	1822.1
13.10	160	4.518	0.5015	2535.3
21.73	220	1.890	0.2585	1104.9
		Methane-n-Decane		
4.50	40	0.674	0.1187	345.3
4.12	40	4.820	0.5431	2483.8
2.87	40	6.461	0.6396	3357.9
6.42	100	0.904	0.1571	522.9
6.54	100	1.569	0.2515	924.3
7.51	100	2.245	0.3336	1333.7
6.68	100	4.039	0.5023	2377.4
5.64	100	5.922	0.6280	3416.1
15.76	220	1.071	0.1963	810.6
16.24	220	2.157	0.3452	1603.1
13.59	220	4.748	0.5897	3326.7
11.55	220	5.792	0.6614	3870.6
20.26	280	0.389	0.0818	333.0
19.55	280	0.977	0.1884	816.6
18.38	280	1.984	0.3365	1600.4
15.66	280	3.111	0.4667	2422.3
17.69	280	3.370	0.4927	2602.9

TABLE 1 (cont'd.)

Chapman-Cowling Diffusion Coefficient sq ft/sec $\times 10^8$	Temperature deg. F	Concentration of Light Component lb/cu ft	Mole Fraction of Light Component	Pressure psi
		Methane-White Oil		
0.43	40	0.538	0.1730	513.4
0.55	40	0.573	0.1823	546.7
1.41	100	0.520	0.1685	553.2
1.51	100	1.002	0.2883	1054.9
1.21	100	1.526	0.3858	1556.6
1.78	160	1.855	0.4422	2053.7
1.74	160	2.949	0.5661	3061.0
4.13	220	0.419	0.1486	548.7
3.81	220	0.815	0.2562	1050.4
2.66	220	1.980	0.4659	2427.0
2.98	220	2.889	0.5678	3431.2
6.83	280	0.373	0.1379	540.8
7.51	280	0.732	0.2413	1042.8
4.88	280	2.271	0.5131	3071.5
9.31	340	0.413	0.1552	641.6
7.87	340	0.748	0.2514	1145.5
		Ethane-n-Pentane		
11.56	40	2.86	0.1615	56.6
8.32	40	6.20	0.3268	112.9
11.76	40	9.29	0.4626	160.4
17.55	100	1.17	0.0731	56.4
12.81	100	11.63	0.5798	375.9
14.40	160	5.52	0.3278	329.0
15.48	160	9.08	0.5229	533.4
28.45	280	3.69	0.2822	597.6
		Ethane-n-Decane		
4.10	40	5.82	0.4275	164.3
4.45	40	12.05	0.6802	262.2
5.35	100	0.78	0.0782	47.4
5.67	100	1.185	0.1160	72.6
5.79	100	4.825	0.3829	251.3
5.80	100	7.165	0.5086	345.6
5.46	100	10.30	0.6382	448.6
7.82	160	1.70	0.1667	150.8
6.52	160	3.53	0.3108	294.7
7.85	160	4.96	0.4046	398.2
7.62	160	6.78	0.5070	522.0
6.52	160	8.54	0.5899	629.2
6.21	160	11.08	0.6920	770.0
9.22	220	0.875	0.0940	111.1

TABLE 1 (cont'd.)

Chapman-Cowling Diffusion Coefficient sq ft/sec $\times 10^8$	Temperature deg. F	Concentration of Light Component lb/cu ft	Mole Fraction of Light Component	Pressure psi
9.99	220	2.083	0.2067	254.5
9.76	220	4.875	0.4147	549.5
9.47	220	6.48	0.5092	706.1
9.15	220	10.45	0.6959	1070.0
13.09	280	1.610	0.1719	254.6
13.47	280	2.483	0.2513	383.5
12.43	280	3.202	0.3108	489.3
13.66	280	3.911	0.3648	590.2
13.14	280	4.589	0.4135	687.0
15.01	340	0.737	0.0874	159.4
16.55	340	1.490	0.1683	302.1
15.34	340	2.248	0.2423	439.7
15.43	340	2.291	0.2536	555.9
19.22	400	2.120	0.2438	516.9
18.96	400	2.650	0.2954	629.2
17.03	400	3.222	0.3484	746.4
		Ethane-White Oil		
1.94	100	2.34	0.3440	218.4
1.94	100	3.98	0.4867	330.0
2.18	100	5.94	0.6053	451.2
3.51	100	8.53	0.7140	596.5
2.05	220	0.70	0.1352	142.6
4.41	220	2.25	0.3531	453.4
7.92	220	4.07	0.5119	802.4
5.80	280	1.15	0.2117	288.7
5.62	340	0.88	0.1731	264.0
11.90	340	1.95	0.3200	600.0
6.49	400	0.94	0.1865	319.0
		n-Butane-n-Decane		
7.33	220	11.61	0.516	112.5
9.24	220	17.74	0.714	158.4
12.92	280	6.32	0.331	115.5
11.84	280	14.09	0.633	232.5
11.65	280	16.24	0.704	265.4
19.51	340	4.27	0.249	130.6
21.65	340	8.13	0.433	230.0
19.83	340	11.87	0.593	326.2

TABLE 2. Liquid Hydrocarbon Diffusion Data

Author	System	Temperature deg. F	Diffusion Coefficient sq ft/sec X 10^8	Mole Fraction Light Component
Fishman	n-Pentane	96.0	6.76	
		77.0	6.05	
		32.0	4.45	
		-9.25	3.20	
		-109.5	1.485	
	n-Heptane	204.5	7.06	
		176.4	6.31	
		143.8	4.54	
		90.5	3.47	
		32.0	2.24	
		-9.25	1.64	
		-109.5	0.446	
McCall	n-Pentane	77.0	5.87	
	n-Hexane	77.0	4.54	
	n-Heptane	77.0	3.36	
	n-Octane	77.0	2.15	
	n-Nonane	77.0	1.83	
	n-Decane	77.0	1.41	
	n-Octadecane	122.0	0.495	
	n-Dicetyl	212.0	0.323	
Trevoy	nC_7-nC_{12}	77	1.69	0.5
		113	2.30	0.5
		149	2.88	0.5
	nC_7-nC_{14}	77	1.38	0.5
	nC_7-nC_{16}	77	1.08	0.5
		113	1.55	0.5
		149	2.20	0.5
	nC_7-nC_{18}	77	0.99	0.5
Bidlack	nC_7-nC_{16}	77	0.818	0.0239
		77	0.965	0.2080
		77	1.147	0.4179
		77	1.331	0.6066
		77	1.562	0.7976
		77	1.698	0.8936
		77	1.911	0.9944

TABLE 2 (cont'd.)

Author	System	Temperature deg. F	Diffusion Coefficient sq ft/sec $\times 10^8$	Mole Fraction Light Component
Bidlack	nC_6-nC_{12}	77	1.561	0.0245
		77	1.740	0.2091
		77	1.935	0.4019
		77	2.22	0.6377
		77	2.51	0.8011
		77	2.72	0.8987
		77	2.94	0.9942
	nC_6-nC_{16}	77	0.935	0.0146
		77	1.191	0.2578
		77	1.350	0.3975
		77	1.610	0.6076
		77	1.793	0.7496
		77	1.960	0.8469
		77	2.082	0.9047
		77	2.360	0.9958
	nC_6-$CC\ell_4$	77	4.15	0.9958
Van Geet	nC_8-nC_{12}	77	1.297	0.1412
		77	1.422	0.3892
		77	1.547	0.5980
		77	1.675	0.7763
		77	1.791	0.9302
		140	2.23	0.1412
		140	2.42	0.3892
		140	2.56	0.5980
		140	2.71	0.7763
		140	2.83	0.9302
	n-Octane	77	2.54	-
		140	3.72	-
	n-Dodecane	77	0.875	-
		140	1.598	-

TABLE 3. Comparison of Diffusion Coefficients Evaluated with Truncated and Untruncated Formulas

Pressure psi	Temperature deg. F	Chapman-Cowling Diffusion Coefficient, sqft/sec $\times 10^8$		-M
		Truncated Formula	Untruncated Formula	
		Methane-n-Pentane		
342.2	40	10.58	11.81	0.0478
1484.8	40	9.68	12.47	0.1081
409.3	100	13.54	14.78	0.0384
1053.5	100	14.23	15.96	0.0498
1702.7	100	12.62	15.39	0.0856
377.2	160	18.68	20.06	0.0313
849.8	160	17.71	19.55	0.0431
1338.8	160	15.61	18.07	0.0635
1784.1	160	14.17	18.08	0.1042
452.7	220	25.06	27.25	0.0367
823.5	220	21.72	24.66	0.0552
1529.7	220	16.93	21.22	0.0970
918.1	280	31.81	39.13	0.0891
1123.2	280	24.19	32.27	0.1227
		Methane-n-Decane		
345.3	40	4.39	4.57	0.0174
2483.8	40	4.51	5.03	0.0472
3357.9	40	3.83	4.48	0.0682
522.9	100	6.39	6.81	0.0280
924.3	100	6.62	6.97	0.0225
1333.7	100	7.66	8.00	0.0190
2377.4	100	7.16	7.59	0.0261
3416.1	100	7.25	7.88	0.0364
810.6	220	15.79	16.39	0.0164
1601.3	220	16.13	16.84	0.0191
3326.7	220	17.32	19.07	0.0419
3870.6	220	17.05	19.61	0.0608
332.9	280	20.11	20.69	0.0124
816.6	280	19.38	20.10	0.0162
1600.4	280	18.36	19.22	0.0201
2422.3	280	16.07	17.44	0.0357
2602.9	280	18.40	20.50	0.0470

TABLE 4. Estimated Uncertainties in Evaluation of Diffusion Coefficients

Pressure psi	Temperature deg. F	Variables and Estimated Uncertainties* $\sigma_{j\ell}$ lb/cu ft	$\overline{V}_{j\ell}$ lb/cu ft	σ_{ko} lb/cu ft	σ_{kbi} lb/cu ft	$10^{12} x_b^2$ lb/sq ft sec	D_{Ckj} sq ft/sec $\times 10^8$
			Methane-n-Pentane				
342.2	40	37.56	0.0242	1.219	0.136	77.97	11.81
		0.1	0.0005	0.05	0.05	5.21	7.57
1484.8	40	27.77	0.0189	5.408	4.142	101.2	12.47
		0.3	0.002	0.15	0.15	4.7	8.14
409.3	100	35.22	0.0260	1.187	0.280	69.06	14.78
		0.2	0.0005	0.03	0.03	0.25	9.77
1053.5	100	30.47	0.0251	3.218	2.264	77.79	15.96
		0.2	0.0005	0.03	0.03	0.44	4.12
1702.7	100	28.02	0.0195	5.340	4.330	74.65	15.39
		0.2	0.002	0.05	0.05	2.78	9.74
377.2	160	33.65	0.0280	0.830	0.069	65.94	20.06
		0.2	0.0005	0.03	0.03	0.85	18.27
849.8	160	30.59	0.0272	2.074	1.280	68.06	19.55
		0.2	0.0005	0.03	0.03	0.90	6.53
1338.8	160	27.07	0.0255	3.361	2.518	66.10	18.07
		0.2	0.0005	0.03	0.03	1.10	3.73
1784.1	160	22.81	0.0224	4.627	3.756	60.06	18.08
		0.3	0.0015	0.05	0.05	0.44	7.38
452.7	220	30.99	0.0300	0.782	0.114	67.73	27.25
		0.2	0.0005	0.03	0.03	0.73	14.51
823.5	220	28.11	0.0291	1.636	0.925	65.29	24.66
		0.2	0.0005	0.03	0.03	0.34	7.41
1529.7	220	23.12	0.0251	3.270	2.551	49.28	21.22
		0.3	0.001	0.05	0.05	0.50	6.88

* Uncertainties listed below variables.

TABLE 4 (cont'd.)

Pressure psi	Temperature deg. F	Variables and Estimated Uncertainties* $\sigma_{j\ell}$ lb/cu ft	$\bar{V}_{j\ell}$ lb/cu ft	σ_{ko} lb/cu ft	σ_{kbi} lb/cu ft	$10^{12} \times b^2$ lb/sq ft sec	D_{Ckj} sq ft/sec $\times 10^8$
918.1	280	25.14	0.0294	1.449	0.843	67.73	39.13
		0.2	0.0005	0.03	0.03	2.00	9.14
1123.2	280	23.35	0.0267	1.881	1.260	53.14	32.27
		0.3	0.0005	0.05	0.05	1.26	8.33
			Methane-n-Decane				
345.3	40	45.3	0.0214	0.674	0.003	11.83	4.57
		0.3	0.0003	0.05	0.05	0.14	6.56
2483.8	40	35.9	0.02085	4.820	3.559	21.04	5.03
		0.5	0.0003	0.05	0.05	3.33	1.67
3357.9	40	32.2	0.02056	6.461	4.840	15.57	4.48
		0.5	0.0003	0.05	0.05	1.79	1.40
522.9	100	42.95	0.02215	0.904	0.0	29.91	6.81
		0.1	0.0002	0.03		0.60	3.73
924.3	100	41.45	0.0220	1.569	0.904	15.32	6.97
		0.1	0.0002	0.03	0.03	0.43	2.30
1333.7	100	39.9	0.0218	2.245	1.729	9.52	8.00
		0.1	0.0002	0.03	0.03	0.17	2.12
2377.4	100	35.65	0.0213	4.039	3.435	8.23	7.59
		0.2	0.0002	0.03	0.03	0.19	1.54
3416.1	100	30.05	0.0208	5.922	5.276	4.74	7.88
		0.3	0.0003	0.03	0.03	0.11	1.90
810.6	220	38.95	0.0238	1.071	0.668	13.91	16.39
		0.1	0.0002	0.02	0.02	0.50	6.07
1601.3	220	36.3	0.0234	2.157	1.739	12.97	16.84
		0.1	0.0002	0.03	0.03	0.25	4.35

* Uncertainties listed below variables.

TABLE 4 (cont'd.)

Pressure	Temperature	Variables and Estimated Uncertainties*					
		$\sigma_{j\ell}$	$\overline{V}_{j\ell}$	σ_{ko}	σ_{kbi}	$10^{12} x_b^2$	D_{Ckj}
psi	deg. F	lb/cu ft	lb/cu ft	lb/cu ft	lb/cu ft	lb/sq ft sec	sq ft/sec $\times 10^8$
3326.7	220	28.3	0.0209	4.748	4.239	8.34	19.07
		0.1	0.0002	0.03	0.03	2.16	6.10
3870.6	220	26.25	0.0188	5.792	5.201	6.74	19.61
		0.1	0.0004	0.03	0.03	0.44	5.32
332.9	280	38.8	0.02515	0.389	0.040	14.45	20.69
		0.1	0.0002	0.02	0.02	0.46	20.41
816.6	280	37.3	0.0249	0.977	0.607	14.43	20.10
		0.1	0.0002	0.03	0.03	0.19	7.99
1600.4	280	34.7	0.0244	1.984	1.589	13.36	19.22
		0.1	0.0002	0.03	0.03	0.45	5.01
2422.3	280	31.65	0.0233	3.111	2.551	18.23	17.44
		0.1	0.0003	0.03	0.03	0.78	3.79
2602.9	280	30.9	0.0230	3.370	2.667	30.55	20.50
		0.1	0.0004	0.03	0.03	1.65	4.82

* Uncertainties listed below variables.

TABLE 5. Empirical Equations for Individual Binary Systems

Equation	Number
$D_{Ckj} = C_1 + C_2t^2 + C_3\chi + C_4t^2\chi$	I
$D_{Ckj} = C_1 + C_2t^2 + C_3\chi + C_4t\chi$	II
$D_{Ckj} = C_1 + C_2t + C_3\chi + C_4t\chi$	III
$D_{Ckj} = C_1 + C_2t + C_3\chi + C_4t^2\chi$	IV
$D_{Ckj} = C_1 + C_2t^2 + C_3t^2\chi$	V
$D_{Ckj} = C_1 + C_2t^{1.5} + C_3t^{1.5}\chi$	VI
$D_{Ckj} = C_1 + C_2t + C_3t^2\chi$	VII
$D_{Ckj} = C_1 + C_2t + C_3t\chi$	VIII

TABLE 6. Value to Be Subtracted from Absolute Temperature

System	Subtracted Temperature, deg. R
Methane-Propane	461.8
Methane-n-Butane	464.0
Methane-n-Pentane	527.0
Methane-n-Heptane	42.
Methane-n-Decane	472.4
Methane-White Oil	296.
Ethane-n-Pentane	521.6
Ethane-n-Decane	586.
Ethane-White Oil	531.8

TABLE 7. Standard Deviation for Empirical Equations for Individual Binary Systems

Equation Number	Standard Deviation $\times 10^8$, sq ft/sec			Average Per Cent Deviation, Mole Frac. C_1
	χ = Concentration of C_1	Weight Fraction C_1	Mole Fraction C_1	
		Methane-Propane		
I	1.16	0.94	0.85	3.8
II	1.66	1.43	1.36	6.1
III	1.54	1.26	1.15	5.3
IV	0.90	0.76	0.72	2.8
V	1.18	0.94	0.90	4.2
VI	1.29	1.05	0.96	4.6
VII	0.86	0.73	0.71	2.8
VIII	1.27		0.93	4.4
		Methane-n-Butane		
I	1.07	0.812	0.77	3.2
II	1.54	1.28	1.31	5.4
III	0.96	1.07	1.02	4.8
IV	1.37	1.44	1.47	6.4
V	1.05	0.80	0.76	3.4
VI	0.86	0.70	0.65	3.2
VII	1.54	1.74	1.86	8.8
VIII	0.97		0.98	4.8
		Methane-n-Pentane		
I	1.65	1.42	1.34	5.2
II	2.10	1.93	1.92	8.4
III	1.64	1.59	1.62	5.5
IV	1.83	1.93	2.11	7.9
V	1.57	1.38	1.31	5.5
VI	1.54	1.40	1.37	4.9
VII	1.77	1.84	2.03	7.8
VIII	1.84		1.76	6.4
		Methane-n-Heptane		
I	1.67	1.65	1.68	9.8
II	1.67	1.65	1.68	10.0
III	2.17	2.15	2.18	11.2
IV	2.09	2.06	1.99	10.8
V	1.62	1.62	1.63	10.6
VI	1.78	1.77	1.80	10.7
VII	2.11	2.11	2.07	11.2
VIII	1.72		1.75	10.0

TABLE 7 (cont'd.)

Equation Number	Standard Deviation $\times 10^8$, sq ft/sec			Average Per Cent Deviation, Mole Frac. C_1
	χ = Concentration of C_1	Weight Fraction C_1	Mole Fraction C_1	
		Methane-n-Decane		
I	1.34	1.34	1.34	10.6
II	1.39	1.38	1.40	11.0
III	0.92	0.91	0.94	8.2
IV	0.93	0.92	0.99	9.0
V	1.36	1.35	1.34	11.3
VI	1.03	1.01	1.03	8.0
VII	0.91	0.90	0.99	9.7
VIII	0.89		0.91	8.0
		Methane-White Oil		
I	0.54	0.54	0.52	12.8
II	0.56	0.56	0.55	15.9
III	0.68	0.69	0.67	23.8
IV	0.70	0.70	0.67	22.2
V	0.52	0.52	0.50	12.1
VI	0.51	0.52	0.50	13.0
VII	0.78	0.80	0.86	41.9
VIII	0.66		0.66	25.5
		Ethane-n-Pentane*		
I	3.36	3.26	2.95	13.3
II	3.87	3.83	3.59	16.2
III	2.67	2.65	2.34	10.5
IV	2.50	2.91	3.00	11.1
V	3.13	3.02	2.75	13.3
VI	2.75	2.68	2.33	11.6
VII	2.35	2.70	2.85	11.9
VIII	2.23		2.26	11.3
		Ethane-n-Decane*		
I	0.83	0.83	0.85	6.7
II	0.81	0.82	0.82	6.2
III	0.73	0.75	0.80	7.1
IV	0.86	0.87	0.90	8.5
V	0.85	0.84	0.85	7.1
VI	0.64	0.63	0.65	4.8
VII	0.85	0.86	0.89	8.5
VII	0.80		0.83	7.9

* Values for Ethane are for C_2 instead of C_1.

TABLE 7 (cont'd.)

Equation Number	Standard Deviation $\times 10^8$, sq ft/sec			Average Per Cent Deviation, Mole Frac. C_2
	χ = Concentration of C_2	Weight Fraction C_2	Mole Fraction C_2	
		Ethane-White Oil		
I	0.94	1.00	0.87	12.5
II	1.27	1.31	1.15	15.0
III	1.31	1.35	1.17	15.7
IV	0.94	1.00	0.93	14.0
V	0.95	1.00	0.82	13.4
VI	1.20	1.26	0.96	15.0
VII	0.93	0.99	0.88	14.3
VIII	1.51		1.17	17.4
		n-Butane-n-Decane*		
VIII	1.66			8.7

* Values for n-Butane-n-Decane are for C_4 instead of C_2.

TABLE 8. Generalized Empirical Equations

Equation	Number
$D_{Ckj} = C_1 + C_2/M_j + [C_3/M_j + (C_4 + C_5/M_j^2)\chi]t^{1.5}$	I
$D_{Ckj} = C_1 + C_2/M_j + [C_3/M_j + (C_4 + C_5/M_j)\chi]t^{1.5}$	II
$D_{Ckj} = C_1 + C_2/M_j^{0.5} + [C_3/M_j^{0.5} + (C_4 + C_5/M_j^{0.5})\chi]t^{1.5}$	III
$D_{Ckj} = [C_1 + (C_2 + C_3\chi)t^{1.5}]/M_j$	IV
$D_{Ckj} = (C_1 + C_2t^{1.5})/M_j + C_3\chi t^{1.5}/M_j^{0.5}$	V
$D_{Ckj} = C_1 + [C_2 + (C_3 + C_4\chi)t^{1.5}]/M_j$	VI
$D_{Ckj} = C_1 + (C_2 + C_3t^{1.5})/M_j + C_4\chi t^{1.5}/M_j^{0.5}$	VII
$D_{Ckj} = (C_1 + C_2t^{1.5})/M_j^{0.5} + C_3\chi t^{1.5}/M_j^2$	VIII
$D_{Ckj} = C_1 + (C_2 + C_3t^{1.5})/M_j^{0.5} + C_4\chi t^{1.5}/M_j^2$	IX
$D_{Ckj} = (C_1 + C_2t^{1.5})/M_j + C_3\chi t^{1.5}/M_j^2$	X
$D_{Ckj} = C_1 + (C_2 + C_3t^{1.5})/M_j + C_4\chi t^{1.5}/M_j^2$	XI
$D_{Ckj} = [C_1 + (C_2 + C_3\chi)t^{1.5}]/M_j^{0.5}$	XII
$D_{Ckj} = C_1 + [C_2 + (C_3 + C_4\chi)t^{1.5}]/M_j^{0.5}$	XIII
$D_{Ckj} = C_1 + (C_2 + C_3t^{1.5})/M_j$	XIV
$D_{Ckj} = C_1 + C_2/M_j + [C_3/M_j + (C_4 + C_5/M_j^2)\chi]T^{1.5}$	XV
$D_{Ckj} = C_1 + C_2/M_j + [C_3 + C_4/M_j + (C_5 + C_6/M_j^2)\chi]t^{1.5}$	XVI
$D_{Ckj} = C_1 + (C_2 + C_3\chi)t + (C_4 + C_5\chi t)/M_j^3$	XVII
$D_{Ckj} = C_1 + [C_2 + (C_3 + C_4\chi)/M_j^3]t$	XVIII

TABLE 8 (cont'd.)

Equation	Number
$D_{Ckj} = C_1 + (C_2 + C_3\chi)t + (C_4 + C_5\chi t)/M_j^2$	XIX
$D_{Ckj} = C_1 + [C_2 + (C_3 + C_4\chi)/M_j^2]t$	XX
$D_{Ckj} = C_1 + [C_2 + (C_3 + C_4\chi)t^{1.5}](1/M_k + 1/M_j)^{0.5} + C_5\chi t^{1.5}$	XXI

TABLE 9. Standard Deviations for Generalized Empirical Equations

Equation Number	Standard Deviation $\times 10^8$, sq ft/sec			Average Per Cent Deviation, Mole Frac. C_1
	χ = Concentration of C_1	Weight Fraction C_1	Mole Fraction C_1	
		Methane-Hydrocarbon		
I	2.11	1.98	2.29	30.2
II	2.55	2.26	2.87	40.0
III	2.03	1.89	2.19	15.8
IV	2.90	2.54	2.98	28.7
V	3.01	2.91	3.01	29.6
VI	2.83	2.51	2.88	42.7
VII	2.93	2.83	2.94	42.5
VIII	3.63	3.61	3.63	68.1
IX	1.80	1.71	1.89	24.4
X	2.19	2.10	2.14	31.2
XI	2.21	1.98	2.29	33.0
XII	3.58	3.59	3.40	64.1
XIII	2.06	1.96	2.18	15.8
XV	2.98	2.66	2.78	36.6
XVI	2.11	1.98	2.30	30.9
XVII		5.09		78.2
XVIII		4.80		97.5
XIX	4.69	4.52		57.2
XX	4.33			-

TABLE 9 (cont'd.)

Equation Number	Standard Deviation $\times 10^8$, sq ft/sec			Average Per Cent Deviation Mole Frac. C_2
	χ = Concentration of C_2	Weight Fraction C_2	Mole Fraction C_2	
	Ethane-Hydrocarbon			
I	1.35	1.36	1.57	12.8
II	1.54	1.35	1.74	14.2
III	2.39	1.89	2.33	21.8
IV	1.59	1.61	1.60	15.7
V	1.58	1.59	1.39	14.5
VI	1.32	1.33	1.34	11.8
VII	1.33	1.33	1.36	11.8
VIII	2.47	2.40	2.41	27.4
IX	1.89	1.86	1.88	17.8
X	1.62	1.62	1.62	16.0
XI	1.34	1.36	1.35	12.2
XII	2.81	2.76	2.82	34.1
XIII	1.91	1.91	1.91	18.7
XIV	1.60			13.2
XV	1.71	1.72	1.64	15.7
XVI	1.36	1.37	1.77	14.4
XVIII		2.44		29.1
XIX	2.35			
XX	2.07			
	Both Methane and Ethane Hydrocarbon			
XXI	5.26	5.11	5.00	89.0

TABLE 10. Constants for the Best Generalized Empirical Equations

Equation Number	Constants and 95 Per Cent Uncertainties × 10^8				
	C_1	C_2	C_3	C_4	C_5
			Methane-Hydrocarbon Systems		
III	-12.17	191.1	0.0388	0.02031	-0.3138
	2.0	17.4	0.0040	0.0143	0.145
IX	-13.29	203.7	0.04058	-105.9	
	1.60	14.6	0.00330	22.6	
XIII	-10.40	174.6	0.03851	-0.1166	
	1.58	13.5	0.00414	0.0452	
			Ethane-Hydrocarbon Systems		
II	-1.463	819.9	0.2734	0.0001906	-0.2172
	1.367	164.2	0.0295	0.00469	0.5518
VI	-1.426	815.8	0.2735	-0.1970	
	1.011	127.4	0.0290	0.2349	
VII	-1.262	796.6	0.2742	-0.01916	
	0.977	118.8	0.0292	0.02244	

TABLE 11. Constants and Standard Deviations for Equations Relating Diffusion Coefficient and Total Concentration

System	Standard Deviation $\times 10^8$ sq ft/sec	Constant Number	Constant $\times 10^8$	Est. Uncertainty on Constant $\times 10^8$
C_1-C_3	1.81	1	-33.9	52.1
		2	- 0.107	0.54
		3	1.57	1.85
		4	0.0081	0.0199
C_1-nC_4	1.65	1	-31.1	20.3
		2	0.159	0.103
		3	1.20	0.579
		4	- 0.00163	0.00324
C_1-nC_5	2.40	1	-16.6	30.8
		2	0.107	0.152
		3	0.621	0.896
		4	- 0.000491	0.00493
C_1-nC_7	1.78	1	-40.3	43.3
		2	0.325	0.301
		3	1.13	1.08
		4	- 0.00643	0.00798
C_1-nC_{10}	1.00	1	- 2.98	17.0
		2	0.00137	0.0879
		3	0.0691	0.415
		4	0.00179	0.00226
C_1-WO	0.72	1	-65.3	32.3
		2	0.170	0.100
		3	1.18	0.591
		4	- 0.00247	0.00203
C_2-nC_5	4.02	1	-50.2	78.0
		2	0.198	0.343
		3	1.49	2.15
		4	- 0.00182	0.0108
C_2-nC_{10}	0.81	1	- 9.67	8.73
		2	0.0822	0.0340
		3	0.275	0.219
		4	- 0.00105	0.000922
C_2-WO	2.42	1	37.9	104.0
		2	- 0.0744	0.588
		3	- 0.752	2.13
		4	0.00189	0.0122

TABLE 12. Equations of Eyring Form for Individual Binary Systems

Equation	Number
$D_{Ckj} = \exp[C_1 + (C_2 + C_3 \overset{n}{\cdot}_k)/T]$	I
$D_{Ckj} = \exp[C_1 + (C_2 + C_3 \sigma_k)/T]$	II
$D_{Ckj} = \exp[C_1 + C_2 \sigma_k + (C_3 + C_4 \sigma_k)/T]$	III
$D_{Ckj} = T \exp[C_1 + (C_2 + C_3 \overset{n}{\cdot}_k)/T]$	IV
$D_{Ckj} = T^{0.5} \exp[C_1 + (C_2 + C_3 n_k)/T]$	V

TABLE 13. Standard Deviation for Equations of Table 12

Equation No.	Standard Deviation × 10^8 sq. ft./sec.	Average Per Cent Deviation
	Methane-Propane	
I	2.12	10.9
II	2.46	
III	1.58	
IV	2.11	10.9
V	2.17	11.0
	Methane-n-Butane	
I	1.55	7.1
II	1.80	
III	0.87	
IV	1.49	6.7
V	1.55	7.0
	Methane-n-Pentane	
I	2.10	8.8
II	2.26	
III	1.48	
IV	2.04	8.6
V	2.12	9.0
	Methane-n-Heptane	
I	1.60	9.1
II	1.59	
III	1.93	
IV	1.57	9.1
V	1.54	9.1
	Methane-n-Decane	
I	0.98	7.9
II	0.96	
III	0.98	
IV	1.02	8.1
V	0.96	7.0
	Methane-White Oil	
I	0.51	12.4
II	0.51	
IV	0.52	13.1
V	0.52	13.5
	Ethane-Pentane	
I	2.24	11.2
II	2.31	
IV	2.17	11.2

TABLE 13 (cont'd.)

V	2.27	11.7
	Ethane-Decane	
I	0.69	6.1
II	0.68	
IV	0.67	5.8
V	0.66	5.9
	Ethane-White Oil	
I	1.53	23.1
II	2.02	
IV	1.57	23.5
V	2.05	29.7
	Butane-Decane	
I	1.30	7.0
IV	1.29	6.9

TABLE 14. Activation Energies for Diffusion at Infinite Dilution of Light Component

Equation Number	Activation Energy, k cal/g mole: Calculated at $n_k = 0$	McCall's Self-Diffusion Value
	Methane-Propane	
I	-2.60	
II	-3.37	
III	3.72	
IV	-4.55	
V	-3.34	
	Methane-n-Butane	
I	3.16	
II	2.75	
III	5.44	
IV	1.15	
V	2.27	
	Methane-n-Pentane	
I	5.19	1.5
II	5.00	
III	7.83	
IV	2.92	
V	4.08	
	Methane-n-Heptane	
I	5.33	2.2
II	5.22	
III	5.58	
IV	3.26	
V	4.32	
	Methane-n-Decane	
I	7.61	3.6
II	7.50	
III	7.94	
IV	5.36	
V	6.55	

TABLE 14 (cont'd)

Equation Number	Activation Energy, k cal/g mole: Calculated at $n_k = 0$	McCall's Self-Diffusion Value
	Methane-White Oil	
I	11.42	
II	11.50	
III	11.48	
IV	8.96	
V	10.43	
	Ethane-n-Pentane	
I	4.75	1.5
II	4.54	
III	7.76	
IV	2.56	
V	3.68	
	Ethane-n-Decane	
I	6.86	3.6
II	6.83	
III	7.36	
IV	4.36	
V	5.58	
	Ethane-White Oil	
I	17.17	
II	13.32	
III	8.94	
IV	14.65	
V	11.60	
	n-Butane-n-Decane	
I	15.42	3.6
IV	12.78	

TABLE 15. Constants for Generalized Equations of Eyring Form

Equation No.*	Constant No.	Constant	Est. Uncertainty on Constant	Standard Deviation $\times 10^8$ sq. ft. /sec.
		Methane-Hydrocarbon		
			with white oil	
1	1	-13.6	0.37	2.98
	2	-1480.0	312.	
	3	-445.0	224	
	4	24900.0	6280	
			without white oil	
1	1	-13.5	0.30	2.42
	2	-1400	255	
	3	-512	184	
	4	20,500	5240	
			with white oil	
2	1	-13.4	0.493	2.03
	2	-.670	1.85	
	3	-846.0	291.	
	4	-4.30	.701	
	5	121.	1240.	
	6	-18100.	22,000.	
			without white oil	
2	1	-13.4	.554	2.20
	2	-.721	2.06	
	3	-818.	320.	
	4	-4.76	1.48	
	5	288.	1450.	
	6	-27100.	32,400.	
		Ethane-Hydrocarbon		
			with white oil	
1	1	-13.3	.278	1.49
	2	-2460.	265.	
	3	-154.	168.	
	4	81300.	8480.	

* Equation 1: $D_{Ckj} = \exp[C_1+(C_2+C_3 n_k+C_4/M_j)/T]$

2: $D_{Ckj} = \exp[C_1+C_2 n_k+(C_3+C_4 M_j+C_5 n_k+C_6 n_k/M_j)/T]$

Equation No.	Constant No.	Constant	Est. Uncertainty on Constant	Standard Deviation $\times 10^8$ sq. ft. / sec.
			without white oil	
1	1	-13.3	.227	1.14
	2	-2420.	220.	
	3	-209.	136.	
	4	79400.	7490.	
			with white oil	
2	1	-14.8	.963	2.29
	2	3.67	3.22	
	3	-387.	589.	
	4	-2.29	1.16	
	5	-3420.	2230.	
	6	96400.	53900.	
			without white oil	
2	1	-12.7	.595	1.04
	2	-1.56	1.84	
	3	-854.	292.	
	4	-9.95	1.66	
	5	1440.	1460.	
	6	-66000.	45200.	

TABLE 16. Molecular Radii of Eyring and of Longuet-Higgins and Pople Determined from Viscosity and Diffusion Coefficients

Temperature, Deg. F	Mole Fraction, Light Component	Viscosity$\times 10^7$ lb. sec. /sq. ft.	Molecular Radius, Ångstroms, of Eyring	of Pople
		Methane-Propane System		
40	0.1550	20.52	12.5	3.96
40	0.2474	17.71	16.3	3.43
40	0.2925	16.39	17.8	3.28
70	0.0994	18.54	13.4	3.94
70	0.1425	17.39	15.4	3.66
70	0.1838	16.27	17.3	3.46
70	0.3101	13.09	27.6	2.72
100	0.1482	14.15	22.4	3.14
100	0.2044	12.74	25.6	2.94
100	0.2446	11.83	33.4	2.59
100	0.2866	10.90	45.8	2.21
100	0.3325	8.78	79.5	1.74
130	0.0793	12.69	18.9	3.58
130	0.1622	10.96	32.8	2.73
		Methane-n-Butane System		
10	0.1174	42.38	8.28	5.11
10	0.2020	38.65	8.75	4.86
10	0.2765	35.15	9.79	4.50
40	0.1128	36.18	9.50	4.84
40	0.2262	31.11	11.7	4.25
40	0.3275	26.59	12.8	3.96
40	0.4349	21.85	18.4	3.24
100	0.1888	24.10	14.1	4.05
100	0.2843	20.78	16.9	3.64
100	0.2858	20.77	16.3	3.70
100	0.3791	17.40	22.4	3.12
100	0.3793	17.34	21.8	3.16
160	0.1029	19.62	13.4	4.42
160	0.2864	14.69	21.0	3.46
160	0.3491	12.88	26.4	3.08
160	0.4158	10.96	33.9	2.73
220	0.1149	13.40	16.7	4.22
220	0.3076	9.45	33.9	2.98
		Methane-White Oil System		
100	0.1685	2090.	1.90	20.3
100	0.2883	1107.	3.33	14.4
100	0.3858	860.	5.36	10.8

TABLE 16 (cont'd.)

Ethane-White Oil System

100	0.3440	955.	3.02	14.8
100	0.4867	580.	4.96	10.5
100	0.6053	255.	10.07	6.76

TABLE 17. Solubility Parameters and Molar Volumes

Hydrocarbon	Solubility Parameter, $(psi)^{1/2}$	Molar Volume ml/gmole
Methane	140.0	52
Ethane	149.1	68
Propane	157.7	84
n-Butane	165.8	101.4
n-Pentane	173.0	116.1
n-Heptane	183.1	147.5
n-Decane	190.2	196.0

TABLE 18. Molecular Radii of Longuet-Higgins and Pople Calculated from Diffusion Coefficients and Estimated Thermal Pressures

Temperature Deg. F	Mole Fraction Lt. Component	Estimated Thermal Pressure $\times 10^{-3}$, psi	Molecular Radius, Ångstroms
	Methane-Propane		
40	0.1550	24.7	4.24
40	0.2474	24.6	3.52
40	0.2925	24.5	3.40
70	0.0994	24.9	4.64
70	0.1425	24.8	4.19
70	0.1838	24.8	3.92
70	0.3101	24.5	2.84
100	0.1482	24.3	3.62
100	0.2044	24.8	3.52
100	0.2446	24.8	2.89
100	0.2866	23.8	2.15
100	0.3325	23.6	1.63
130	0.0793	25.1	5.44
130	0.1622	25.0	3.56
130	0.2025	24.9	2.52
	Methane-n-Butane		
10	0.1174	27.2	4.70
10	0.2020	27.0	4.43
10	0.2765	26.8	3.98
40	0.1128	27.3	4.78
40	0.2262	27.0	4.01
40	0.3275	26.7	2.86
40	0.4349	26.3	2.86
100	0.1888	27.2	4.54
100	0.2843	27.0	4.00
100	0.2858	27.0	4.13
100	0.3791	26.7	3.30
100	0.3793	26.7	3.41
160	0.1029	27.5	6.63
160	0.2864	27.1	4.90
160	0.3491	27.0	4.27
160	0.4158	26.7	3.78
220	0.1149	27.6	8.51
220	0.3076	27.1	5.46
	Methane-n-Pentane		
40	0.1274	29.6	4.85
40	0.4669	28.3	2.99
100	0.3221	29.0	4.44
100	0.1316	29.6	5.50

TABLE 18 (cont'd.)

100	0.4920	28.3	3.27
160	0.0999	29.8	7.17
160	0.2337	29.4	5.87
160	0.3584	29.0	4.58
160	0.4170	29.0	4.36
220	0.1019	29.8	9.12
220	0.2075	29.6	7.18
220	0.3888	29.0	4.70
280	0.2059	29.7	10.37
280	0.2660	29.4	7.53
		Methane-n-Heptane	
40	0.1453	33.0	7.99
40	0.2524	32.6	5.61
40	0.3454	32.2	4.36
40	0.4256	31.8	3.84
40	0.4943	31.4	3.19
100	0.1049	33.2	6.37
100	0.2953	32.6	7.09
100	0.3754	32.2	5.86
100	0.4371	32.0	4.76
160	0.2029	33.0	8.48
160	0.4186	32.2	5.17
160	0.5015	32.1	4.69
220	0.2585	32.9	10.14
220	0.3947	32.4	8.63
		Methane-n-Decane	
40	0.1187	35.9	6.27
40	0.5431	34.2	2.57
40	0.6396	33.7	1.39
100	0.1571	35.8	7.23
100	0.2515	35.5	6.37
100	0.3336	35.3	6.38
100	0.5023	34.6	4.06
100	0.6280	33.9	2.51
220	0.1963	35.8	13.59
220	0.3452	35.5	10.96
220	0.5897	34.4	5.56
220	0.6614	33.8	3.93
280	0.0818	36.1	18.92
280	0.1884	35.9	15.67
280	0.3365	35.5	11.64
280	0.4667	35.1	7.81
280	0.4927	35.0	8.38

TABLE 18 (cont'd.)

		Ethane-n-Pentane	
40	0.1615	29.2	5.31
40	0.3268	28.2	3.22
40	0.4626	27.4	3.91
100	0.0731	29.6	7.85
100	0.5798	26.7	3.27
160	0.0865	29.6	10.36
160	0.3278	28.4	4.52
160	0.5229	27.3	4.15
280	0.1478	29.6	13.26
280	0.2822	29.0	9.27
		Ethane-n-Decane	
40	0.4275	33.2	3.48
40	0.6802	30.1	2.13
100	0.0782	35.8	6.83
100	0.1160	35.6	6.91
100	0.3829	33.7	4.66
100	0.5086	32.5	3.68
100	0.6382	30.9	2.57
160	0.1667	35.3	7.90
160	0.3108	34.4	5.31
160	0.4046	33.7	5.46
160	0.5070	32.7	4.39
160	0.5899	31.8	3.15
160	0.6920	30.4	2.35
220	0.0940	35.7	9.28
220	0.2067	35.1	8.59
220	0.4147	33.7	6.11
220	0.5092	32.9	4.99
220	0.6959	30.7	3.22
280	0.1719	35.4	10.96
280	0.2513	34.9	10.11
280	0.3108	34.6	8.56
280	0.3648	34.2	8.65
280	0.4135	33.9	7.70
340	0.0874	35.8	13.09
340	0.1683	35.5	13.07
340	0.2423	35.1	10.99
340	0.2536	35.1	11.32
400	0.2438	35.1	13.19
400	0.2954	34.8	12.15
400	0.3484	34.5	10.16

TABLE 18 (cont'd.)

n-Butane-n-Decane

220	0.516	33.1	4.61
220	0.714	31.3	4.48
280	0.331	34.4	9.56
280	0.633	32.2	6.07
280	0.704	31.5	5.42
340	0.249	35.0	14.98
340	0.433	33.8	13.62
340	0.592	32.6	10.42

APPENDIX*

This appendix will serve to demonstrate the use of correlations of diffusion coefficients in real situations. Specifically, two problems involving diffusion will be treated in which non-idealities occur, such as when the diffusion coefficient varies with composition or the partial volumes of the two components are constant but unequal. The two illustrative situations will be (1) diffusion into a stagnant liquid layer and (2) diffusion through a U-tube when one component is non-volatile.

Stagnant Liquid Layer

The prediction of the molecular flux in a binary system under isobaric, isothermal conditions was described earlier in this work. If the solution obtained there is applied to the flux of one component crossing the interface into the liquid phase, the result is

$$\dot{m}_{ki} = -M\left(\frac{D_{Ckj}}{\theta}\right)^{\frac{1}{2}} \frac{1-\sigma_{jd}\overline{V}_{j\ell}}{\overline{V}_{k\ell}} \tag{1}$$

with the coordinates measured from the interface and M determined from Equation 29 of EVALUATION. The extended equation for the transient solution of the above problem, but with the diffusion coefficient variable is

$$\frac{\partial \sigma_k}{\partial \theta} = -\frac{\dot{m}_{ki}\overline{V}_{k\ell}}{1-\sigma_{jd}\overline{V}_{j\ell}} \frac{\partial \sigma_k}{\partial x} + \frac{\partial}{\partial x}\left(D_{Ckj}\frac{\partial \sigma_k}{\partial x}\right) \tag{2}$$

---

* The material for this appendix was presented in a talk given by Professor B. H. Sage at the April 7, 1964, meeting of the American Chemical Society in Philadelphia.

from Equation 25 of EVALUATION. When the variation of the Chapman-Cowling diffusion coefficient with composition is taken as

$$D_{Ckj} = a + b\,\sigma_k \quad , \tag{3}$$

Equation 2 becomes

$$\frac{\partial \sigma_k}{\partial \theta} = - \frac{\mathring{m}_{ki}\,\overline{V}_{k\ell}}{1-\sigma_{jd}\overline{V}_{j\ell}} \frac{\partial \sigma_k}{\partial x} + b\left(\frac{\partial \sigma_k}{\partial x}\right)^2 + (a+b\,\sigma_k)\frac{\partial^2 \sigma_k}{\partial x^2} \quad . \tag{4}$$

In finite difference form, Equation 4 can be expressed (32) as

$$C_{m+1,n} = C_{m,n} - \frac{\mathring{m}_{ki}\,\overline{V}_{k\ell}}{1-\sigma_{jd}\overline{V}_{j\ell}} \frac{\Delta\theta}{2\Delta x}(C_{m,n+1} - C_{m,n-1}) + \frac{b\Delta\theta}{4(\Delta x)^2} \times$$

$$(C_{m,n+1}-C_{m,n-1})^2 + (a+bC_{m,n})\frac{\Delta\theta}{(\Delta x)^2}(C_{m,n+1} - 2C_{m,n}+C_{m,n-1}) \tag{5}$$

where the subscript m denotes the time interval, n denotes the distance interval, and C denotes σ_k. The weight flux of component k across the interface is found from

$$\mathring{m}_{ki} = - \frac{D_{Ckj}}{\overline{V}_{j\ell}} \frac{1-\sigma_{jd}\overline{V}_{j\ell}}{\sigma_{jb}-\sigma_{jd}} \left(\frac{\partial \sigma_k}{\partial x}\right)_i \quad . \tag{6}$$

This equation in finite difference form is

$$\mathring{m}_{ki} = - \frac{(a+bC_{m,o})}{12\Delta x \overline{V}_{j\ell}} \frac{(1-\sigma_{jd}\overline{V}_{j\ell})}{(\sigma_{jb}-\sigma_{jd})} (-25C_{m,o}+48C_{m,1}-36C_{m,2}$$

$$+16C_{m,3}-3C_{m,4}) \quad . \tag{7}$$

Figure A1 shows the results of numerical solution of Equations 5 and 7 for the ethane-white oil system at 160° F ($a = 8.8\times10^{-10}$, $b = 1.155\times10^{-8}$) over a typical time period for the above experiment. The characteristics of the process shown are as follows:

$\bar{V}_{k\ell}$ = 0.0389 cu. ft./lb. $\quad\quad$ σ_{jd} = 0. lb./cu. ft.

$\bar{V}_{j\ell}$ = 0.0183 cu. ft./lb. $\quad\quad$ σ_{ko} = 0. lb./cu. ft.

σ_{jb} = 40.57 lb./cu. ft. $\quad\quad$ σ_{kb} = 6.41 lb./cu. ft.

The solid curve gives the numerically determined value of the flux of ethane at the interface as a function of time; the upper and lower dashed curves are the analytical approximation of the solid curve when the diffusion coefficient is determined at surface conditions and at the average of surface and initial conditions, respectively. The dashed curves are obviously reasonable approximations of the solid curve, yet they are both in error by as much as twenty per cent over the time period shown. Therefore, for precise work they would be inadequate descriptions of the process. It is very interesting to note that in this time period the numerical flux could have been characterized very accurately by a very nearly constant diffusion coefficient calculated from a weighted average concentration of 0.7 times the surface concentration of component k plus 0.3 times the initial concentration of that component.

U-tube

Another problem of interest deals with a one-dimensional system of constant cross section with a liquid-gas interface at each end (a U-tube of liquid described in one dimension). A transient process involving this configuration might be the compression of a gas phase composed of a volatile component at one end of the tube and a reduction in pressure at the other end. If the second liquid-phase component were non-volatile, the result would be diffusion of the light

component through the tube and a consequent migration of the heavy component toward the end with the reduced pressure. The initial conditions of a transient process of interest might be the following for an ethane-white oil mixture at 160° F:

$$n_{c_2}(o, x) = 0.5 \qquad n_{c_2}(o, o) = 0.9$$
$$\bar{V}_{k\ell} = 0.0390 \text{ cu. ft./lb.} \qquad L_o = 3.0 \text{ ft.}$$
$$\bar{V}_{j\ell} = 0.0180 \text{ cu. ft./lb.}$$

The above problem would be difficult to solve analytically if the partial volume of component k were zero; having it non-zero and letting the diffusion coefficient be variable complicate the situation a great deal more. However, the problem can be handled in a straightforward manner numerically.

The differential equation describing the transport process was taken as

$$\frac{\partial \sigma_k}{\partial \theta} = -\sigma_k \frac{\partial u}{\partial x} - u \frac{\partial \sigma_k}{\partial x} + \frac{1}{\bar{V}_{j\ell}} \frac{\partial}{\partial x}\left(\frac{D_{Ckj}}{\sigma} \frac{\partial \sigma_k}{\partial x}\right) \tag{8}$$

while the equation of continuity was expressed in the following way:

$$\frac{\partial u}{\partial x} = -\frac{1}{\sigma}\left(1 - \frac{\bar{V}_{k\ell}}{\bar{V}_{j\ell}}\right)\left(u \frac{\partial \sigma_k}{\partial x} + \frac{\partial \sigma_k}{\partial \theta}\right) . \tag{9}$$

When Equations 3, 8, and 9 were combined, the equation to be solved for the concentration of component k was

$$\frac{\partial \sigma_k}{\partial \theta} = -u \frac{\partial \sigma_k}{\partial x} + (a+b\sigma_k) \frac{\partial^2 \sigma_k}{\partial x^2} + \left[\frac{a(\bar{V}_{k\ell} - \bar{V}_{j\ell}) + b}{1 - \sigma_k(\bar{V}_{k\ell} - \bar{V}_{j\ell})}\right]\left(\frac{\partial \sigma_k}{\partial x}\right)^2 . \tag{10}$$

The variation in pressure along the diffusion path may be evaluated from the conservation of momentum in the following way when

viscosity is neglected:

$$\frac{\partial P}{\partial x} = -\frac{1-\sigma_k(\overline{V}_{k\ell}-\overline{V}_{j\ell})}{\overline{V}_{j\ell}\, g}\left(\frac{\partial u}{\partial \theta} + u\frac{\partial u}{\partial x}\right) . \tag{11}$$

Finally, since the partial volumes were taken as constant, the overall change in volume may be simply evaluated from

$$\frac{dL}{d\theta} = \frac{1}{A}\frac{dV}{d\theta} = (\mathring{m}_{ko}-\mathring{m}_{kL})\,\overline{V}_{k\ell} . \tag{12}$$

Equations 9, 10, and 11 will now be expressed in finite difference form, but with a variable value for the size of the distance increment. This modification was necessitated since the system grows in length during the process and the moving end must be allowed to move, numerically, any fraction of a distance increment during a time step, as determined from Equation 12. Therefore, the symbol h_{n+1} denotes the distance from point n to point n+1 ; h_n denotes the distance from point n-1 to point n . Now Equation 10 can be expressed as

$$C_{m+1,n} = C_{m,n}\left[1 - \frac{2(a+bC_{m,n})\Delta\theta}{h_n h_{n+1}}\right] + C_{m,n+1}\frac{\Delta\theta}{(h_n+h_{n+1})} \times$$

$$\left[\frac{2(a+bC_{m,n})}{h_n} - u_{m,n}\right] + C_{m,n-1}\frac{\Delta\theta}{(h_n+h_{n+1})}\left[\frac{2(a+bC_{m,n})}{h_{n+1}} + u_{m,n}\right]$$

$$+ \frac{\Delta\theta}{(h_n+h_{n+1})^2}\left[\frac{a(\overline{V}_{k\ell}-\overline{V}_{j\ell})+b}{1-C_{m,n}(\overline{V}_{k\ell}-\overline{V}_{j\ell})}\right](C_{m,n+1} - C_{m,n-1})^2 \tag{13}$$

Similarly, Equation 9 becomes

$$u_{m+1,n+1} = u_{m+1,n}\left[1 + \frac{(\overline{V}_{k\ell}-\overline{V}_{j\ell})(C_{m+1,n+1}-C_{m+1,n})}{1 - C_{m,n}(\overline{V}_{k\ell}-\overline{V}_{j\ell})}\right] +$$

$$+\frac{h_{n+1}}{\Delta\theta}\left[\frac{\bar{V}_{k\ell}-\bar{V}_{j\ell}}{1-C_{m,n}(\bar{V}_{k\ell}-\bar{V}_{j\ell})}\right](C_{m+1,n}-C_{m,n}) \quad . \tag{14}$$

Equation 11 then is

$$P_{m+1,n+1}=P_{m+1,n}-\frac{1}{g\bar{V}_{j\ell}}\left[1-C_{m+1,n}(\bar{V}_{k\ell}-\bar{V}_{j\ell})\right] \tag{15}$$

$$(u_{m+1,n+1}-u_{m,n+1})\frac{h_{n+1}}{\Delta\theta}-u_{m+1,n}(u_{m+1,n+1}-u_{m+1,n}) \quad .$$

The flux of component k at the ends was determined from the evaluation of the following equation:

$$\dot{m}_{ki}=-\frac{a+bC_{m,i}}{1-C_{m,i}\bar{V}_{k\ell}}\left\{\frac{C_{m,i}[h_1^2-(h_1+h_2)^2]+C_{m,i+1}(h_1+h_2)^2-C_{m,i+2}h_1^2}{h_1h_2(h_1+h_2)}\right\} \tag{16}$$

Now that the problem has been formulated, the solution is easy to obtain; the main point where care must be exercised is in the proper adding on of increments during the growth process of the liquid phase.

In Figures A2 and A3 are presented some of the more interesting results of solutions for the U-tube problem which has been set up. The dashed lines apply to a solution with constant diffusion coefficient (8.345×10^{-4} sq. ft. /hr.), and the solid lines apply to a solution with variable diffusion coefficient ($a = 3.165\times10^{-6}$ sq. ft. /hr., $b = 4.157\times10^{-5}$ ft^5/lb. hr.).

Figure A2 shows that the flux of ethane into the tube looks very much like diffusion into a semi-infinite layer of liquid until the outward flux of ethane makes itself felt and the two fluxes converge to a steady state situation. The approach to steady state is also evident in the slowing of the growth rate of the liquid phase. It is of interest

to note from Figure A3 the large amount of white oil which has been transported to the downstream end of the tube. Only some twenty-four per cent of the white oil is present in the original length of the phase as steady state is approached(8280 hr.) even though the new length is little more than double the original. The solutions of this particular problem with and without a variable diffusion coefficient show again that the assumption of constancy of the coefficient introduces errors which can be tolerated in some situations and which cannot in others.

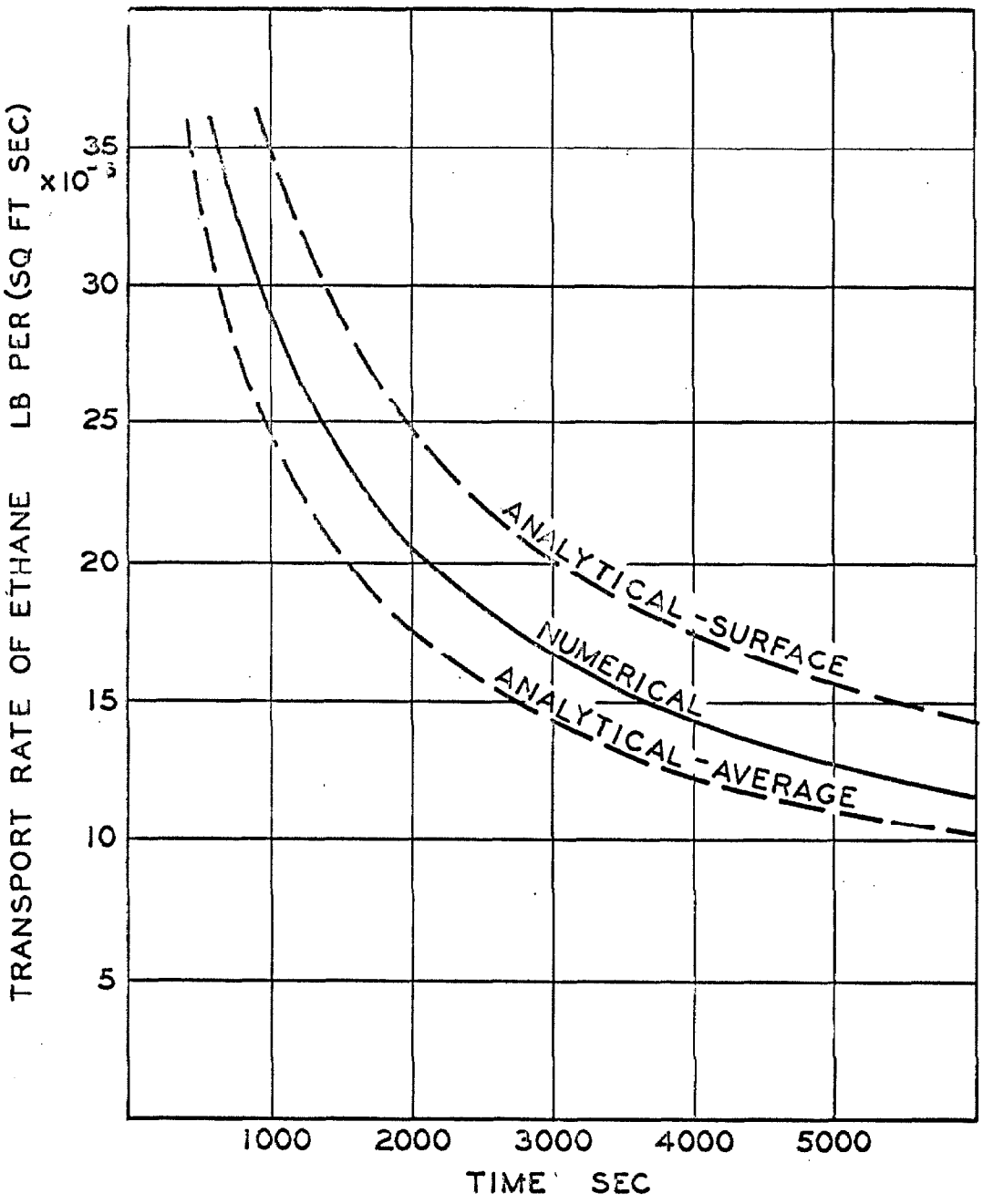

Fig. A1. Transport Rate of Ethane into a Liquid Film.

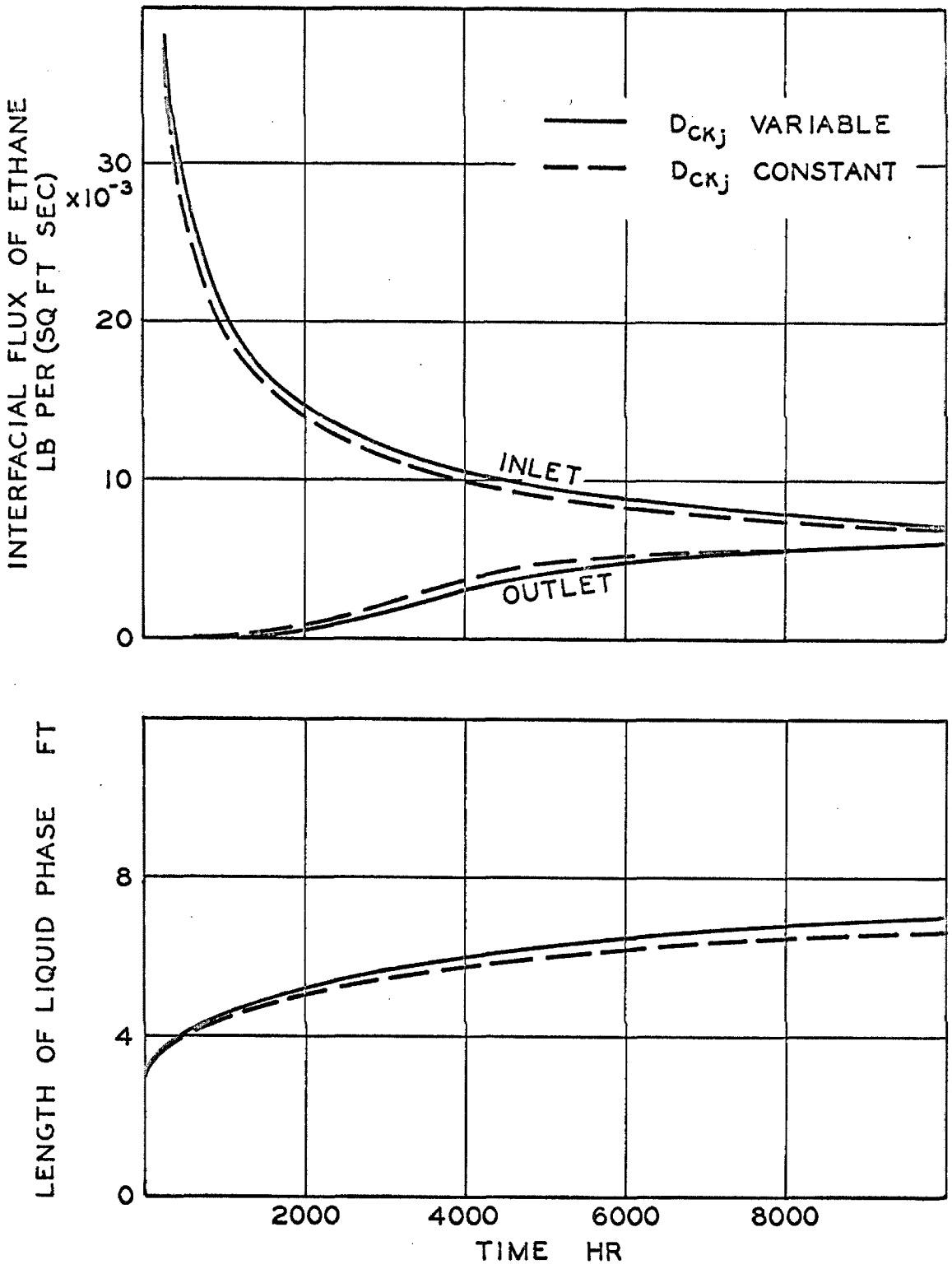

Fig. A2. Effects of Transient Diffusion Through a U-tube.

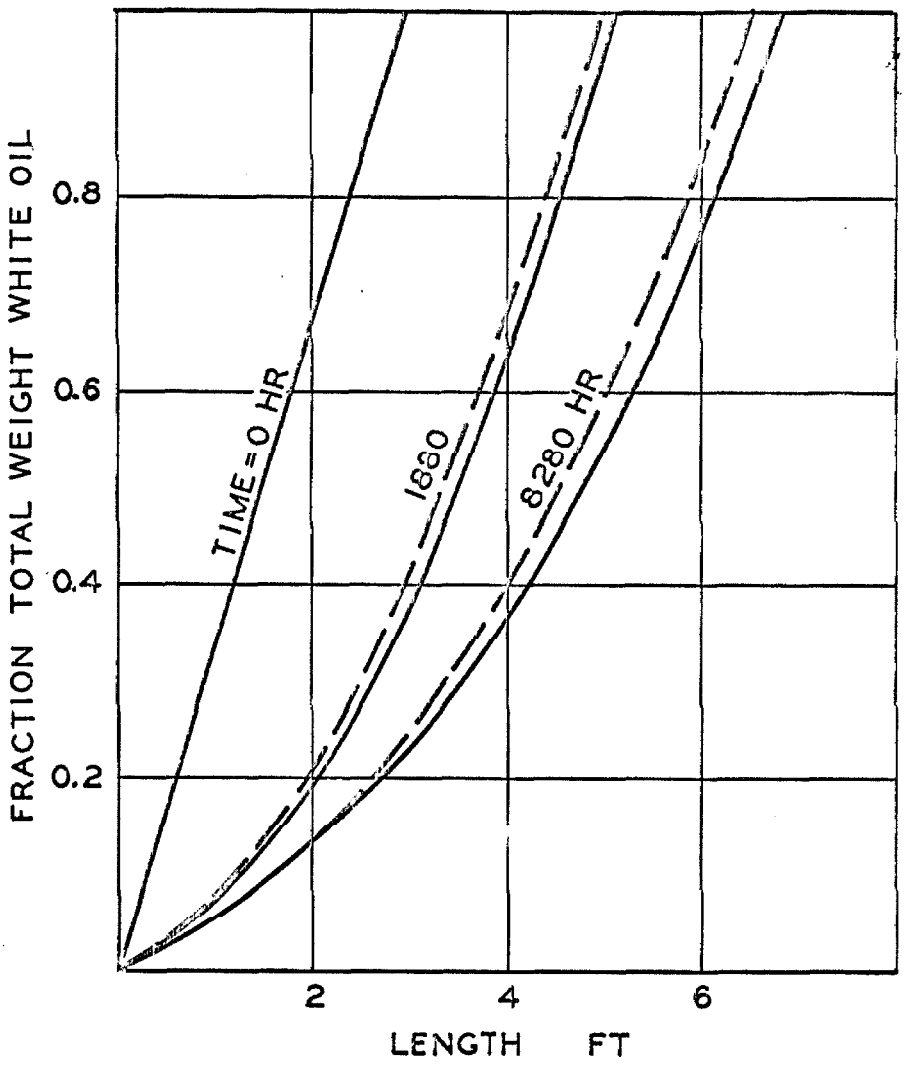

Fig. A3. Migration of Heavy Component During Transient Diffusion in a U-tube.

PROPOSITIONS

PROPOSITION I

It is proposed that a concentric cylinder viscometer which is operated as a transient device be used in industry as a replacement of the widely-used rolling-ball type viscometer in high pressure work. The cylindrical viscometer would have the characteristics of low cost and ease of operation with the additional advantage that it would give results which could be related to hydrodynamic theory and which would differentiate non-Newtonian fluids from Newtonian fluids.

The excellent viscometers in use for very precise work at high pressures are either too expensive (4) or too limited in range (1) for practical use in many industries. Falling cylinder viscometers constitute another alternative which is constantly being improved (2).

The proposed viscometer consists of an outer, stainless steel, pressure cylinder which is geared to a small electrical motor. One or more small loops of copper wire are imbedded in the inner wall of the cylinder where they are insulated from the steel; their leads connect, through pressure seals, with slip rings on the outside of the cylinder. An inner cylinder of desired radius and moment of inertia is suspended within the pressure cylinder on bearings which are as friction-free as possible. Built into the inner cylinder is a small, permanent magnet which induces current in the copper coils with each relative rotation of the cylinders.

In operation, the outer cylinder would be accelerated quickly to a constant speed by the motor, and the impulses from the copper loops would be recorded as a function of time. As shown by the fol-

lowing analysis, the viscosity would be a function of θ and $\Delta\omega$.

The reduced Navier-Stokes equation which is applicable to the situation is (3)

$$\frac{1}{\nu}\frac{\partial u_\psi}{\partial \theta} = \frac{\partial^2 u_\psi}{\partial r^2} + \frac{1}{r}\frac{\partial u_\psi}{\partial r} - \frac{u_\psi}{r^2} , \tag{1}$$

with the initial and boundary conditions

$$\begin{aligned} u_\psi &= 0 && \text{at} && \theta = 0 \\ u_\psi &= \omega_o r_o && \text{at} && r = r_o \\ u_\psi &= \omega_i r_i && \text{at} && r = r_i \end{aligned} \tag{2}$$

where

$$\frac{d\omega_i}{d\theta} = \frac{M}{I} = \frac{2\pi r_i^2 L}{I}\tau_{r_\psi} . \tag{3}$$

But, for a Newtonian fluid, the shear is

$$\tau_{r_\psi} = \eta\left(\frac{\partial u_\psi}{\partial r} - \frac{u_\psi}{r}\right) . \tag{4}$$

Combining Equations 1, 3, and 4 gives

$$u_\psi = \frac{2\pi r_i^4 L\eta}{2\pi r_i^4 L\rho - I}\int_0^\theta \frac{\partial^2 u_\psi}{\partial r^2}\bigg|_{r_i} d\theta . \tag{5}$$

An exact solution to Equation 1 would give the viscosity as a complicated, implicit function of the cell parameters, elapsed time, θ, and measured velocity, ω_i. To permit a simpler solution to be found, the conditions will be determined under which the instantaneous flow pattern between the cylinders can be approximated by its steady state form, Equation 6.

$$u_\psi = \left[\omega_i + \frac{r - r_i}{r_o - r}(\omega_o - \omega_i)\right] r . \tag{6}$$

This approximation will be accurate if the cell parameters are restricted so that the steady-state flow pattern is approached much more rapidly than the inner cylinder is accelerated.

Using the steady-state flow pattern approximation, a combination of Equations 4 and 6 gives the relation

$$\tau_{r_\psi} = \eta r \left(\frac{\omega_o - \omega_i}{r_o - r_i} \right) . \tag{7}$$

Then, Equation 3 becomes

$$\frac{d\omega_i}{d\theta} = \frac{2\pi r_i^3 L}{I(r_o - r_i)} \eta (\omega_o - \omega_i) \tag{8}$$

at $r = r_i$. The solution to Equation 8 is

$$\Delta\omega = \omega_o - \omega_i = \omega_o e^{-\frac{2\pi r_i^3 L}{I(r_o - r_i)} \eta \theta} . \tag{9}$$

This expression is only as valid as the assumption of a steady-state flow pattern in the space between the cylinders. The circumstances for which the assumption is valid will now be determined.

The space between the cylinders can be approximated as that between two infinite, parallel plates. In the case where one of the plates is suddenly accelerated to a steady velocity, the expression describing the flow of the fluid in the space is easily determined to be

$$\frac{u}{u_o} = \frac{y}{d} + \frac{2}{\pi} \sum_{n=1}^{\infty} \frac{(-1)^n}{n} e^{-\frac{n^2 \pi^2}{d^2} \nu \theta} \sin n\pi \frac{y}{d} . \tag{10}$$

Equation 10 includes the assumption that one surface does not move.

Now, it will be required that when the speed of the inner cylinder reaches a low fraction, F_i, of its steady state value, the velocity of the fluid at a point midway between the two cylinders be

equal to or greater than a large fraction, F_f, of its steady state value. In equation form, from Equation 9,

$$1 - F_i = e^{-\frac{2\pi r_i^3 L}{I(r_o - r_i)}\eta\theta} . \tag{11}$$

The first term of the summation in Equation 10 will be taken as adequate to describe the behavior of the fluid velocity. Then, from Equation 10,

$$\frac{1}{2} F_f = \frac{1}{2} - \frac{2}{\pi} e^{-\frac{\pi^2}{d^2}\nu\theta} \tag{12}$$

at $y = \frac{1}{2}d$. If the approximation in Equation 10 can be used for the space between the concentric cylinders,

$$r_o - r_i = d . \tag{13}$$

Equations 11, 12, and 13 can be combined to give the equation which expresses the criteria for the validity of Equation 9.

$$\frac{\pi I}{2\rho r_i^3 L d} \geq \frac{\ell n \left[\frac{\pi}{4}(1 - F_f)\right.}{\ell n (1 - F_i)} . \tag{14}$$

If, for example, the values of the parameters in Equation 14 were chosen as

$$F_f = 0.99 \qquad F_i = 0.05 \qquad I = \frac{5\rho\pi L}{2} r_i^4 , \tag{15}$$

where the inner cylinder was approximated as a right, circular cylinder five times as dense as the fluid, Equation 14 becomes

$$\frac{5\pi^2}{4} \frac{r_i}{d} \geq \frac{\ell n\, \pi/400}{\ell n\, 0.95} . \tag{16}$$

The restricting criterion is, approximately,

$$r_o - r_i = d \leq 0.13\, r_i \quad . \tag{17}$$

Thus, if condition 14 is satisfied, Equation 9 can be solved to give the expression for the viscosity of the fluid in terms of the cell parameters and the experimentally measured quantities $\Delta\omega$ and θ.

$$\eta = \frac{I(r_o - r_i)}{2\pi r_i^3 L} \left[\frac{\ell n\, \omega_o - \ell n\, \Delta\omega}{\theta} \right] \quad . \tag{18}$$

Equation 18 shows that by making measurements at different values of θ one can distinguish a non-Newtonian fluid from a Newtonian one by the dependence of its viscosity, η, on θ.

NOMENCLATURE

Symbols

D	Substantive derivative
d	Distance between parallel plates, ft.
F	Fraction of steady state value attained
I	Moment of inertia of inner cylinder, ft. lb. $sec.^2$
L	Length of the inner cylinder, ft.
M	Moment, lb. ft.
P'	Potential, lb. /sq. ft.
r	Radial coordinate, ft., measured from center of cylinders
u	Velocity, ft. /sec.
y	Linear coordinate between parallel plates, ft.
η	Viscosity, lb. sec., /sq. ft.
θ	Elapsed time, sec.
ν	Kinematic viscosity, sq. ft. /sec.
ρ	Density of fluid, lb. $sec.^2/ft^4$
τ	Shear, lb. /sq. ft.
ψ	Angular coordinate
ω	Angular velocity, $sec.^{-1}$

Subscripts

f	Fluid
i	Inner cylinder
o	Outer cylinder
r	Radial direction
ψ	Angular direction

REFERENCES

1. Eakin, B. E., and Ellington, R. T., Petroleum Trans. 216, 85 (1959).

2. Lohren, J., and Kurata, F., A. I. Ch. E. J. 8, 191 (1962).

3. Longwell, P. A., "Mechanics of Fluid Flow," Ch. E. 168 Course Notes, California Institute of Technology (1961).

4. Reamer, H. H., Cockelet, G., and Sage, B. H., Anal. Chem. 31, 1422 (1959).

PROPOSITION II

Calculations are presented which favor one side of the controversy over the circumstances surrounding the deaths of frozen woolly mammoths.

A number of woolly mammoths (elephas primigenius), notably the Berezovka and Mamutava mammoths, have been found in exceptionally good states of preservation due to freezing (9). Controversies have arisen over two factors concerning the frozen remains: 1, the reason for the location of such an herbivorous animal as far north as Siberia (3, 7), and 2, the reasons for the excellent condition of some specimens (2, 5). This proposition deals with the second controversy.

Farrand (2), Pavlovsky (7), and Tolmachoff (9) have proposed methods of the death of the animals by drowning or suffocation followed by slow freezing. Lippman (5) argued that the state of the flesh and the undigested contents of the stomach required extremely rapid solidification by freezing. Some of the alternative methods which were suggested involved natural catastrophies such as widespread volcanic eruptions and raining liquid air. It was argued that without such novel mechanisms for quick-freezing, the animal remains would have decayed to a much greater extent than they did. A further factor which supports the catastrophy argument is the simultaneous deaths of many of the beasts (4). Tolmachoff proposed that the lack of bacteria in the arctic climate permitted slow freezing without decay.

An analysis was made by the author of the unsteady-state heat

transfer in a freezing woolly mammoth to evaluate the various arguments that have been presented. Data on the size of mammoths were taken from Farrand (2) and estimated from information on elephants (1). Data on the thermal properties of animal tissue were not available and were estimated from data on water (8). A summary of the data used is given in Table I. A numerical method similar to the graphical method of Longwell (6) was used to solve the mathematical problem; in it the animals were approximated as infinitely long cylinders.

The results of the study are given in Figure I which shows the time required to freeze a mammoth's center and to cool it to 50° F. Figure I shows that the time required to freeze one of these animals with any outside temperature so far proposed, no matter how extreme, is probably greater than the time required to cause considerable interior decay. Further, the time required to cool the center of an animal to 50° F is also greater than the time required for considerable decay. The temperature 50° F was chosen as representative of the lower point at which bacteria are active. This heat transfer study has shown, therefore, that it is not possible to freeze the center of a mammoth rapidly enough to satisfy the requirements of the "quick-freeze" theory. It is proposed that the more reasonable method of preservation is that of slow freezing accompanied by even slower decay due to a lack of bacteria, as suggested by Tolmachoff and supported by Farrand.

REFERENCES

1. Benedict, F. G., The Physiology of the Elephant, Carnegie Institute of Washington, Washington, D. C. (1936).

2. Farrand, W. R., Science, 133, 729 (1961).

3. Heintz, A., Blyttia, 16, 122 (1958).

4. Kurten, B., Jr. Paleontology, 28, 286 (1954).

5. Lippman, H. E., Science 137, 449 (1962).

6. Longwell, P. A., A. I. Ch. E. J. 4, 53 (1958).

7. Pavlovsky, E. N., Ann. Sci. Mat. Zool. 16, 413 (1954).

8. Perry, J. H., Ed., Chemical Engineers' Handbook, McGraw-Hill Book Co., New York (1950).

9. Tolmachoff, J. P., Trans. Am. Phil. Soc. 23 (1929).

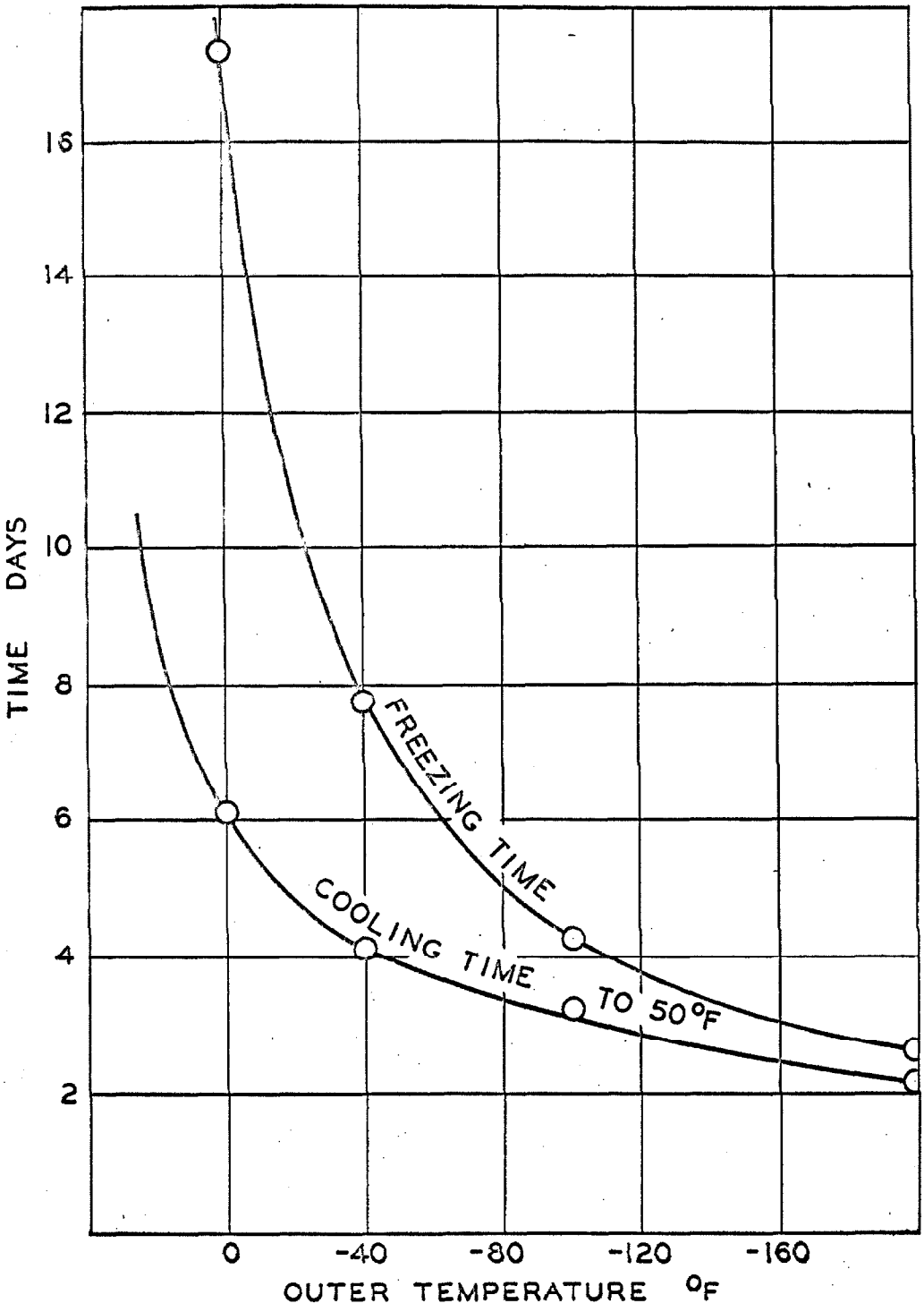

Fig. 1. Freezing and Cooling Time of the Center of a Woolly Mammoth.

TABLE 1. Data Used in Analysis of Heat Transfer in a Woolly Mammoth

Body Temperature	97.5° F
Weight	8100 lb.
Girth	15.4 ft.
Length from Rear to Brow	16.0 ft.
Thermal Conductivity of Tissue	
Unfrozen	0.35 Btu/ft. hr.° F
Frozen	1.28 Btu/ft. hr.° F
Heat Capacity of Tissue	
Unfrozen	1.0 Btu/lb.
Frozen	0.5 Btu/lb.
Density of Tissue	62.4 lb. /ft.^{3}
Heat of Fusion of Tissue	143.6 Btu/lb.

PROPOSITION III

An explanation is proposed for the seemingly paradoxical behavior of forced convective heat transfer under certain conditions of acoustical vibration. It is further proposed that the behavior is worthy of further experimental study as a method for controlling heat transfer coefficients.

Recent research on the effect on heat transfer of pulsation or vibration of the heat transfer fluid and vibration of heat transfer surfaces has shown that substantial increases in heat transfer coefficients may be obtained (3). In free convective heat transfer, vibration of the heat transfer surface at any frequency generally produces increased heat transfer (2). Lemlich (4) has shown that vibrating forced convective heat transfer equipment at resonant frequencies and parallel to the direction of flow produced heat transfer coefficients which were significantly greater than those at non-resonant frequencies. He also has stated that decreases in heat transfer coefficients were possible and that Romie (5) has attempted to explain such a decrease. The latter author blamed fluctuations in wall temperature for decreases in heat transfer coefficients when the fluid was pulsed. In a slightly different area, Scanlan (6) found increases in heat transfer coefficients to be a very marked function of frequency when he vibrated a surface normal to a fluid which was in laminar flow.

The general theory is that longitudinal vibration of a heat transfer surface reduces the thickness of a laminar boundary layer when the fluid is in turbulent flow and thus increases the eddy conduc-

tivity. When the fluid is in laminar flow, longitudinal vibration of the surface is supposed to stimulate turbulence and to partially change the transfer mechanism from molecular conductivity to include some eddy conductivity.

A short study by the author at the University of Colorado on the effect of vibration on forced convective heat transfer resulted in the curve shown in Figure 1. The data were obtained for sixty-cycle longitudinal vibrations of a condensing steam-water heat exchanger. No attempt was made to obtain resonance within the heat exchanger. Figure 1 shows that, in agreement with theory, heat transfer coefficients were increased by vibration of the heat exchanger when the water was in turbulent flow. However, contrary to the usual reports and predictions, in the laminar region the opposite occurred -- heat transfer coefficients were reduced by vibration. The following explanation is proposed to explain the behavior.

The heat transfer equation for forced convection is

$$dq/d\theta = h A \Delta T \ . \qquad (1)$$

A correlation for the heat transfer coefficient is given in Equation 2.

$$\frac{hD}{k} = 1.86 \left(Re \cdot Pr \cdot \frac{D}{L}\right)^{1/3} \left(\frac{\mu_f}{\mu_w}\right)^{0.14} . \qquad (2)$$

This equation is an empirical modification (7) of the Graetz solution (1) for heat transfer in fully developed laminar flow with constant wall temperature. Considering all quantities except the instantaneous bulk velocity to be constant, and considering the bulk velocity to vary sinusoidally with time, the heat transfer coefficient at a point in a

vibrating heat exchanger would vary as

$$h = h_o(1 + a \sin \omega\theta)^{1/3} \quad . \tag{3}$$

The temperature drop variation is then given as

$$\Delta T = \Delta T_o(1 + b \sin \omega\theta) \quad . \tag{4}$$

After substitution from Equations 3 and 4, Equation 1 becomes

$$\frac{dq}{d\theta} = h_o A \Delta T_o(1 + b \sin \omega\theta)(1 + a \sin \omega\theta)^{1/3} \quad . \tag{5}$$

If Equation 5 is integrated over one period of vibration and q_o is taken as the heat which would have been transferred in the absence of vibration, Equation 6 results:

$$\frac{q_{vib}}{q_o} = 1 + a\left(\frac{b}{3} - \frac{a}{9}\right) + \frac{3a^3}{8}\left(\frac{5b}{8!} - \frac{10a}{243}\right) + \ldots \quad . \tag{6}$$

This equation states that if the mechanism of heat transfer in laminar flow remains the same with or without vibration, the heat which is transferred can decrease due to vibration of the exchanger if

$$b < a/3 \quad . \tag{7}$$

The inequality 7 can be satisfied in laminar flow, since the relative magnitude of the periodic variation in the bulk velocity, a , can be much greater than the relative magnitude of the periodic variation in temperature drop at a point along the exchanger. This is true because the temperature change with axial position is not large when the fluid is in laminar flow, whereas the variation in the bulk velocity due to vibration can be an appreciable fraction of the average bulk velocity under those conditions.

Presumably, at a resonant frequency in the heat exchanger, the acoustic energy would be used to more advantage to give the in-

creases in heat transfer which have been reported (3). The secondary proposition is, then, that heat transfer coefficients to fluids in laminar flow could be controlled as desired by varying the frequency of acoustic oscillations of the heat exchanger.

NOMENCLATURE

Symbols

A	Heat exchange area, sq. ft.
a	Approximate relative amplitude of vibration of exchanger
b	Relative amplitude of variation of temperature drop
D	Diameter of tube, ft.
h	Heat transfer coefficient, Btu/ft.^{2}hr.$^\circ$F
k	Thermal conductivity of fluid, Btu/ft. hr.$^\circ$F
L	Length of heat exchange tube, ft.
q	Heat transferred, Btu
θ	Time, hr.
ω	Period of vibration of exchanger, hr.$^{-1}$

Subscripts

o	Without vibration or mean value
vib	With vibration

Groups

Nu	Nusselt number
Re	Reynolds number
Pr	Prandtl number

REFERENCES

1. Graetz, L., Ann. d. Physik, 25, 337 (1885).
2. Holman, J. P., J. Heat Transfer, 82, 393 (1960).
3. Lemlich, R., Chem. Eng. 68, 171 (1961).
4. Lemlich, R., and Hwu, C. K., A. I. Ch. E. J. 7, 102 (1961).
5. Romie, R. E., Ph. D. Thesis, University of California (1956).
6. Scanlan, J. A., Ind. Eng. Chem. 50, 1565 (1958).
7. Sieder, E. N., and Tate, G. E., Ind. Eng. Chem. 28, 1429 (1936).

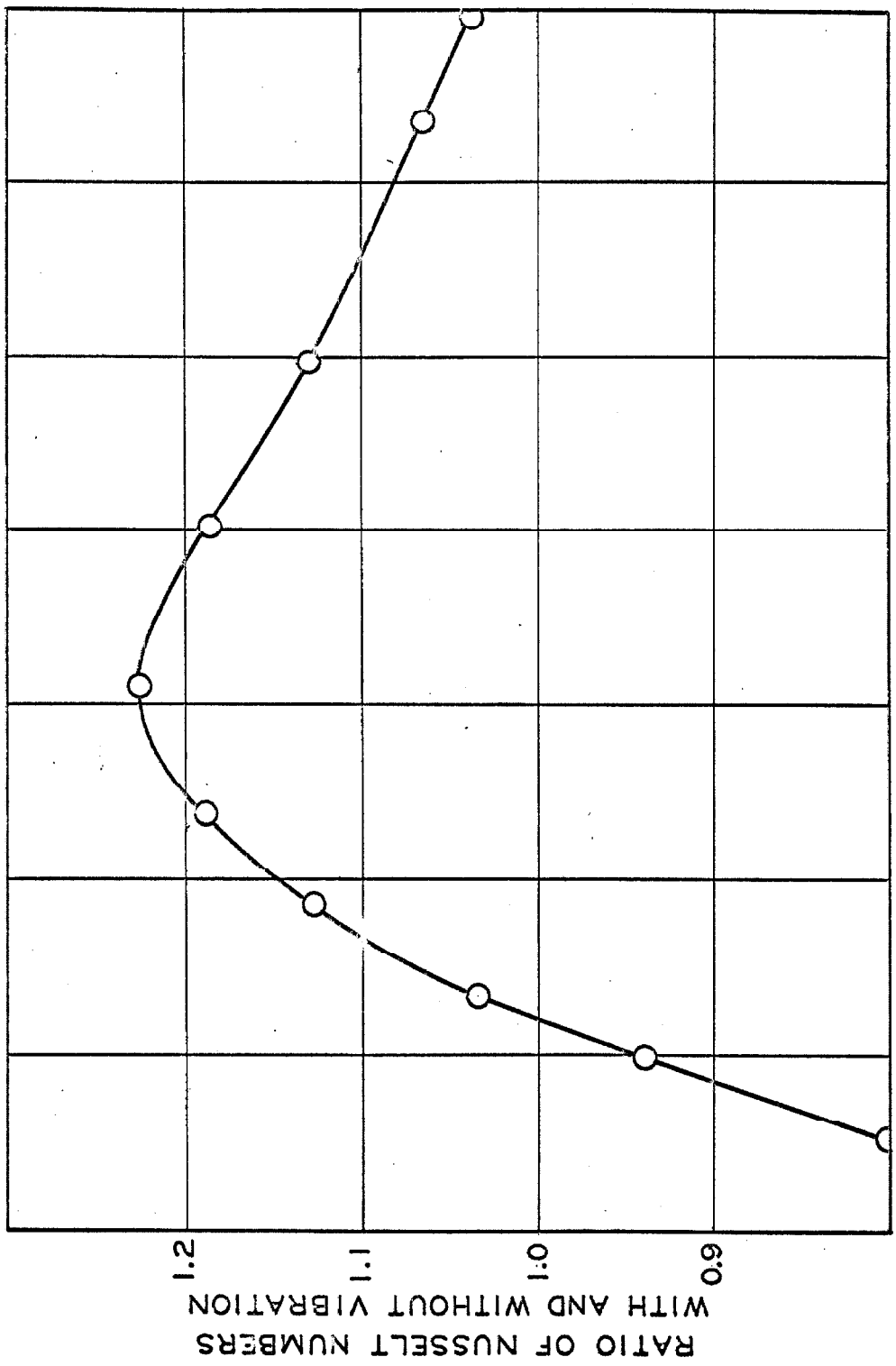

Fig. 1. Effect of Vibration on Heat Transfer.

PROPOSITION IV

A scheme is proposed for choosing the constant diffusion coefficient which best describes diffusion into a liquid layer when the diffusion coefficient is a known function of composition.

When the diffusion coefficient is a known function of composition, the most accurate way of calculating diffusion into a semi-infinite liquid layer is a numerical one. Since for relatively short times even a thin layer of liquid can be approximated as semi-infinite, the above problem for machine calculation can be important for a wide variety of diffusion problems. An often unsatisfactory approximation of the process is sometimes made by calculating the diffusion coefficient from the surface, equilibrium composition and using that in an analytical expression. However, an incidental result found in the Appendix of Part III of this thesis which concerned characterizing the diffusion process by a single, constant diffusion coefficient can be generalized to apply to diffusion in liquid layers in general. The constant diffusion coefficients which are thus estimated can be used in analytical expressions for predicting diffusion processes.

The result found in the Appendix was that a weighted average composition of the liquid phase could be used to calculate the diffusion coefficient which would correctly predict the interfacial flux of material at a particular time. To determine whether the weighted average composition found above was general, numerical calculations similar to those in the Appendix were carried out for the three diffusion situations listed below, each with two expressions describing the

behavior of the diffusion coefficient with composition.

I. Ethane-white oil at 160° F, liquid depth 0.1144 ft.

$\sigma_{ko} = 0.$ $\quad\quad$ $\sigma_{jg} = 0.$

$\sigma_{kbi} = 6.41$ lb./cu. ft $\quad\quad$ $\overline{V}_{j\ell} = 0.0183$ cu. ft./lb.

$\overline{V}_{k\ell} = 0.0389$ cu. ft./lb.

$D_{Ckj} = 8.8\times10^{-10} + 1.155\times10^{-8}\ \sigma_k$

or $\quad D_{Ckj} = 2.582\times10^{-9} + 5.339\times10^{-7}\ n_k$

II. Methane-n-butane at 100° F, liquid depth 0.12 ft.

$\sigma_{ko} = 0.$ $\quad\quad$ $\sigma_{jg} = 1.236$ lb./cu. ft.

$\sigma_{kbi} = 1.601$ lb./cu. ft. $\quad\quad$ $\overline{V}_{j\ell} = 0.0279$ cu. ft./lb.

$\overline{V}_{k\ell} = 0.73$ cu. ft./lb.

$D_{Ckj} = 1.954\times10^{-7} - 1.138\times10^{-8}\ \sigma_k$

or $\quad D_{Ckj} = 7.071\times10^{-8} - 2.973\times10^{-7}\ n_k$

III. Methane-n-butane at 100° F, liquid depth 0.12 ft.

$\sigma_{ko} = 1.601$ lb./cu. ft. $\quad\quad$ $\sigma_{jg} = 4.74$ lb./cu. ft.

$\sigma_{kbi} = 5.346$ lb./cu. ft. $\quad\quad$ $\overline{V}_{j\ell} = 0.0204$ cu. ft./lb.

$\overline{V}_{k\ell} = 0.1045$ lb./cu. ft.

$D_{Ckj} = 1.954\times10^{-7} - 1.138\times10^{-8}\ \sigma_k$

or $\quad D_{Ckj} = 7.071\times10^{-8} - 2.973\times10^{-7}\ n_k$

The results of the calculations showed for the three situations listed above that the processes could be described well by a diffusion coefficient which was evaluated by a weighted average composition from the equation

$$\chi_{characteristic} = w\,\chi_{surface} + (1-w)\,\chi_{initial}\ .$$

The variable χ could be either weight fraction or concentration of the light component. Over the time periods used in the calculations, the weights w for the three tests for the above composition variables were, respectively: I. 0.67 - 0.64 and 0.69 - 0.66; II. 0.74 - 0.67 and 0.75 - 0.68; III. 0.75 - 0.71 and 0.69 . Both the constancy and generality of the value of 0.7 for the variable w are evident from these results. In the numerical calculations for the above three cases, the first behaved as though it were semi-infinite; the other two as though they were of finite length. It is therefore proposed that this value be used in the above equation to permit calculation of a more accurate value for a characteristic, constant diffusion coefficient for use in analytical expressions describing diffusion processes.

NOMENCLATURE

D_{Ckj}	Chapman-Cowling diffusion coefficient, sq. ft. per sec.
n	Weight fraction
$\overline{V}$	Partial volume, cu. ft. /lb.
w	Weighting factor
σ	Concentration, lb. /cu. ft.
χ	Composition variable, either concentration or weight fraction of the light component

Subscripts

b	Bubble point
g	Gas phase
i	Value at two-phase interface, in liquid
j	Heavy component
k	Light component
ℓ	Liquid phase
o	Initial value

PROPOSITION V

An improved method is proposed for treating data on material addition to a transient liquid diffusion cell.

The method which has been used in the past for determining the characteristic quantity for a diffusion experiment $m_{kc}\sqrt{\theta}$ was described (2) in Part III of this thesis. It involved fitting a straight line to data for weight of material added to the cell versus the square root of the time after the initiation of the diffusion run. This method introduces unnecessary errors due to the choice of the zero point of time.

Figure 1 shows data for a typical diffusion experiment (1) with the transient liquid diffusion apparatus. The solid line through the data points shows the trend of the data as taken. In the past, the initial weight of material, m_o, was allowed to be arbitrarily determined from the data by a least squares fit of the following equation

$$m = m_o + b\sqrt{\theta} \quad . \tag{1}$$

But this equation forced the constant b to depend on the zero point which was chosen for the variable θ. If that zero point was chosen too early, as in Figure 1, the initial data points would curve down toward the θ axis and could not be used safely to give a fit of Equation 1. This ill is easily cured by allowing the zero point of the variable θ to be determined also by a least squares fit of the data to the equation

$$m - m_o = b\sqrt{\theta - \theta_o} \quad . \tag{2}$$

Equation 2 can be rearranged to the following form

$$m^2 - 2m_o m + (b^2\theta_o + m_o^2) = b^2\theta \quad . \tag{3}$$

The characteristic quantity is then simply

$$m_{kc}\sqrt{\theta - \theta_o} = b/2 \quad . \tag{4}$$

Equation 3 can be fitted easily to data by a nonlinear least squares technique (3).

For the example situation in Figure 1 (diffusion into methane-n-pentane at 40° F and 1484.8 psi), Equation 1 gave a value for b^2 of 101.2×10^{-12} lb.^{2}/sec. (1), while Equation 3 yielded a value of $77.15\times10^{-12} \pm 7.98\times10^{-12}$ lb.^{2}/sec., where the last quantity indicates the 95 per cent confidence limits on b^2. As shown in Part III of this thesis, the Chapman-Cowling diffusion coefficient is directly proportional to b^2; therefore, the differences noted above for the value of this quantity would cause differences in the finally calculated coefficients of 24 per cent. This difference is larger than that between coefficients calculated with truncated and untruncated formulas and undoubtedly contributes to scatter and uncertainties in the data.

The asymptote in Figure 1, which has the slope b, shows that if an experiment were carried out long enough, the effect of a wrong choice for the zero for time in a diffusion experiment would approach zero. However, because the experiments are carried out in a cell which is not semi-infinite, as assumed in the derivation of the equations for the calculation of the diffusion coefficients, the effect of the semi-infinite approximation nullifies any advantages of long experiments. Therefore, the necessity of using Equation 3 for determining the value of b is at least as great as the necessity for using the untruncated formula for the calculation of coefficients as described in

this thesis.

NOMENCLATURE

Symbol

b	Characteristic product for a diffusion experiment, defined by Equation 4, lb. sec.$^{-\frac{1}{2}}$
m	Weight of material added to transient liquid diffusion cell, lb.
θ	Time, sec.

Subscripts

c	Into cell
k	The light component
o	Initial or zero value

REFERENCES

1. Reamer, H. H., Duffy, C. H., and Sage, B. H., Ind. Eng. Chem. 48, 283 (1956).

2. Reamer, H. H., Opfell, J. B., Sage, B. H., and Duffy, C. H., Ind. Eng. Chem. 48, 275 (1956).

3. Woodward, J. W., Ph. D. Thesis, California Institute of Technology (1965).

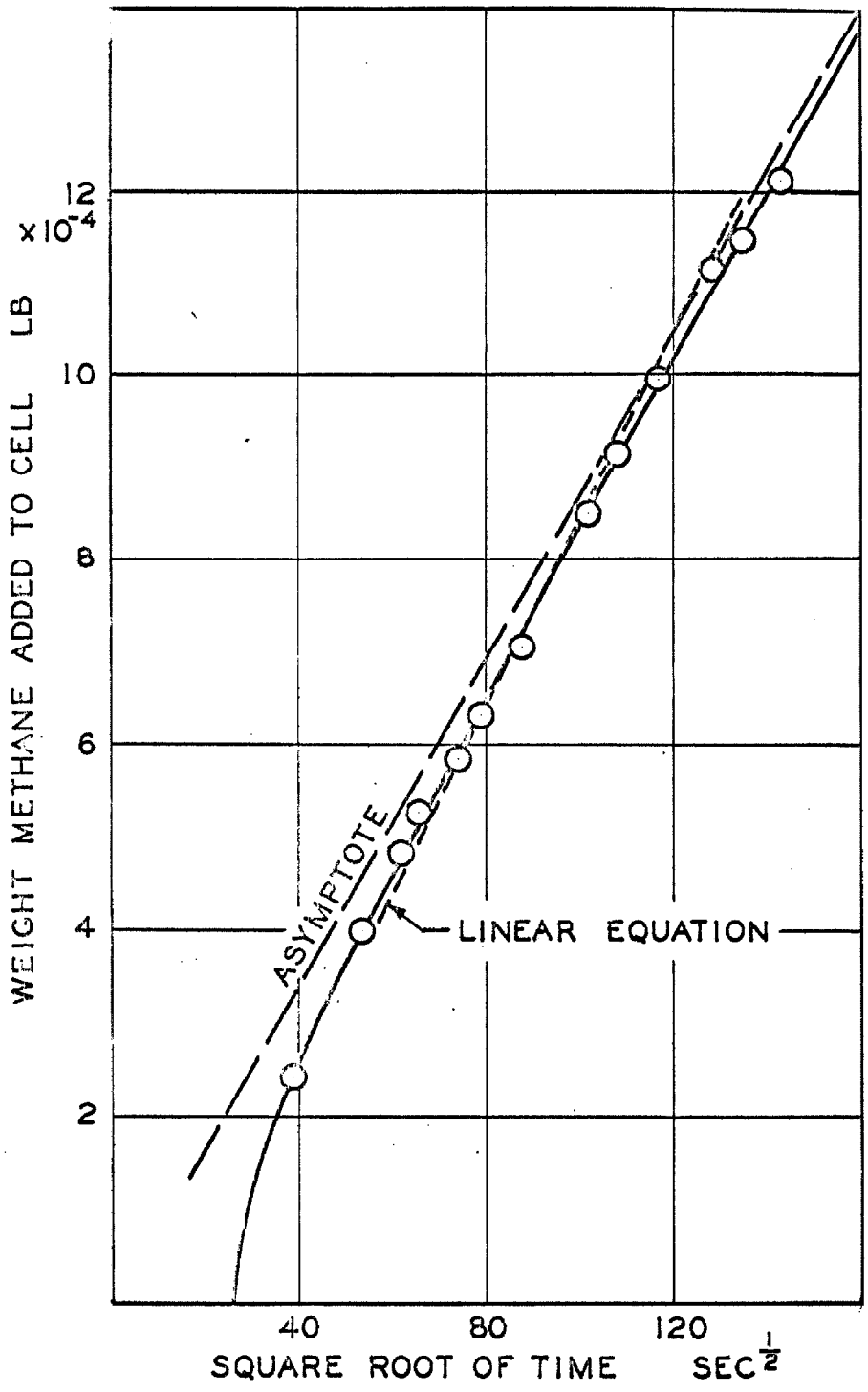

Fig. 1. Transport as a Function of Time.